Nonlinear View on Last Hazardous Tsunamis

Efim Pelinovsky

Department of Nonlinear Geophysical Processes,
Institute of Applied Physics, Nizhny Novgorod, Russia

Applied Mathematics Department,
Nizhny Novgorod State Technical University, Russia

Dynamical System and Applications Laboratory,
Higher School of Economics, Nizhny Novgorod, Russia

Special Research Bureau for Automation of Marine Researches, Yuzhno-Sakhalinsk, Russia

University of Southern Queensland, Toowoomba, Australia

International Tsunami Commission

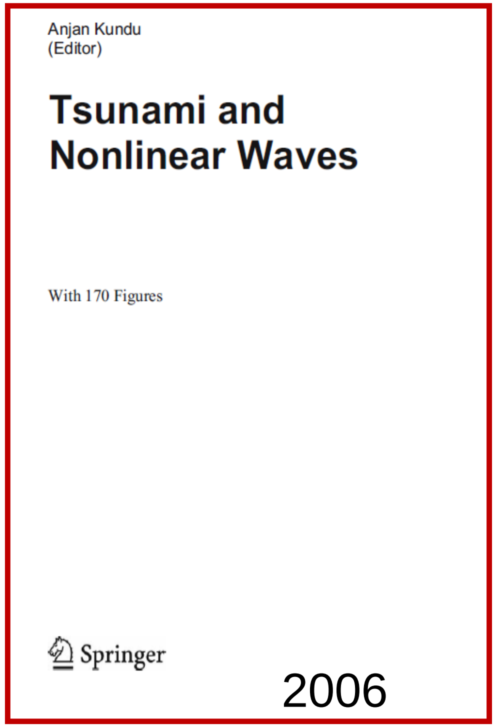
Anjan Kundu
(Editor)
Tsunami and Nonlinear Waves
With 170 Figures
Springer
2006

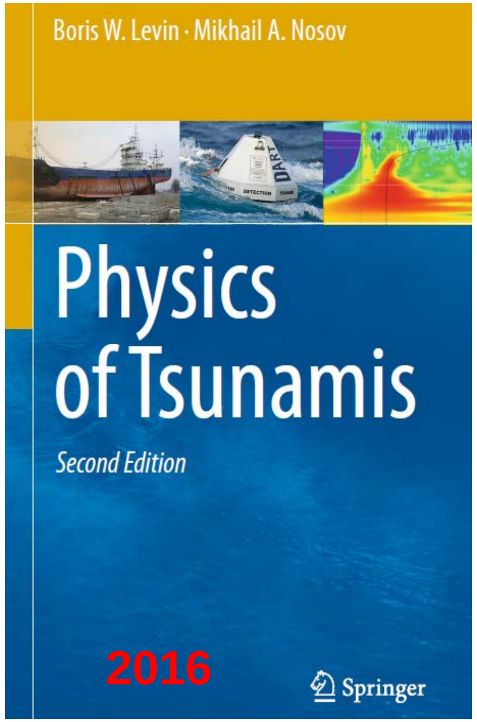
Boris W. Levin · Mikhail A. Nosov
Physics of Tsunamis
Second Edition
2016
Springer

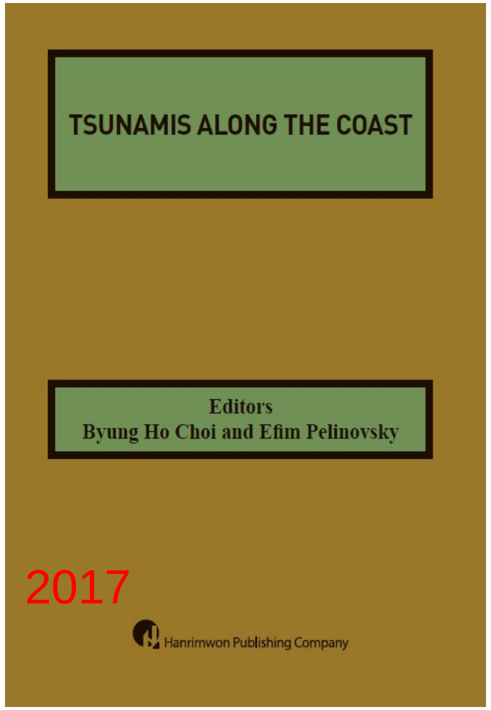
TSUNAMIS ALONG THE COAST
Editors
Byung Ho Choi and Efim Pelinovsky
2017
Hanrimwon Publishing Company

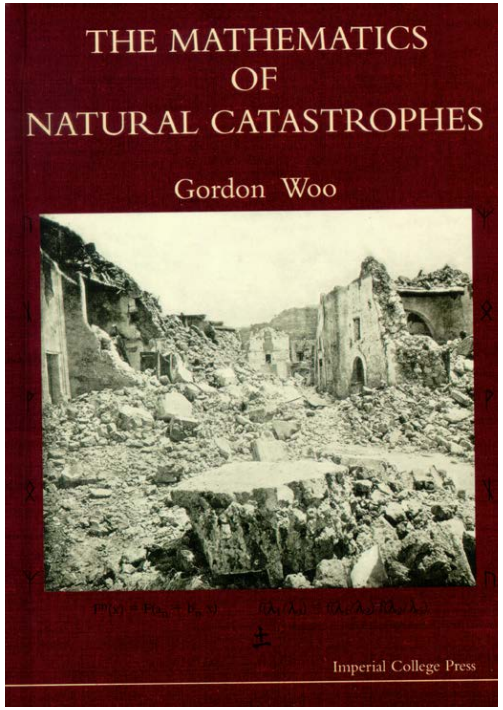
THE MATHEMATICS OF NATURAL CATASTROPHES
Gordon Woo
Imperial College Press

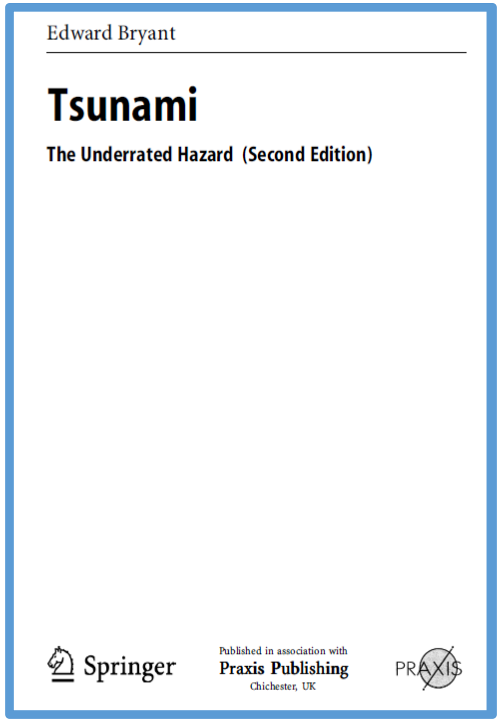
Edward Bryant
Tsunami
The Underrated Hazard (Second Edition)
Springer
Published in association with
Praxis Publishing
Chichester, UK
PRAXIS

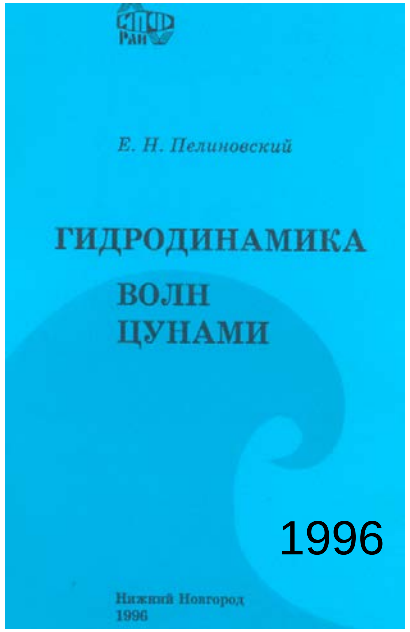
ИПФ РАН
Е. Н. Пелиновский
ГИДРОДИНАМИКА
ВОЛН
ЦУНАМИ
1996
Нижний Новгород
1996

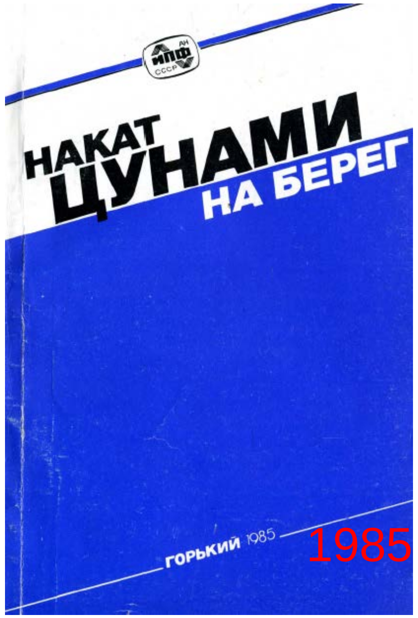
ИПФ АН СССР
НАКАТ
ЦУНАМИ
НА БЕРЕГ
ГОРЬКИЙ 1985
1985

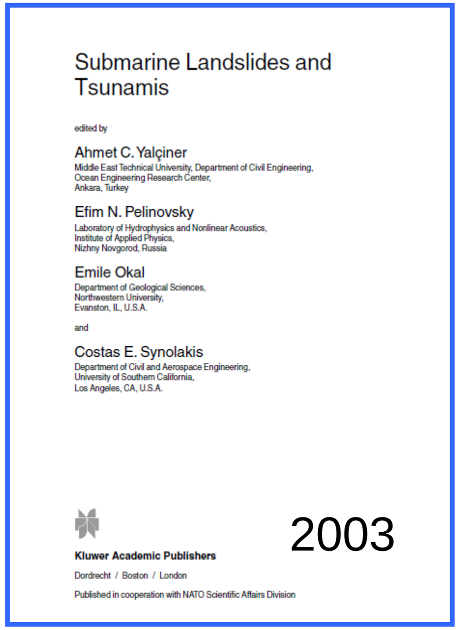
Submarine Landslides and Tsunamis
edited by
Ahmet C. Yalçiner
Middle East Technical University, Department of Civil Engineering,
Ocean Engineering Research Center,
Ankara, Turkey
Efim N. Pelinovsky
Laboratory of Hydrophysics and Nonlinear Acoustics,
Institute of Applied Physics,
Nizhny Novgorod, Russia
Emile Okal
Department of Geological Sciences,
Northwestern University,
Evanston, IL, U.S.A.
and
Costas E. Synolakis
Department of Civil and Aerospace Engineering,
University of Southern California,
Los Angeles, CA, U.S.A.
Kluwer Academic Publishers
Dordrecht / Boston / London
Published in cooperation with NATO Scientific Affairs Division
2003

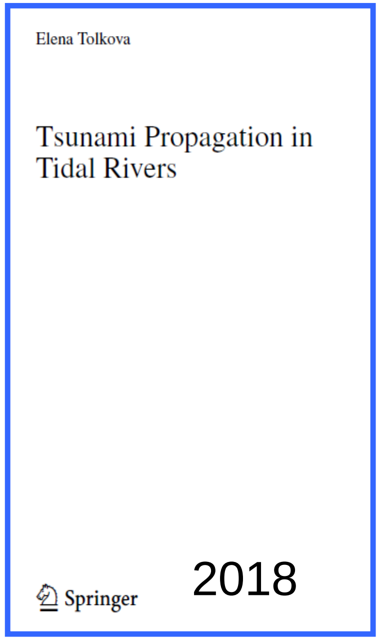
Elena Tolkova
Tsunami Propagation in Tidal Rivers
Springer
2018


Т.С.Мурти
СЕЙСМИЧЕСКИЕ МОРСКИЕ ВОЛНЫ
ЦУНАМИ

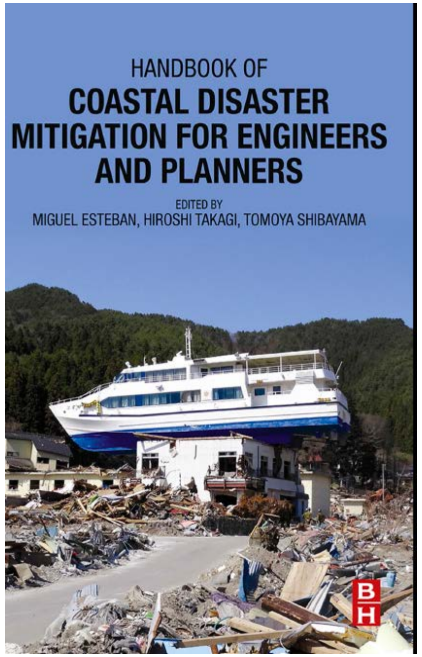
HANDBOOK OF
COASTAL DISASTER MITIGATION FOR ENGINEERS AND PLANNERS
EDITED BY
MIGUEL ESTEBAN, HIROSHI TAKAGI, TOMOYA SHIBAYAMA

Natural Hazard Statistics

1. Flood (40%)
2. Cyclone (20%)
3. Earthquake (15%)
4. Drought (15%)

Cost of the human life: ~$360 000 US

Tsunami is the number FIRST killer in XXI century

津
波

Tsunami
(in Japanese):
Big waves
in harbor

Origin:

1. Earthquakes (85%)
2. Volcanos
3. Landslides
4. Meteo-tsunamis
5. Asteroids
6. Explosions

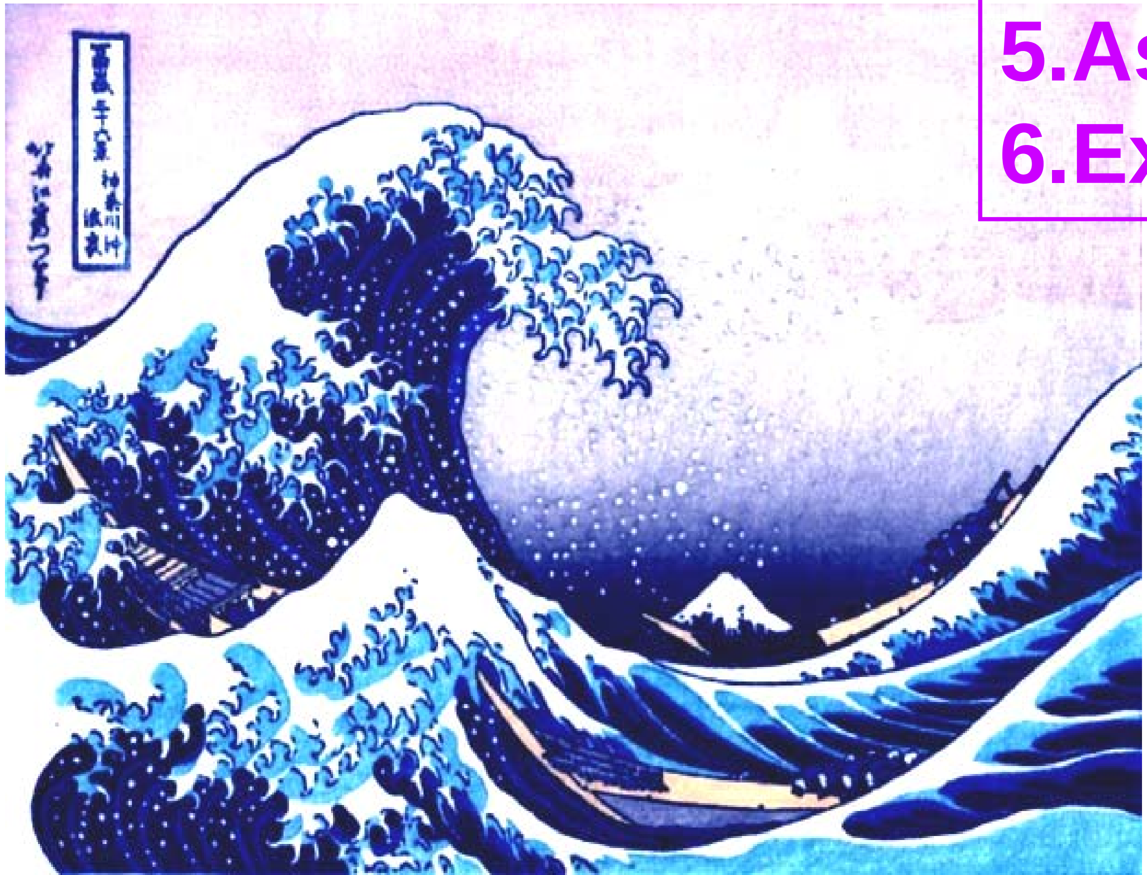

Typical Scales:

Duration 5-30 min
Length 20-100 km
Height 1-30 m

World Tsunami Awareness Day, 5 November

UN General Assembly has designated 5 November as World Tsunami Awareness Day and called on the world to mark it.

The date of 5 November was chosen in honour of a true story from Japan: “Inamura-no-hi”, which means the “burning of the rice sheaves”. During an 1854 earthquake, a farmer saw the tide receding, a sign of a looming tsunami. He set fire to his harvested rice to warn villagers, who fled to high ground. In the aftermath, he helped his community build back better to withstand future shocks, constructing an embankment and planting trees as a tsunami buffer.

28 September 2018, Indonesia, Sulawesi Island

more than 2000 people were killed; wave amplitudes attain up to 11 m

Palu, Sulawesi, Sunday 28 Sept, City Day Holiday

Typical Indonesian House, 0-5 min after the earthquake

Pure Appl. Geophys. 176 (2019), 1379–1395

https://doi.org/10.1007/s00024-019-02145-z

Pure and Applied Geophysics

Check for updates

The September 28th, 2018, Tsunami In Palu-Sulawesi, Indonesia: A Post-Event Field Survey

R. Omira,[1,2] G. G. Dogan,[3] R. Hidayat,[4] S. Husrin,[5] G. Prasetya,[6] A. Annunziato,[7] C. Proietti,[7] P. Probst,[7] M. A. Paparo,[8] M. Wronna,[2] A. Zaytsev,[9] P. Pronin,[10] A. Giniyatullin,[10] P. S. Putra,[11] D. Hartanto,[12] G. Ginanjar,[12] W. Kongko,[13] E. Pelinovsky,[14] and A. C. Yalciner[3]

[1] Portuguese Institute for Sea and Atmosphere (IPMA), Lisbon, Portugal. E-mail: omirarachid10@yahoo.fr
[2] Dom Luiz Institute (IDL), Faculty of Sciences, University of Lisbon, Lisbon, Portugal.
[3] Department of Civil Engineering, Ocean Engineering Research Center, Middle East Technical University, Ankara, Turkey.
[4] Coordinating Ministry for Maritime Affairs (CMMA-RI), Jakarta, Indonesia.
[5] Ministry of Maritime Affairs and Fisheries (MMAF-RI), Jakarta, Indonesia.
[6] Indonesian Tsunami Scientific Community (IATsI), Jakarta, Indonesia.
[7] Joint Research Centre, European Commission, Ispra Site, Ispra, Italy.
[8] Department of Physics and Astronomy, University of Bologna, Bologna, Italy.
[9] Special Research Bureau for Automation of Marine Researches, Nizhny Novgorod, Russia.
[10] Nizhny Novgorod State Technical University n.a. R.E. Alekseev, Nizhny Novgorod, Russia.
[11] Indonesian Institute of Science (LIPI), Jakarta, Indonesia.
[12] Meteorology, Climatology, and Geophysical Agency (BMKG), Jakarta, Indonesia.
[13] Agency for the Assessment and Application of Technology (BPPT), Jakarta, Indonesia.
[14] Institute of Applied Physics, Nizhny Novgorod, Russia.

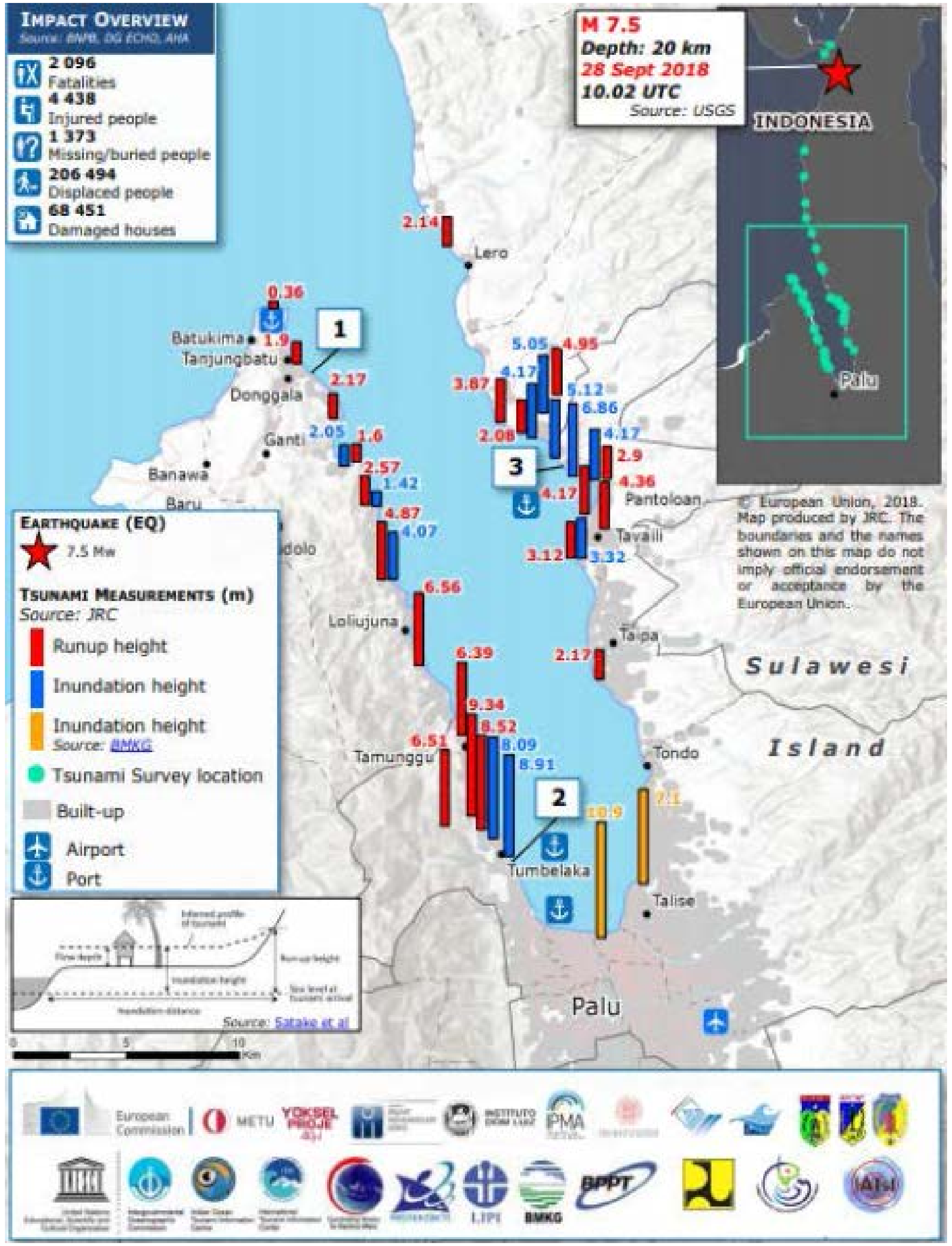

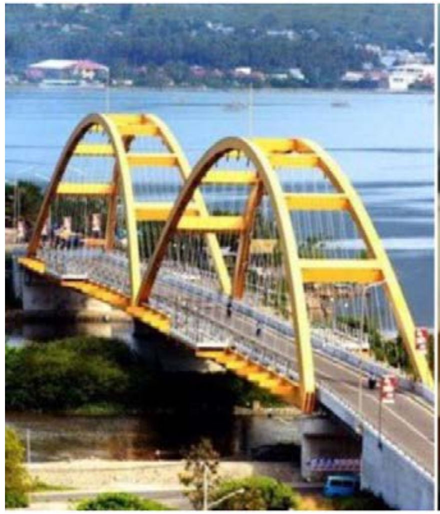

Int. Field Survey, October - November

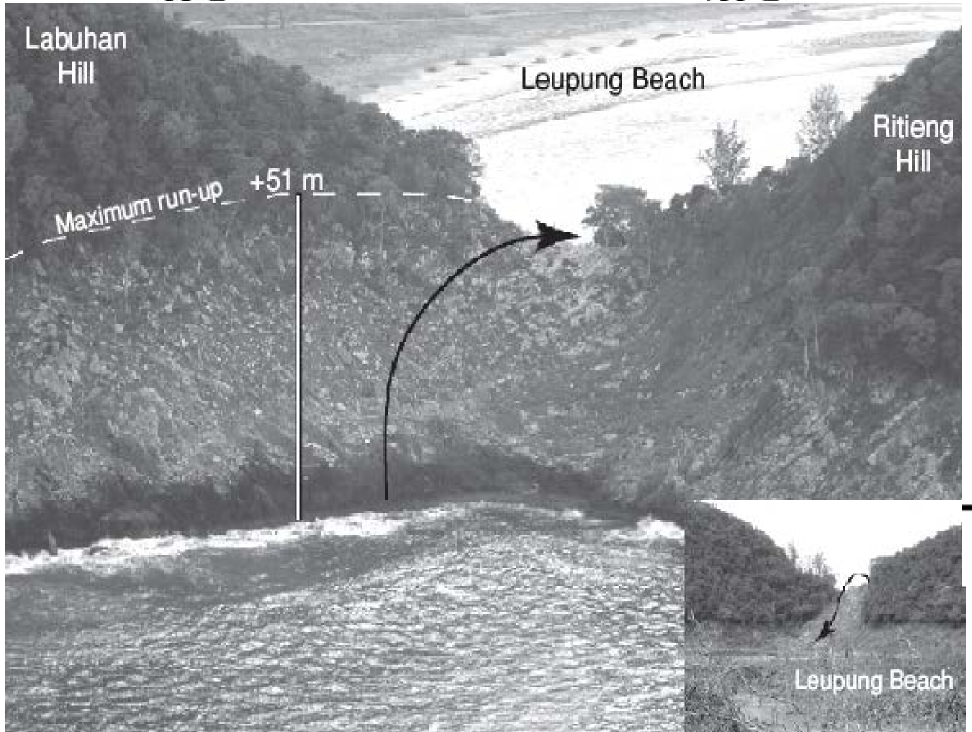

26 December 2004

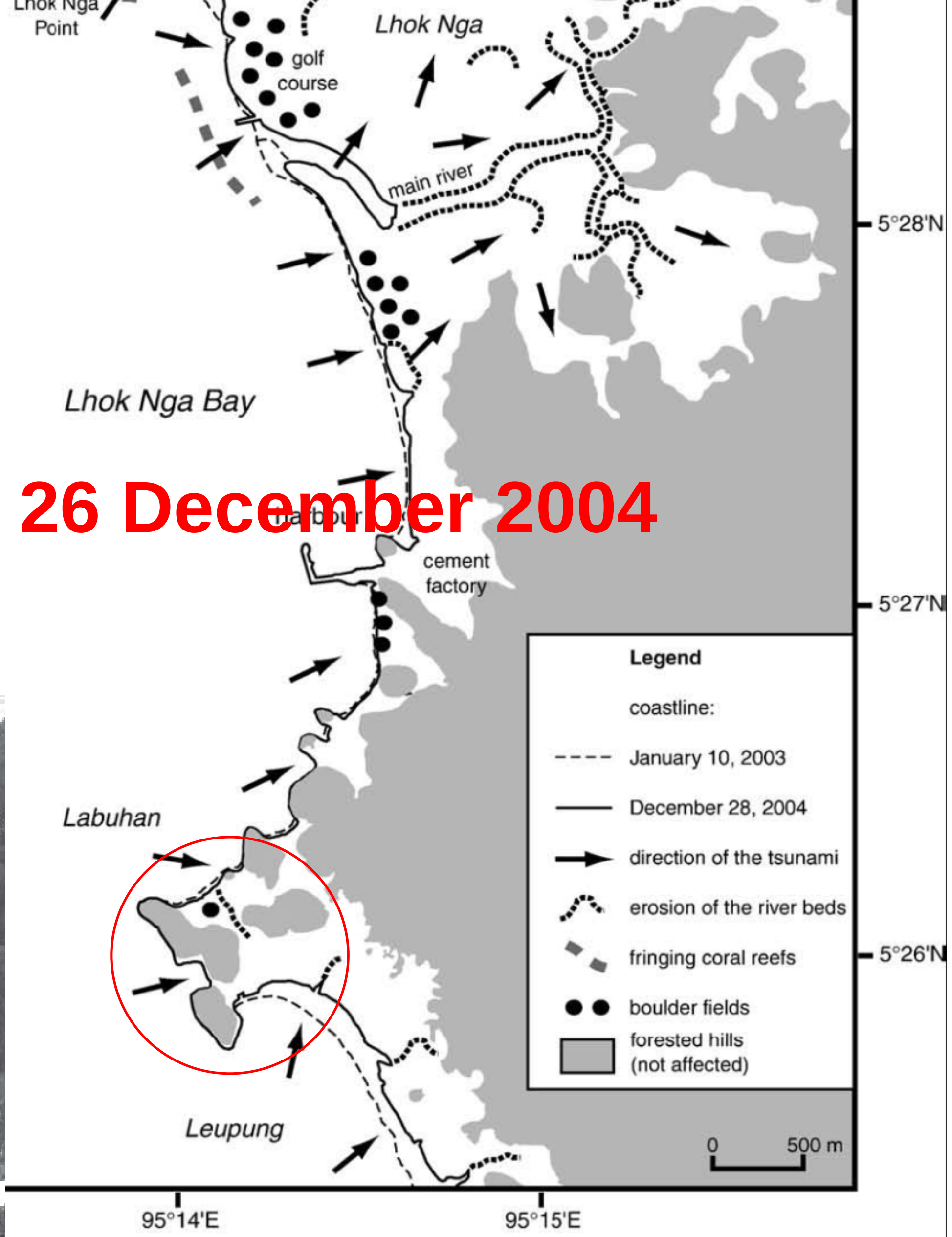

Runup 51 m

Last Tsunami - Puerto-Rico, January 07, 2020

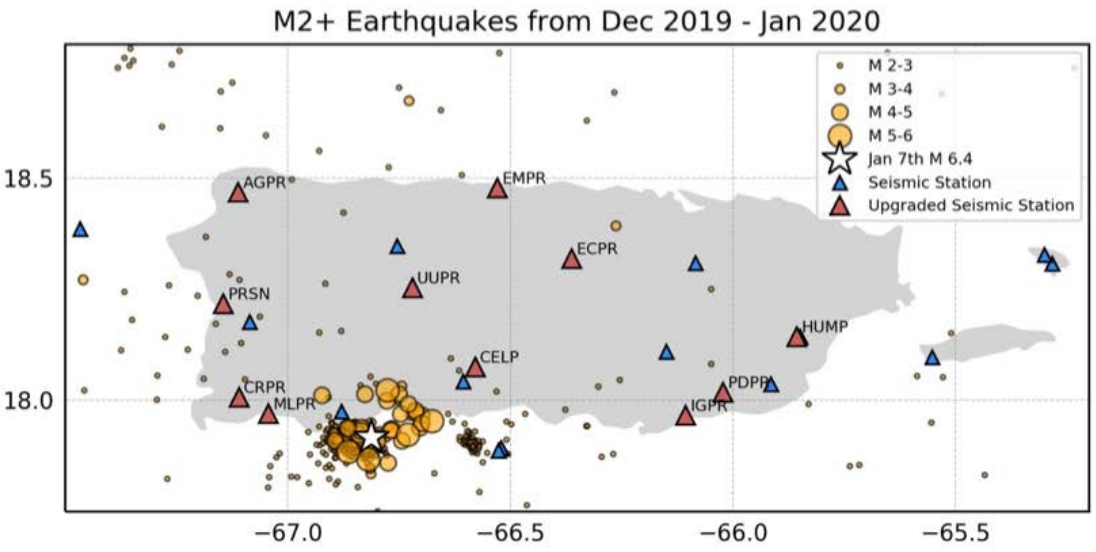

.4

4 died

Tsunami 10 cm

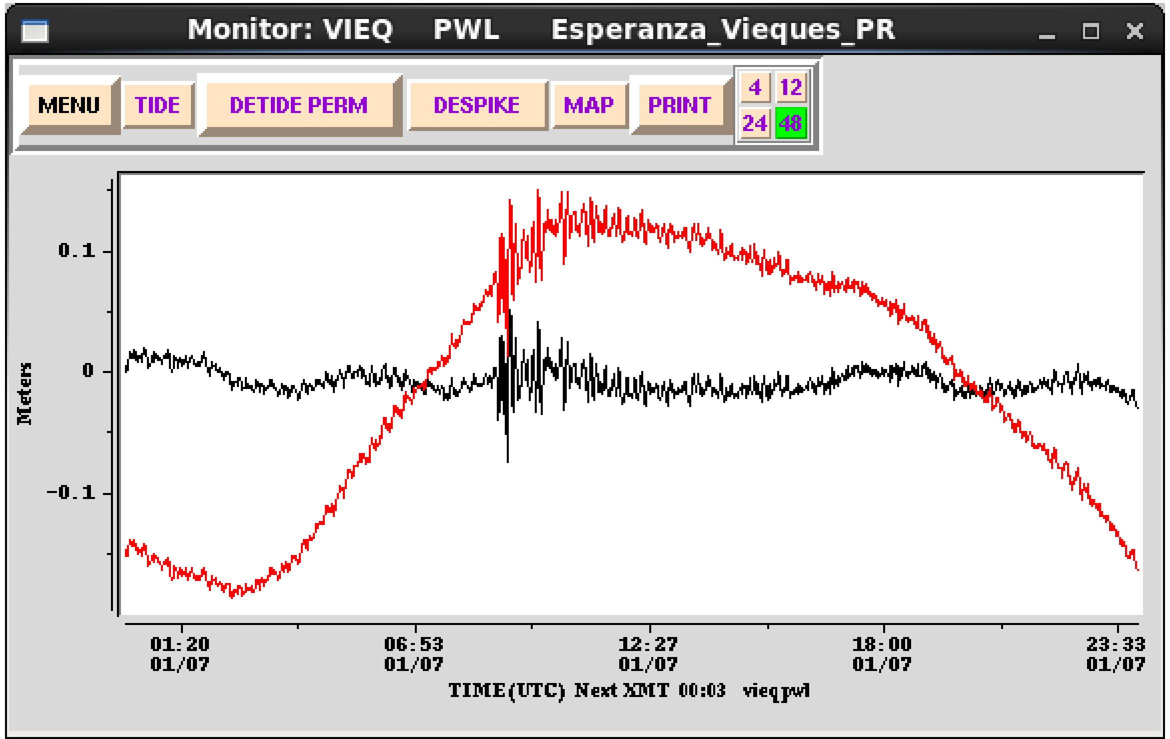

Kubota, T., Saito, T., & Suzuki, W. (2020). Millimeter - scale tsunami detected by a wide and dense observation array in the deep ocean: Fault modeling of an Mw 6.0 interplate earthquake off Sanriku, NE Japan. *Geophysical Research Letters*, *47*, e2019GL085842. https://doi.org/ 10.1029/2019GL085842

Geophysical Research Letters

RESEARCH LETTER
10.1029/2019GL085842

Millimeter-Scale Tsunami Detected by a Wide and Dense Observation Array in the Deep Ocean: Fault Modeling of an Mw 6.0 Interplate Earthquake off Sanriku, NE Japan

T. Kubota[1], T. Saito[1], and W. Suzuki[1]

[1]National Research Institute for Earth Science and Disaster Resilience, Tsukuba, Japan

Key Points:
- Millimeter-scale tsunamis from an Mw 6.0 earthquake were captured by the S-net, a new nationwide pressure gauge array off Sanriku, Japan
- Tsunami signals were identified from the pressure data adjacent to the source, which were contaminated by signals irrelevant to tsunamis
- We inferred the stress drop of the earthquake from the tsunami data more reliably than could be done from seismogram analysis

Supporting Information:
- Supporting Information S1

Correspondence to:
T. Kubota,
kubotatsu@bosai.go.jp

Abstract A new dense and widely distributed tsunami observation network installed off northeast Japan detected millimeter-scale tsunamis from an Mw 6.0 shallow interplate earthquake on 20 August 2016. Based on the fault model deduced from this data set, we obtained a stress drop of 1.5 MPa for this event, similar to those associated with typical interplate earthquakes. The rupture area was unlikely to overlap with regions where slow earthquakes occur, such as low-frequency-tremors and very-low-frequency-earthquakes. The results demonstrated that this new network has dramatically increased the detectability of millimeter-scale tsunamis. Some near-source stations were contaminated by large pressure offset signals irrelevant to tsunami, and we must therefore be careful when analyzing these data. Nonetheless, the new array enables estimations of the stress drops of moderate offshore earthquakes and can be used to elucidate the spatial variation of mechanical properties along the plate interface with much higher resolution than previously possible.

Volcanic Tsunami
22 December 2018
85 m, 430 victims

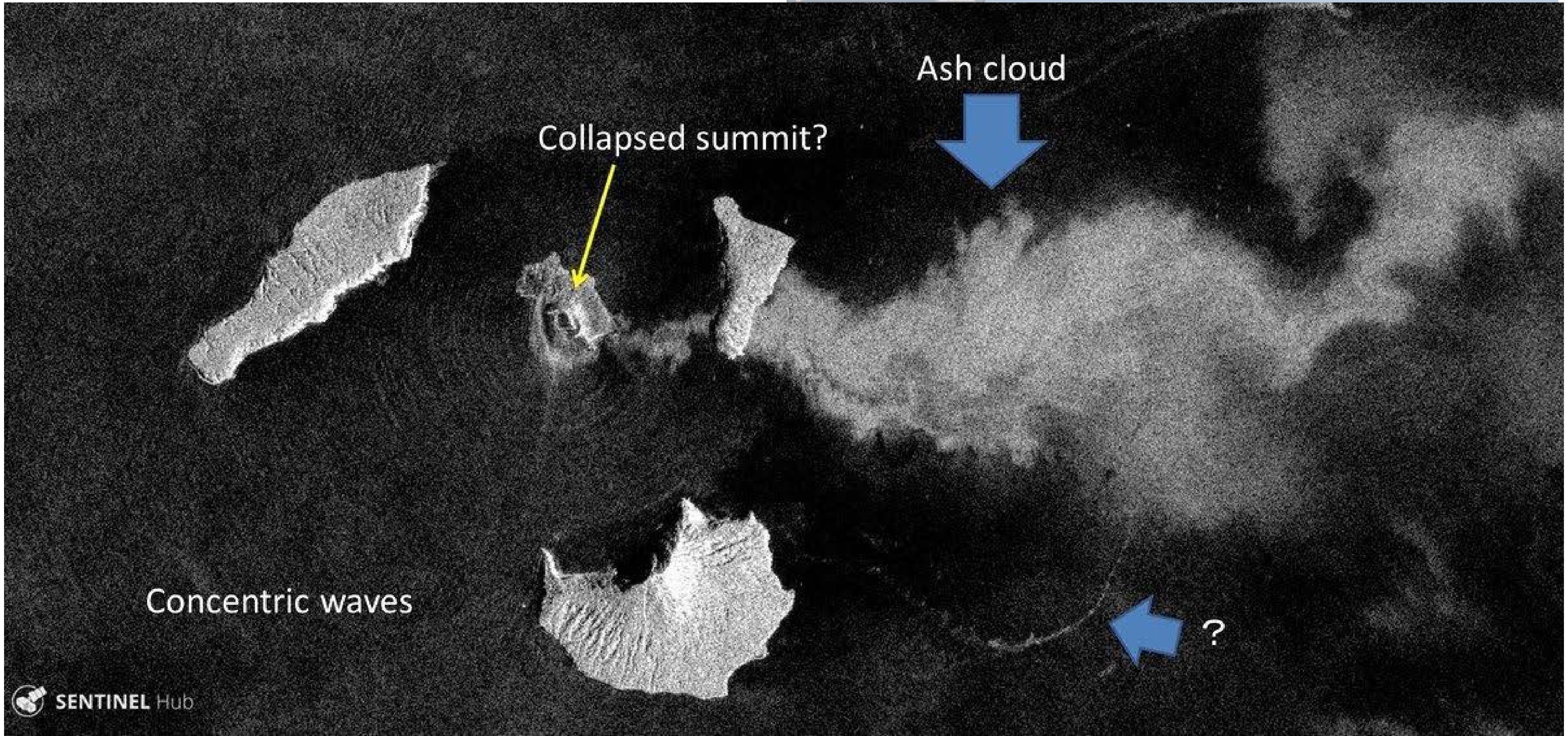

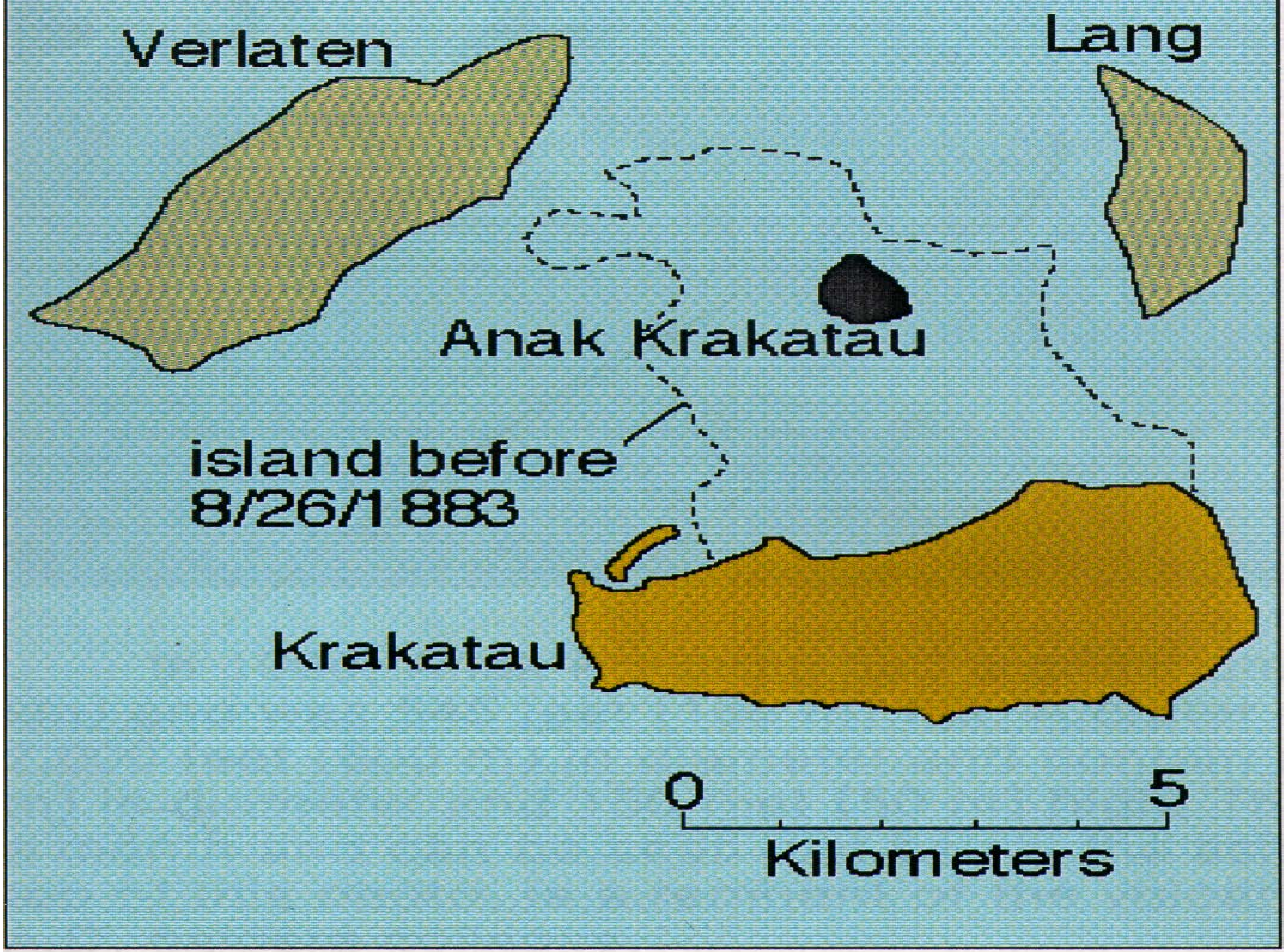

Verlaten
Lang
Anak Krakatau
island before
8/26/1883
Krakatau
0
5
Kilometers

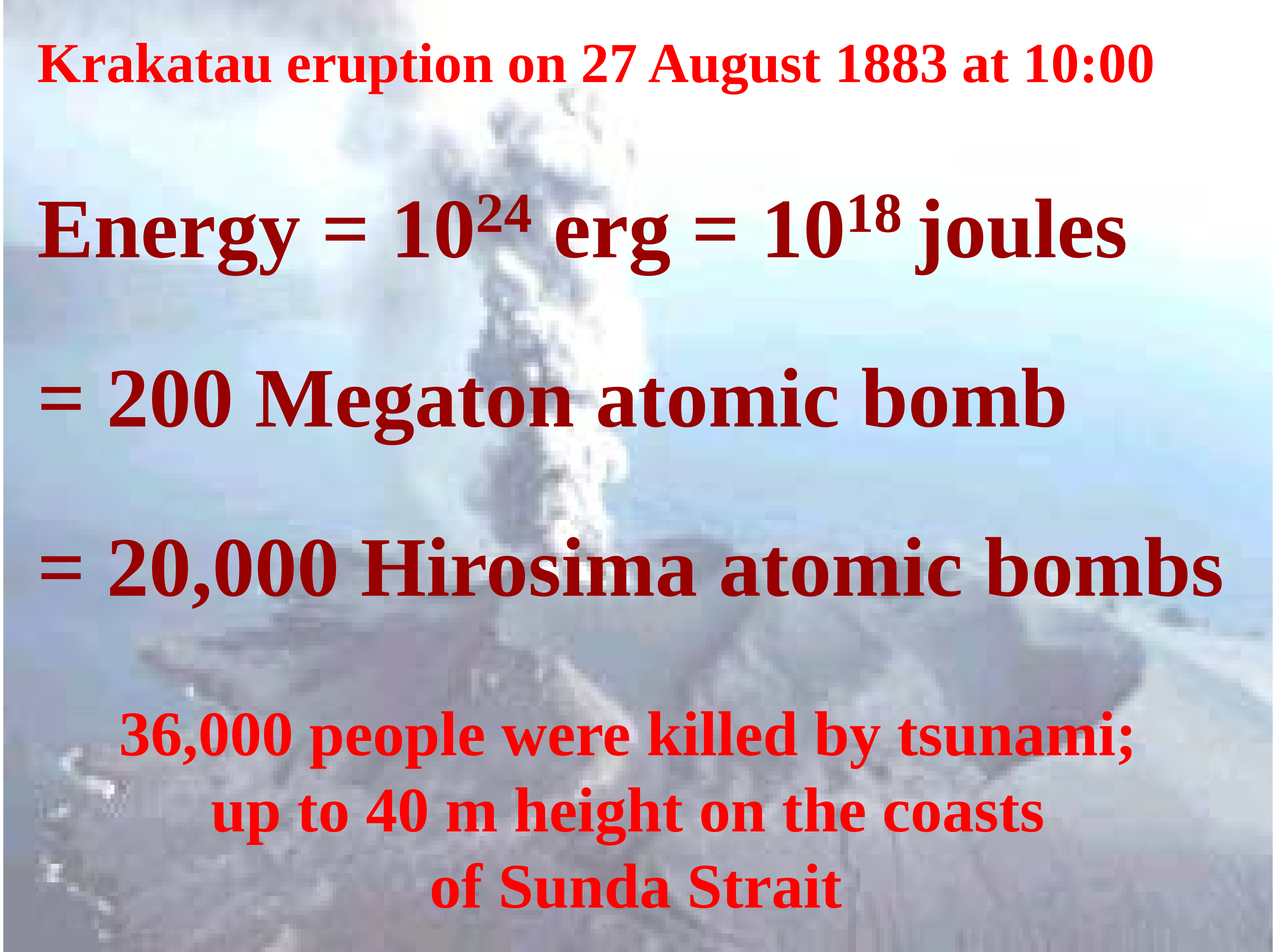

Krakatau eruption on 27 August 1883 at 10:00

Energy = 10^{24} erg = 10^{18} joules

= 200 Megaton atomic bomb

= 20,000 Hirosima atomic bombs

36,000 people were killed by tsunami; up to 40 m height on the coasts of Sunda Strait

Global recording of tsunami waves, 1883

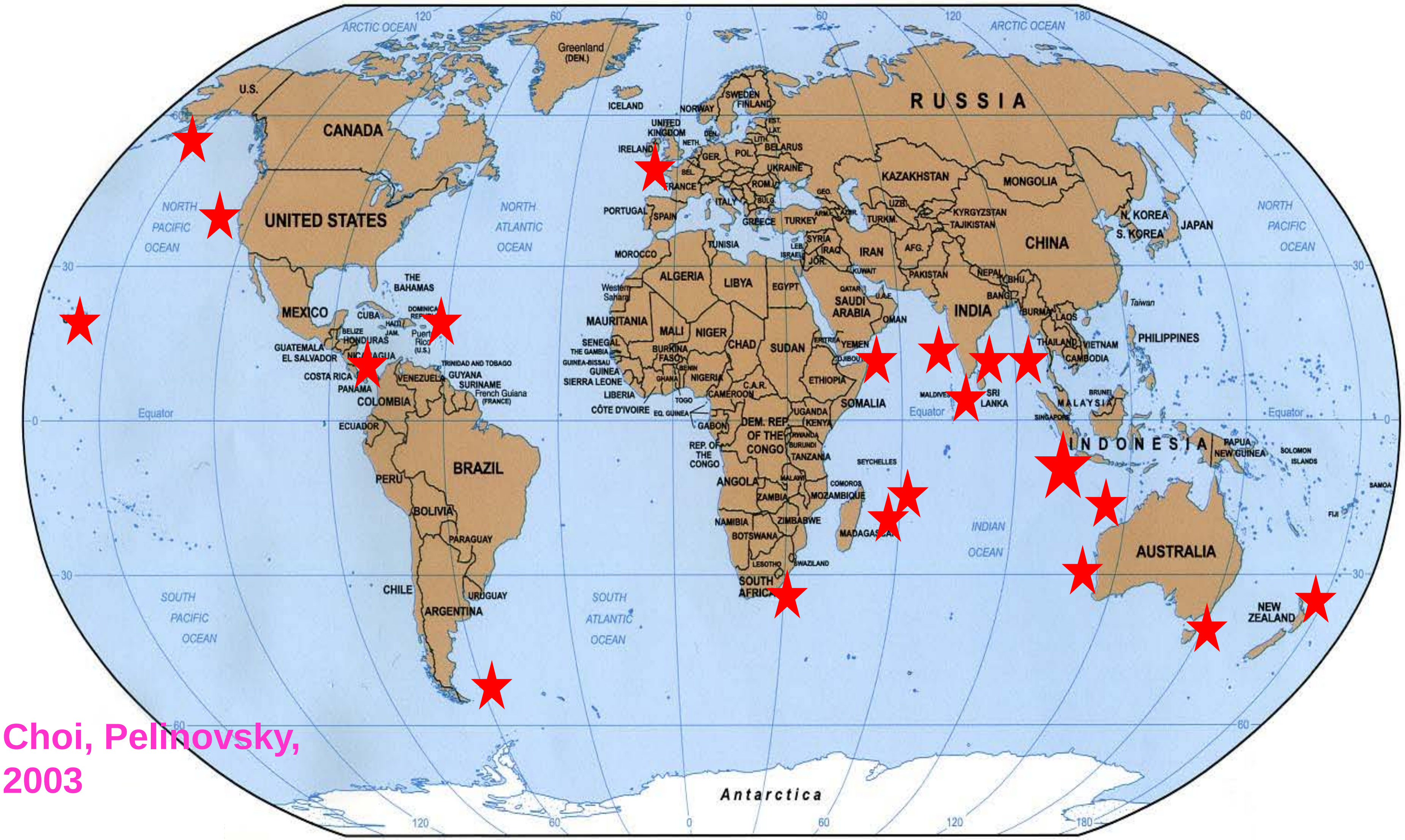

Choi, Pelinovsky, 2003

More than 30 tide-gauge records in Indian Ocean

Landslide Tsunami, 11 December 2018
Bureya River, Russia

25 mln cubic meters

Runup 90 m

A general view of the landslide scar on the southern bank of the Bureya water reservoir and the body of the landslide with a passage, initially made by the militaries in February 2019 and extended by the spring floods in April-May 2019. Photo by A.N. Ostroukhov (IVEP FED RAS) made with the quadcopter "Fantom 4" on June 19, 2019.

This tsunami is 7-8 in list of hugest runup heights

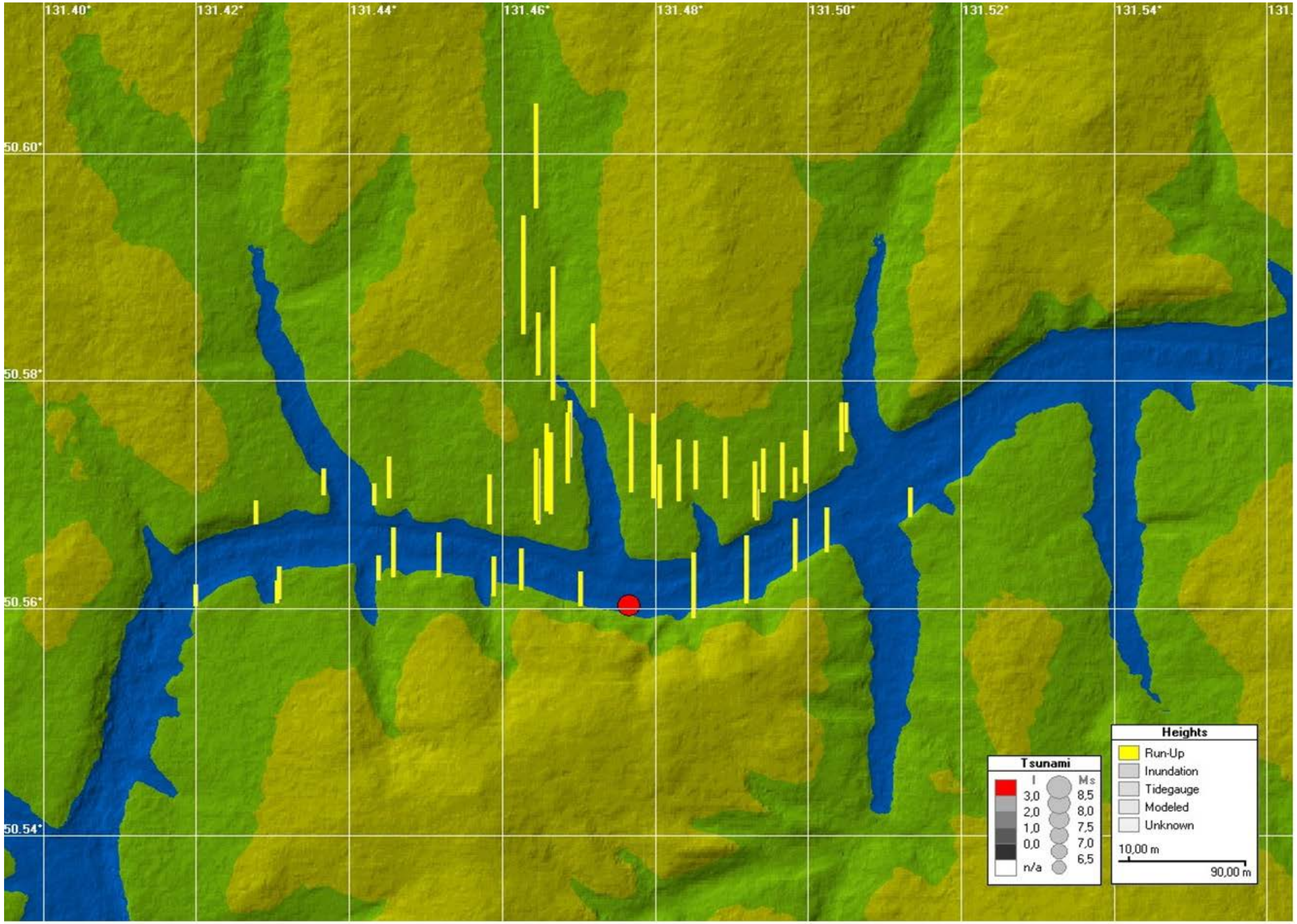

The map of the measured run-up heights of the December 11, 2018 Bureya tsunami plotted in the PDM/TSU graphic shell. The red dot marks a position of the landslide.

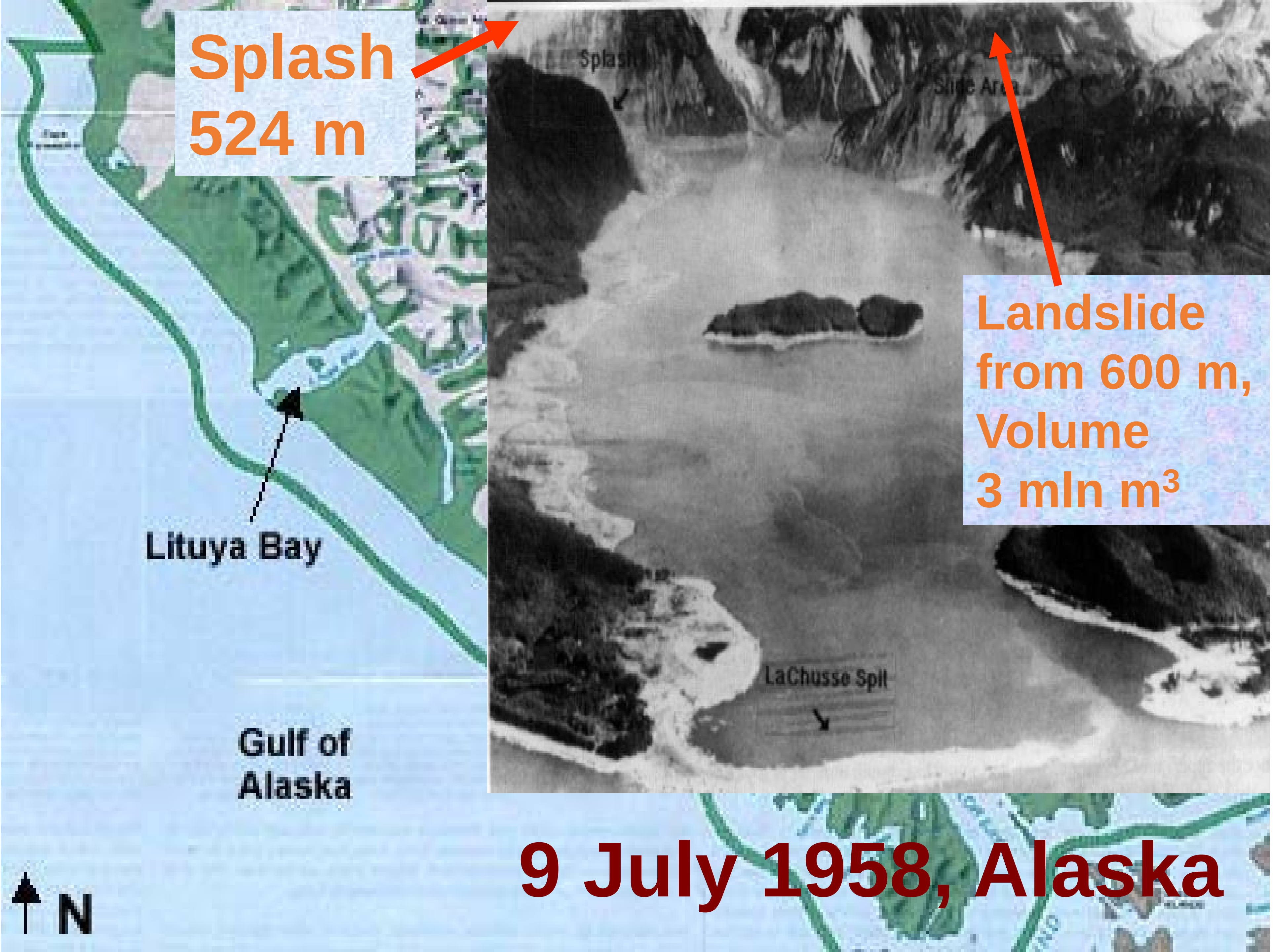

9 July 1958, Alaska

17 October 2015, Alaska

Almost 200 m!

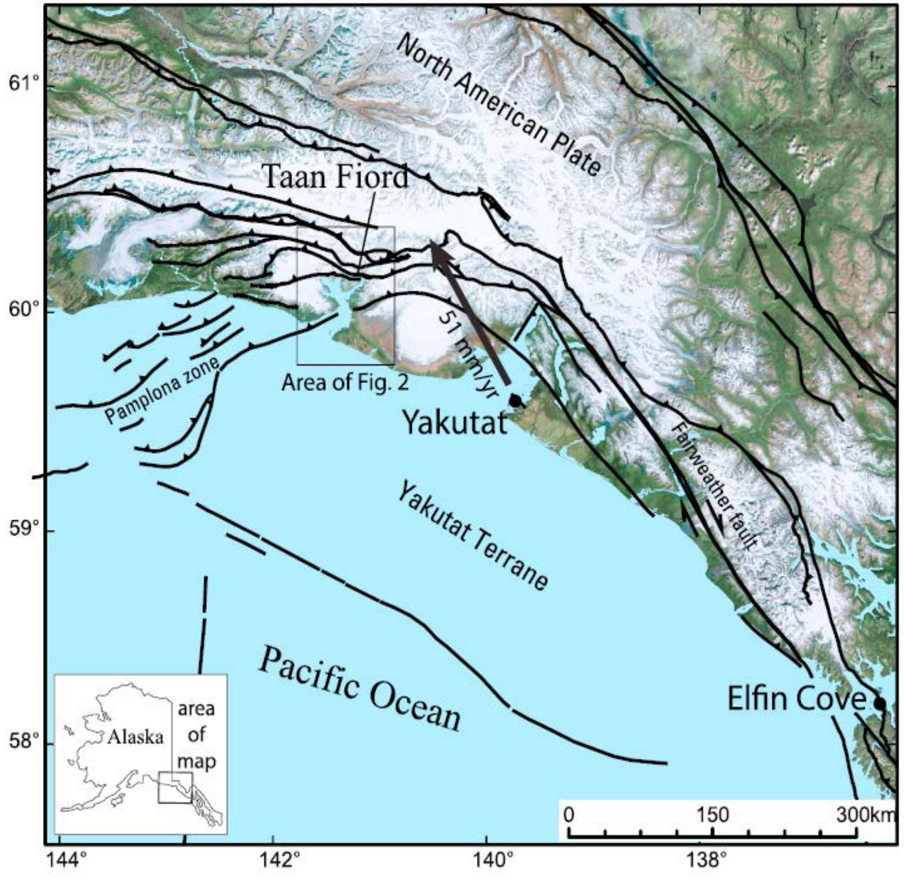

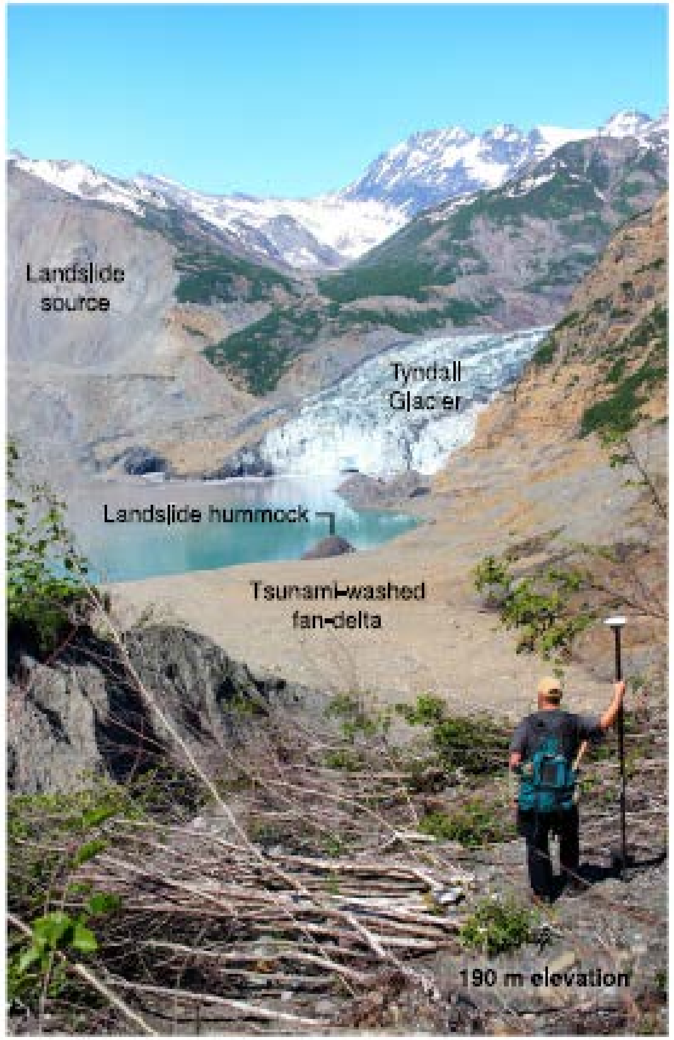

June 18, 2017 Greenland

100 m high,
4 people missing

THE WAVE HEIGHT, AT ITS PEAK, WAS AROUND 100 METERS. DZMITRY MELNIKAU/SHUTTERSTOCK

16 October 1979. A submarine slope failure occurred during construction of *Nice* (France) new harbor. The event cased victims: one person in *Antibes*, and five - worked on the building site. Maximum effects were observed 10 km far from building site near *Antibes*, that was inundated (one person killed). Photos show water heights of 1 m. At *La Salis* (close to *Antibes*), witnesses reported a first wave of 50 cm, 5 min after the landslide. This wave was followed by three 3m-high waves with period of 8 min. At harbor of *Saint Laurent du Var* the water lowered by 2m 1 min after the landslide and then rose by 1 m. Tide-gauge records of *Nice* and of *Villefranche* show that the first wave is a 10 cm trough. The maximum recorded wave amplitudes do not exceed 10 cm in both harbors, whereas witnesses reported wave amplitudes of 1 m.


1 October 1979


16 October 1979

Antibes (60 km from Nice) 16.10.1979

Tide-record of the 1979 Nice tsunami

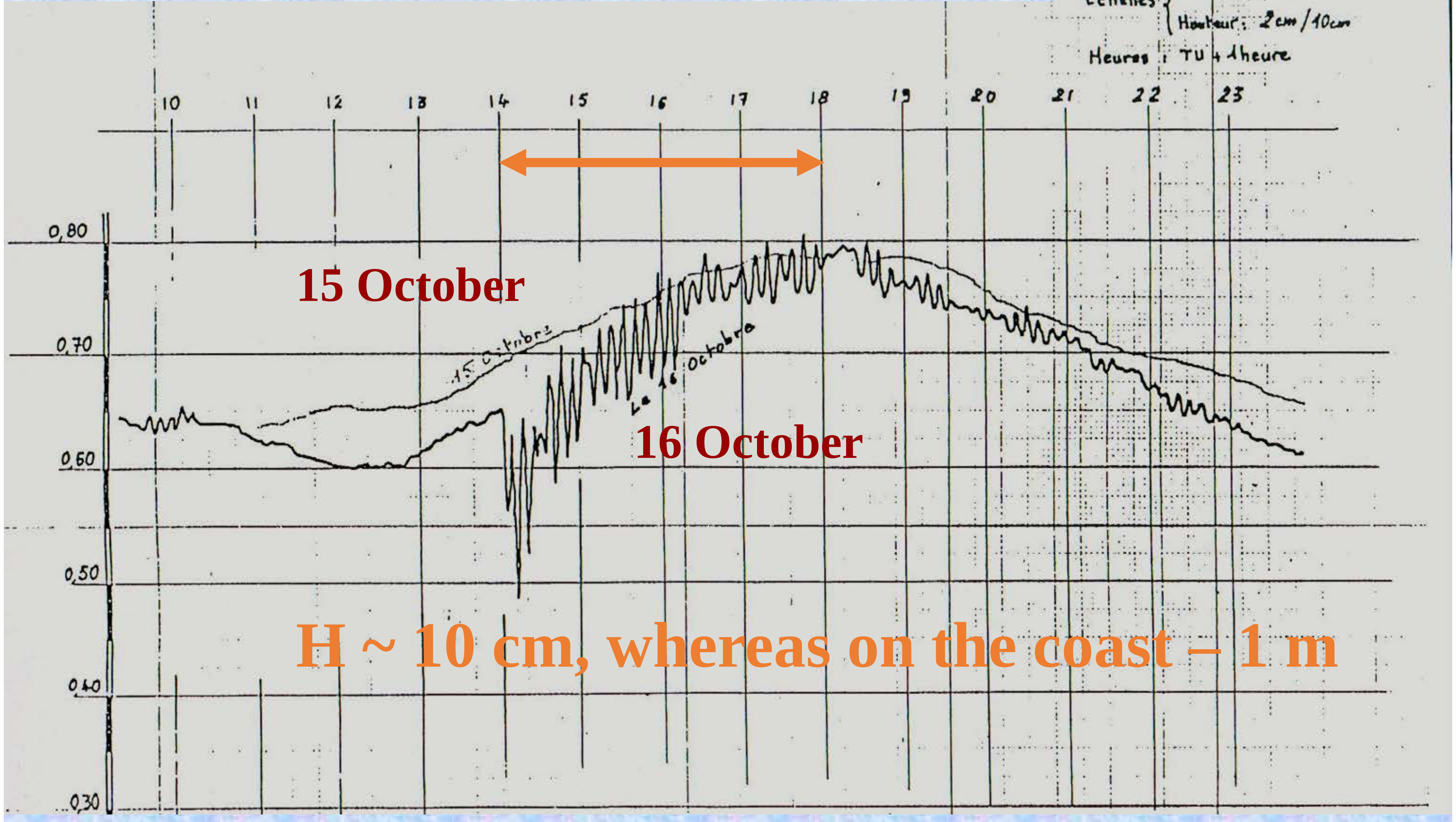

H ~ 10 cm, whereas on the coast – 1 m

Artificial tsunamis of explosive origin

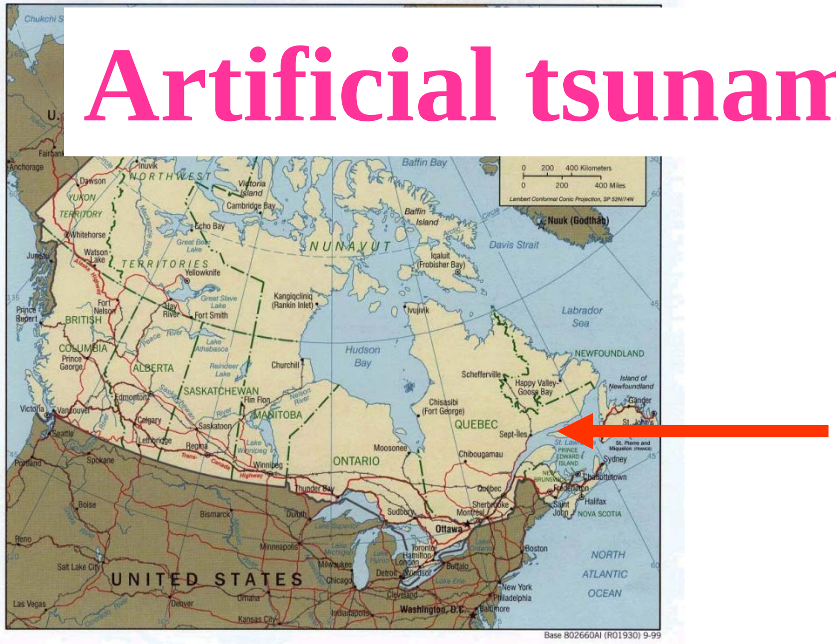

In December 1917 large waves were generated by the greatest explosion before the nuclear era – this happened in the Halifax Harbor (Nova Scotia, Canada) after a collision of the munitions ship *Mont Blanc*, having 3,000 tons of TNT on a board, with the relief ship *Imo*.

At the coast near to the explosion site, the waves were over 10 meters high, but their amplitude diminished greatly further away.

Asteroid collision with Earth

Fulchignoni and Barucci, 2005

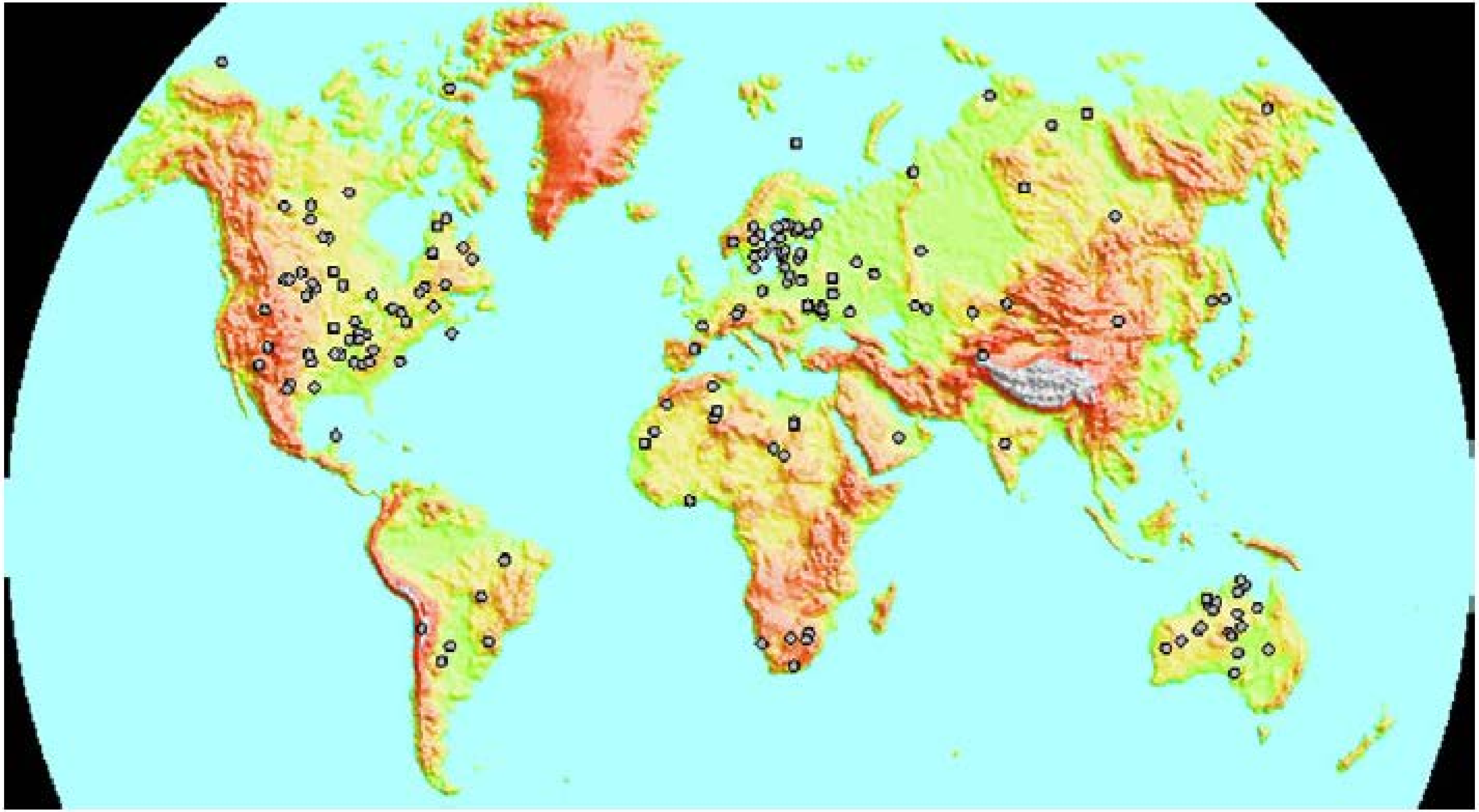

Fig. 1. Geographical distribution of known Earth impact craters.

Asteroid collision with Earth

Asteroids larger than 200 meters in diameter hit Earth about every 3000–5000 years, so the probability of one impact in a given human lifetime is about 2–3%

NASA: 633 known potentially hazardous asteroids

Forecasting time – a few months

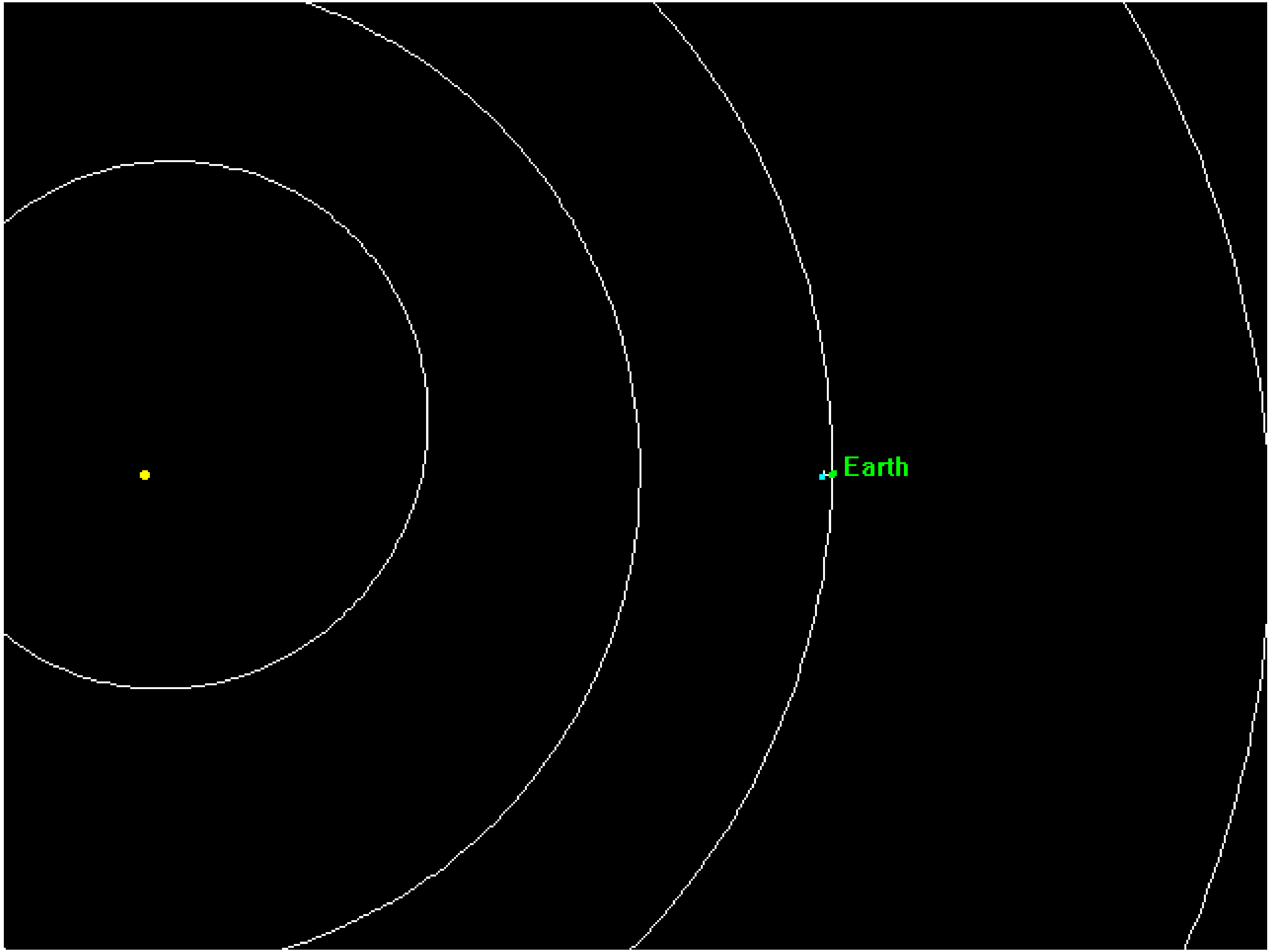
Earth

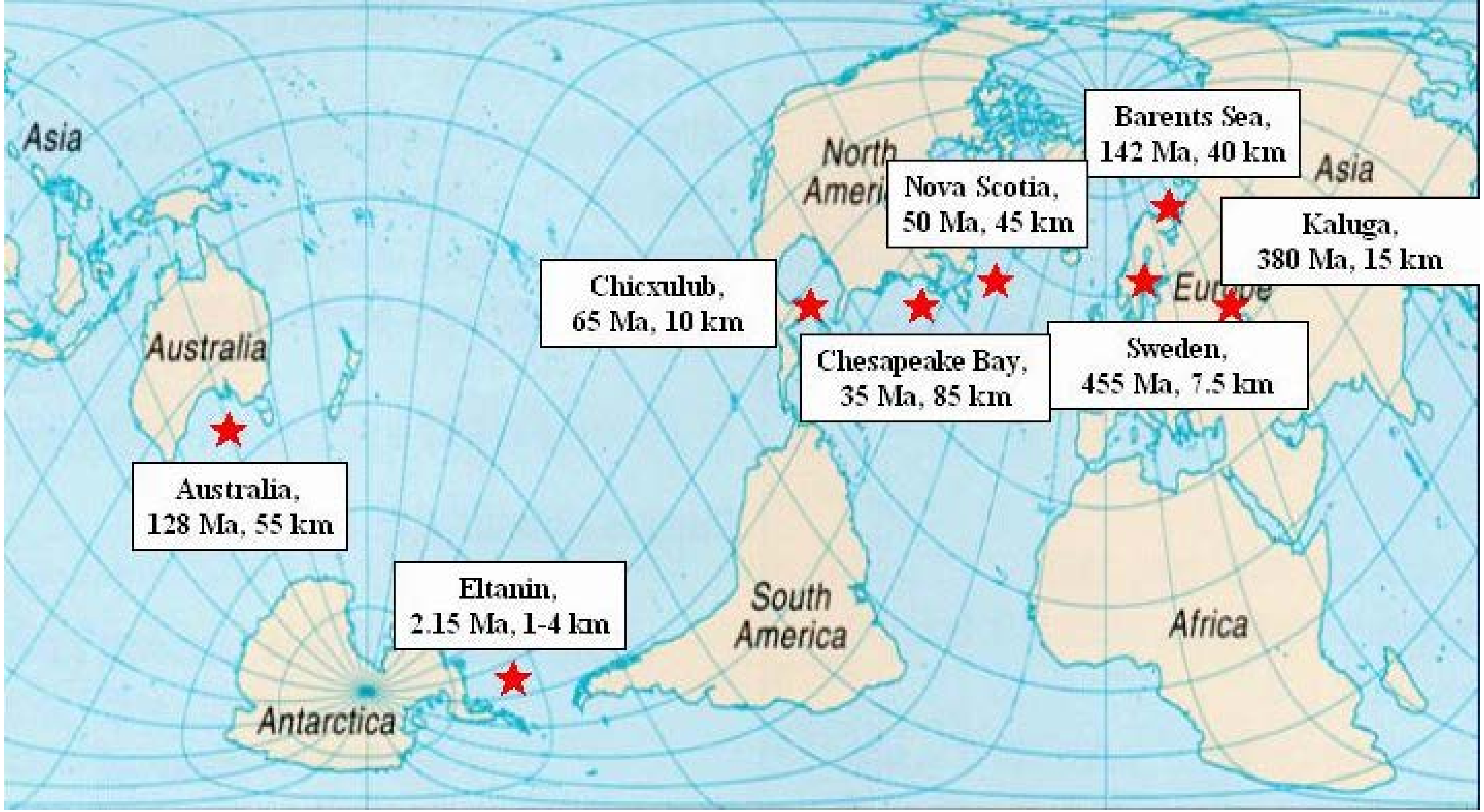

Known asteroid entries into the oceans

(Kharif & Pelinovsky, 2005)

Seismic mapping

Barents Sea,
142 Ma, 40 km

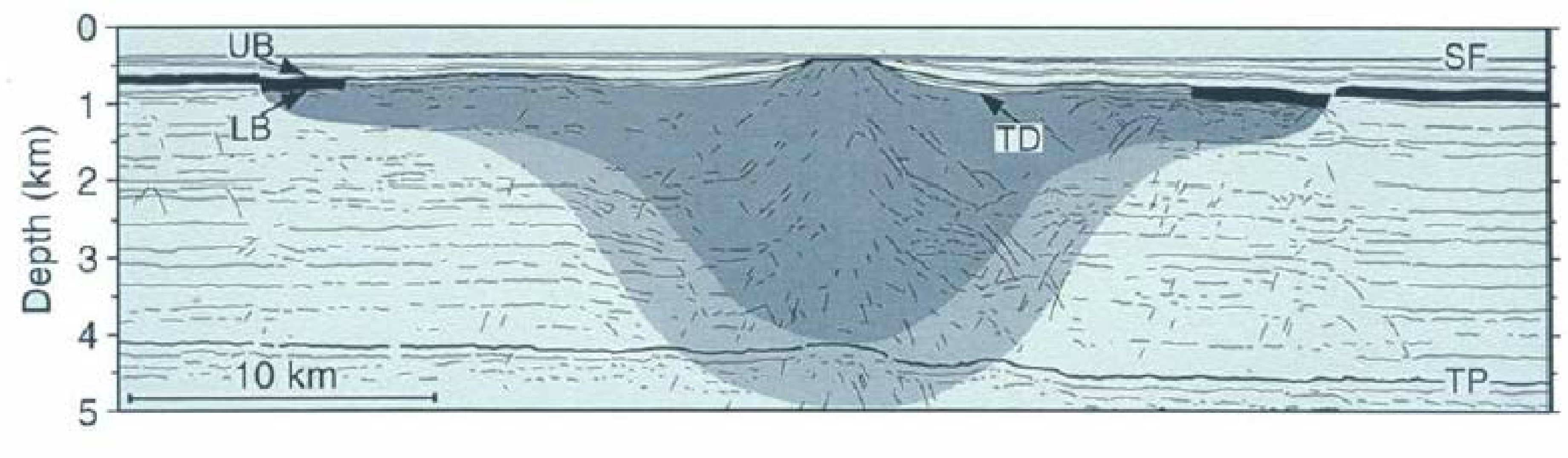

Isolines of the seismic speed

Челябинск, 15 февраля 2013 года

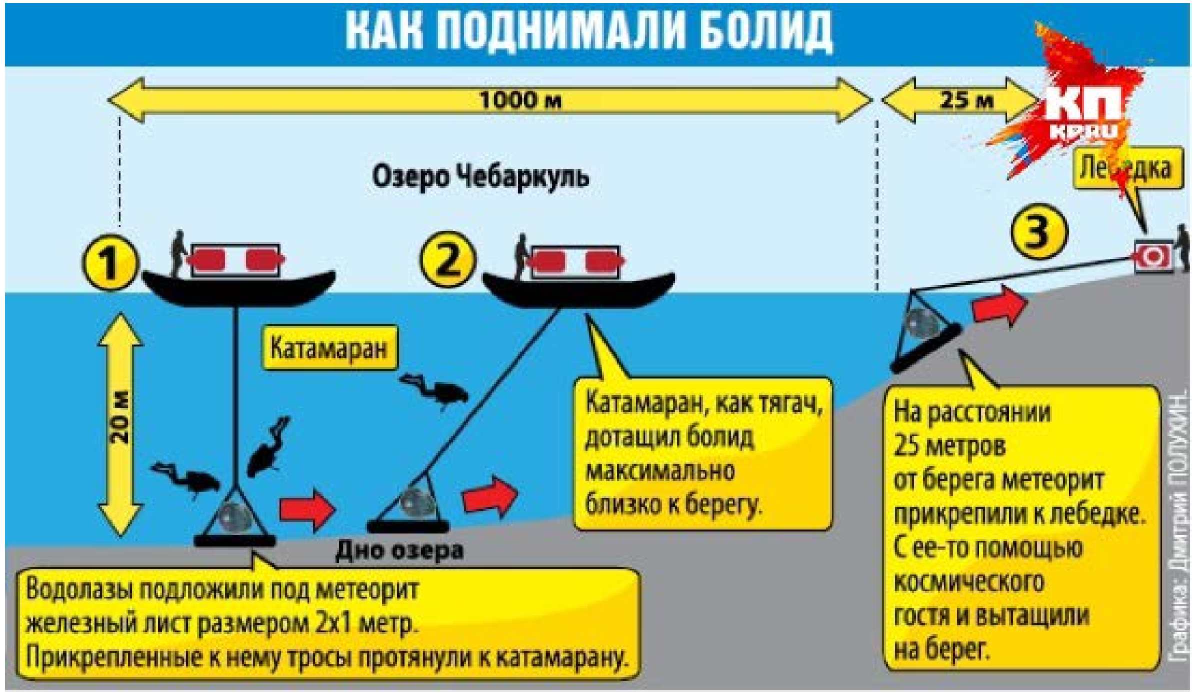

Почему не было цунами?

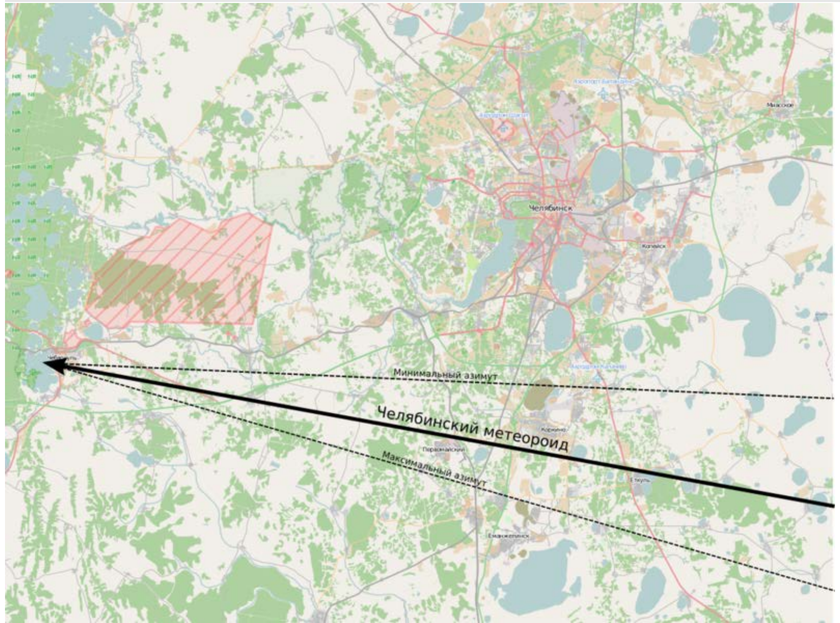

Вес
500 кг

Диаметр
20 м

Meteotsunamis

Storm Surge:
Duration > 12 hours, generated by wind + pressure systems either locally or remotely. Rate of change of water level small. Weak currents

Meteotsunami:
Duration < 6 hours, generated by local pressure systems. Rapid change in water level. Strong currents

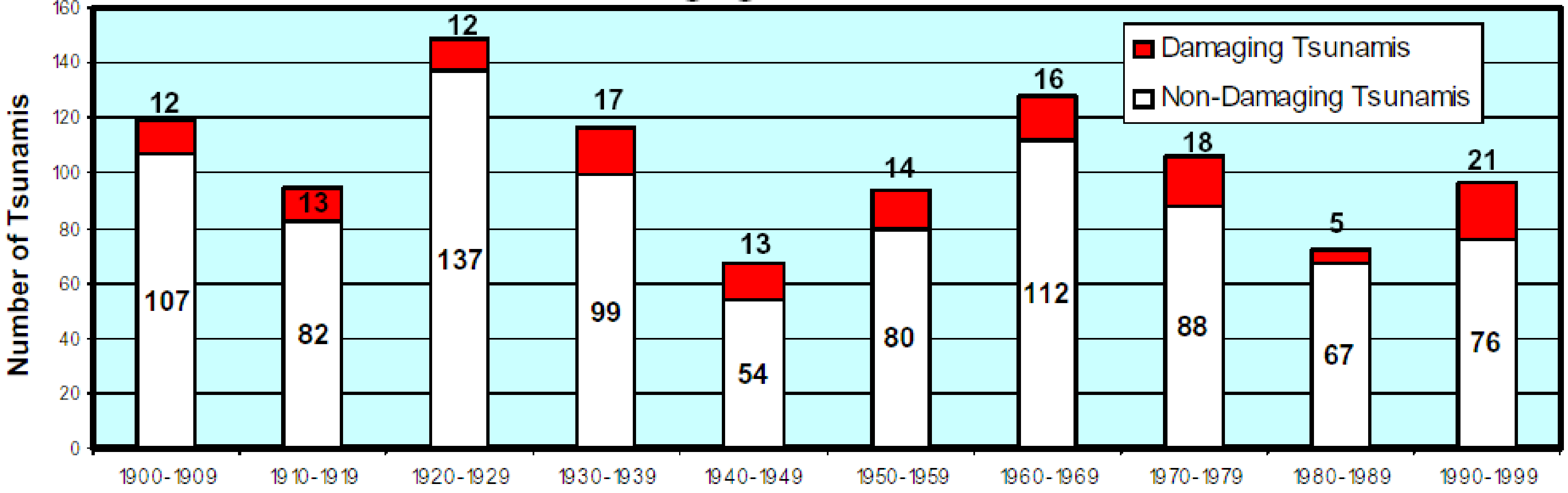

Tsunami statistics for 20th century (NGDC)

Tsunami <u>was</u> the number five killer

(after earthquakes, floods, typhoons and volcanic eruptions)

Now is the First Killer

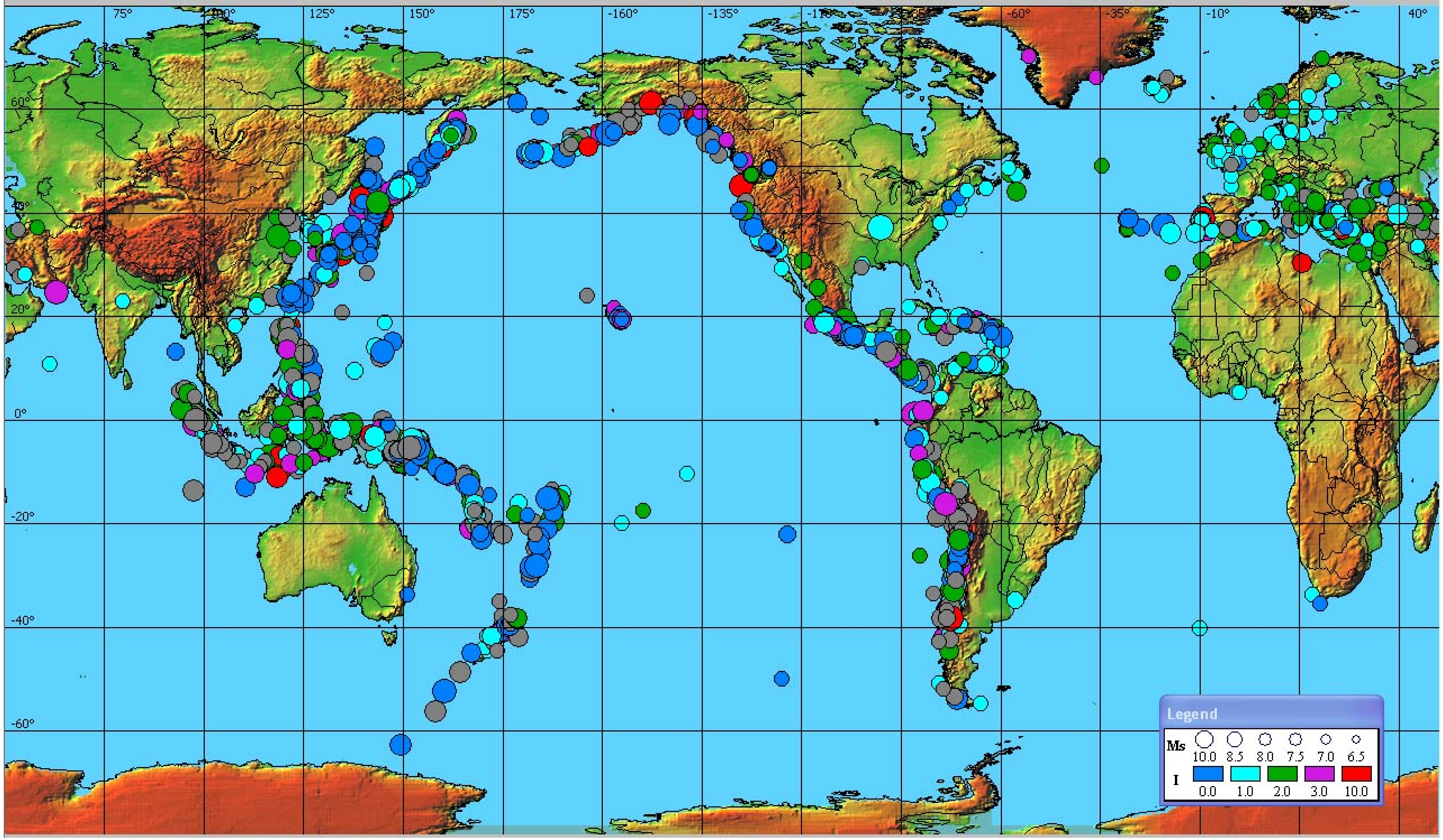

Geographical distribution of tsunamis in the World Ocean

The size of circles is proportional to the earthquake magnitude, density of gray tone – to the tsunami intensity

Gusiakov, 2005

Origin of earthquakes and tsunamis

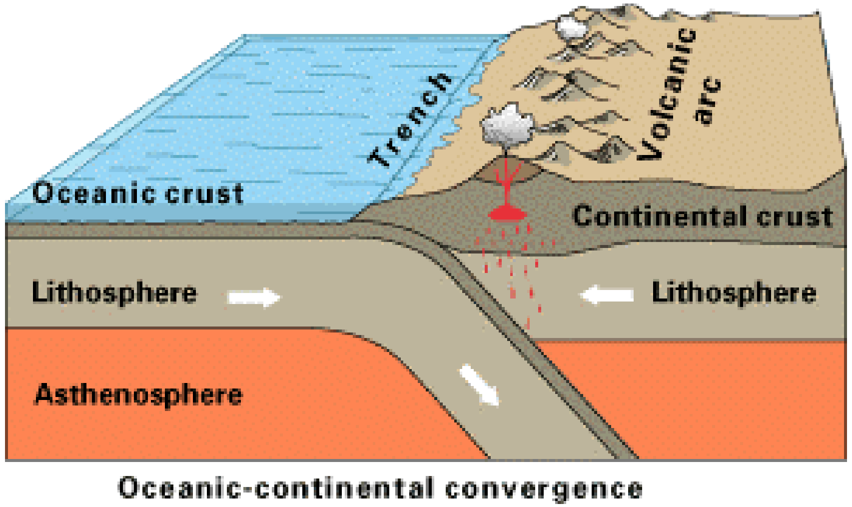

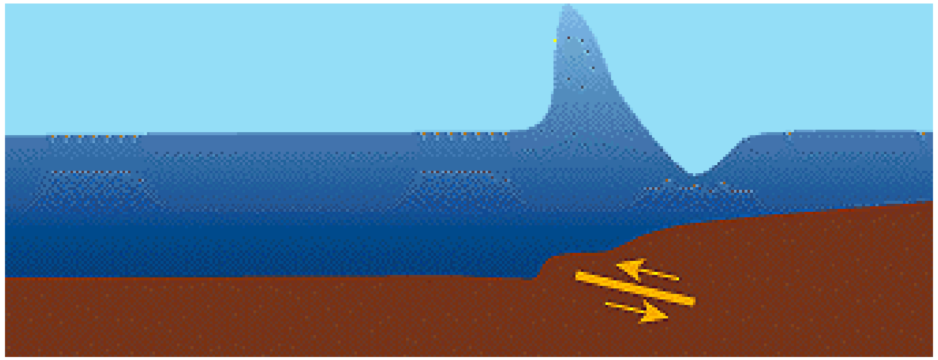

Earthquakes are commonly associated with the ground shaking that is a result of elastic waves travelling through the solid earth. However, near the source of submarine earthquakes, the seafloor is "permanently" uplifted and down-dropped, pushing the entire water column up and down. The potential energy that results from pushing water above mean sea level is then transferred to the horizontal propagation of the tsunami waves (kinetic energy).

Richter magnitude for earthquakes

Logarithm of explosion energy

M = 6 ⟷ 1 atomic bomb

M < 2 – micro-earthquakes

M = 4.5 or greater - several thousand such shocks annually - strong enough to be recorded all over the world

M = 8 – great earthquakes: one event occurs each year

M = 9-10 – limit of “margin of safety” of Earth

Propagation speed of tsunami wave

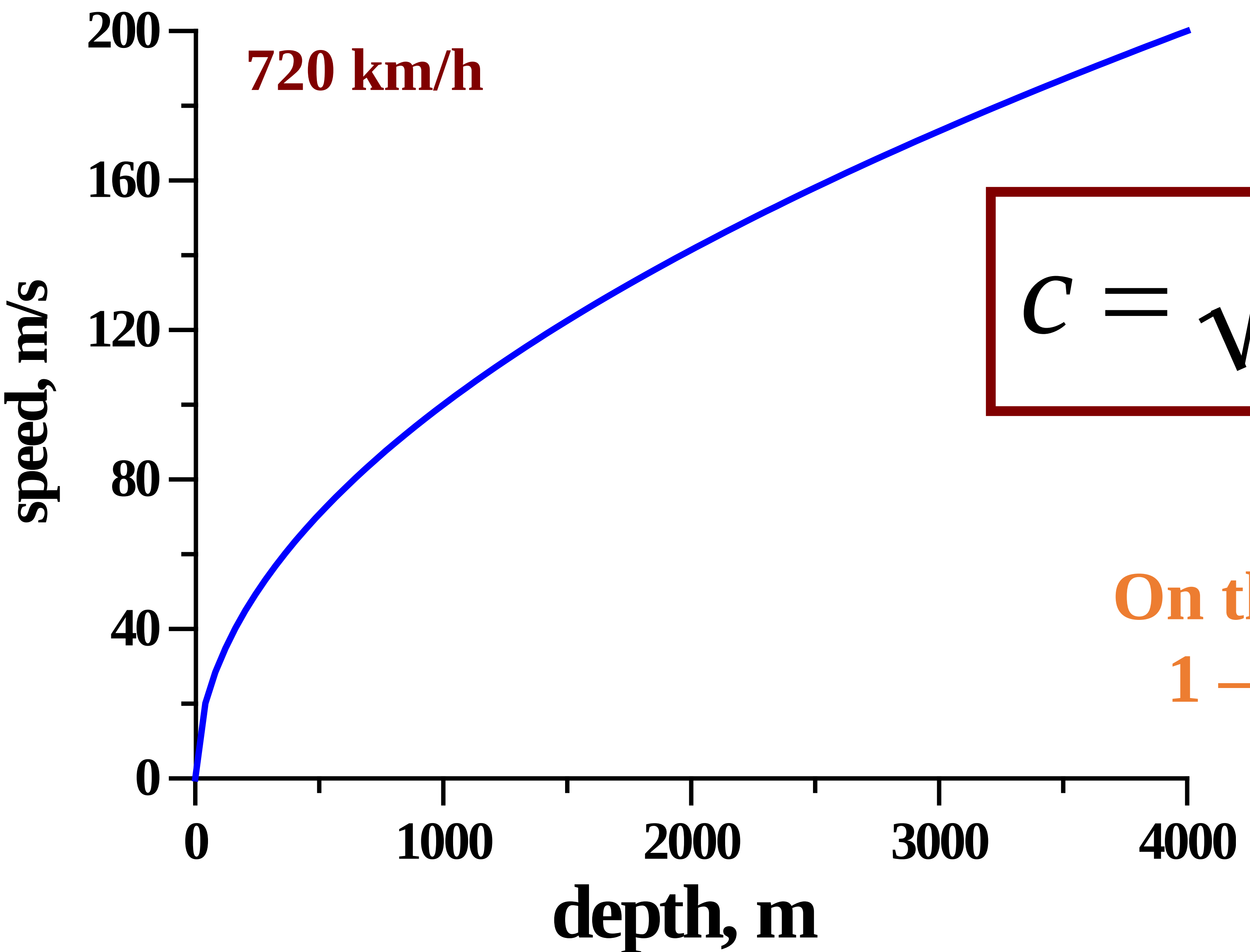

$$c = \sqrt{gh}$$

On the coast
1 – 5 m/s

Ray Tracing Method

30 angle sec Sandwell bathymetry

$$\frac{d\theta}{dt} = \frac{\cos\zeta}{nR} \qquad \frac{d\varphi}{dt} = \frac{\sin\zeta}{R\sin\theta}$$

$$\frac{d\zeta}{dt} = -\frac{\sin\zeta}{n^2R}\frac{\partial n}{\partial\theta} + \frac{\cos\zeta}{n^2R\sin\theta}\frac{\partial n}{\partial\varphi} - \frac{\sin\zeta\cot\theta}{nR}$$

$$n = 1/\sqrt{gh}$$

R, earth radius

θ and φ are latitude and longitude of the ray

ζ is the ray direction measured counter-clockwise

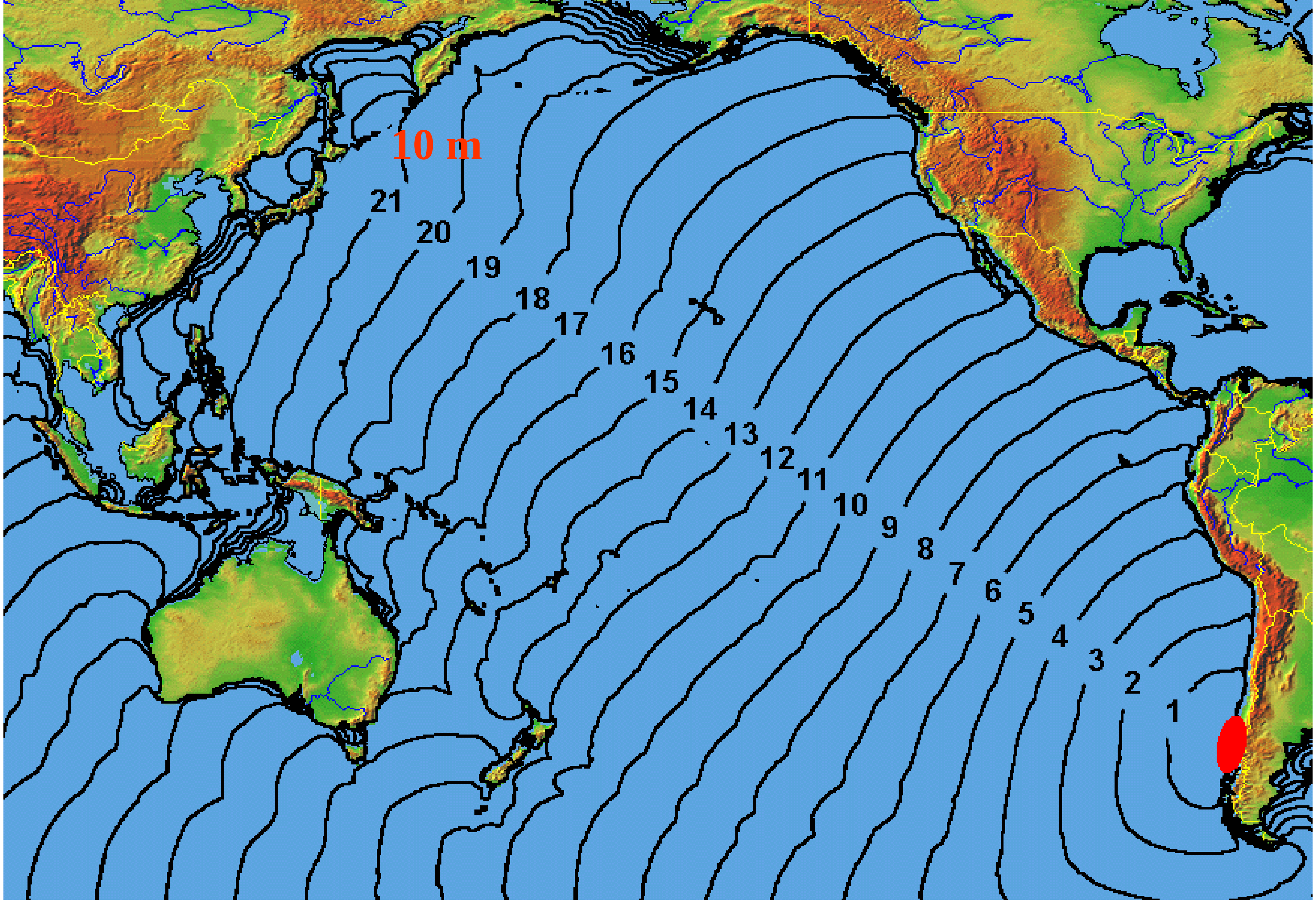

Chile, 22 May 1960

1755 Lisbon Tsunami

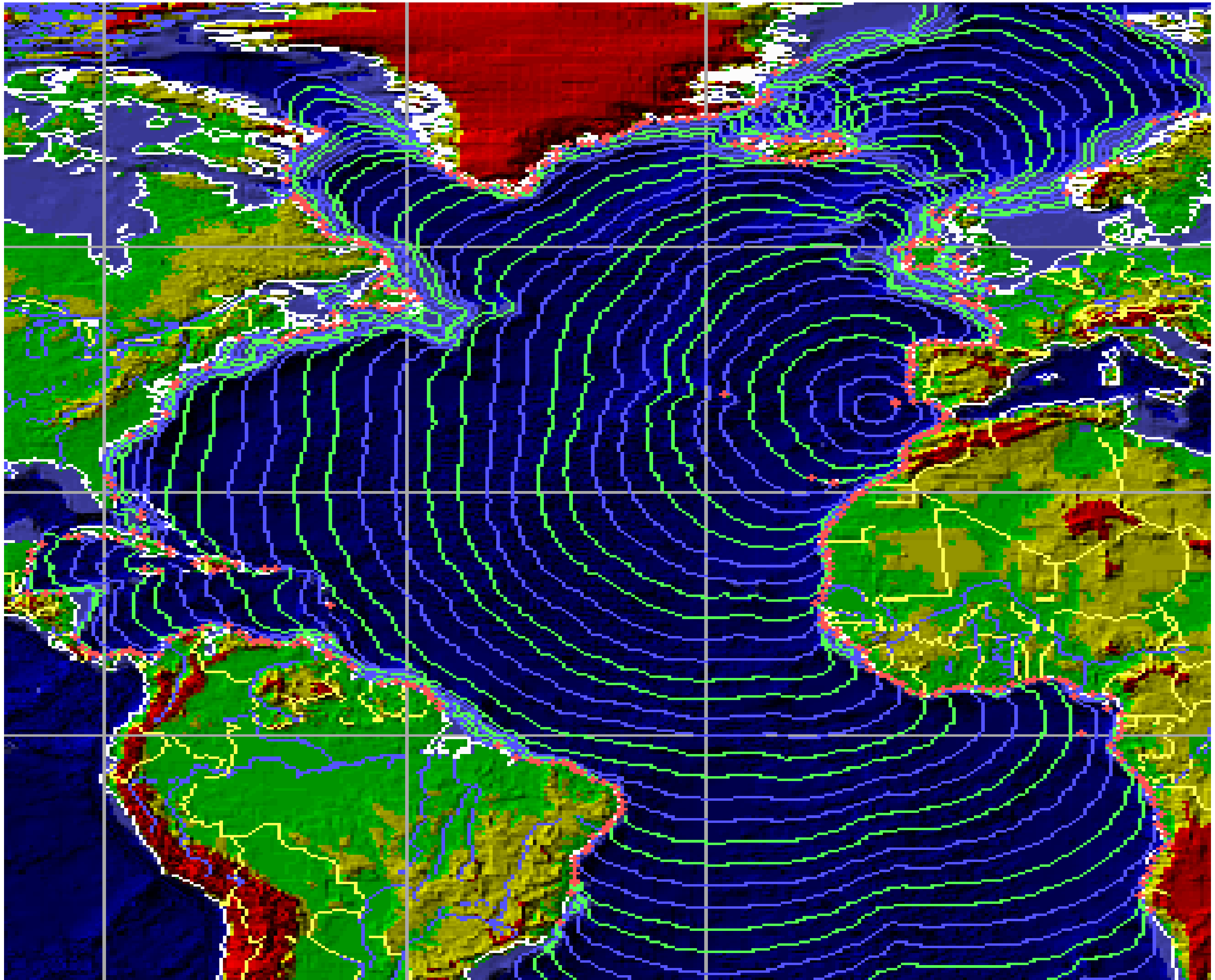

6-7 hours to
Lesser Antilles
4-7 m

"Piston" Model

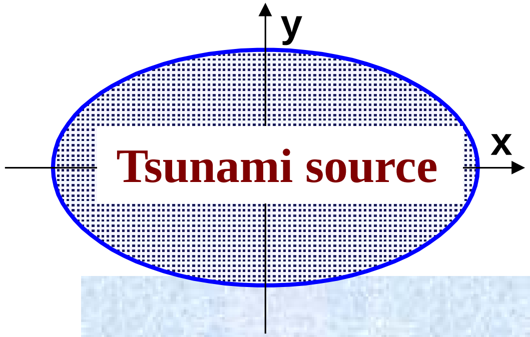

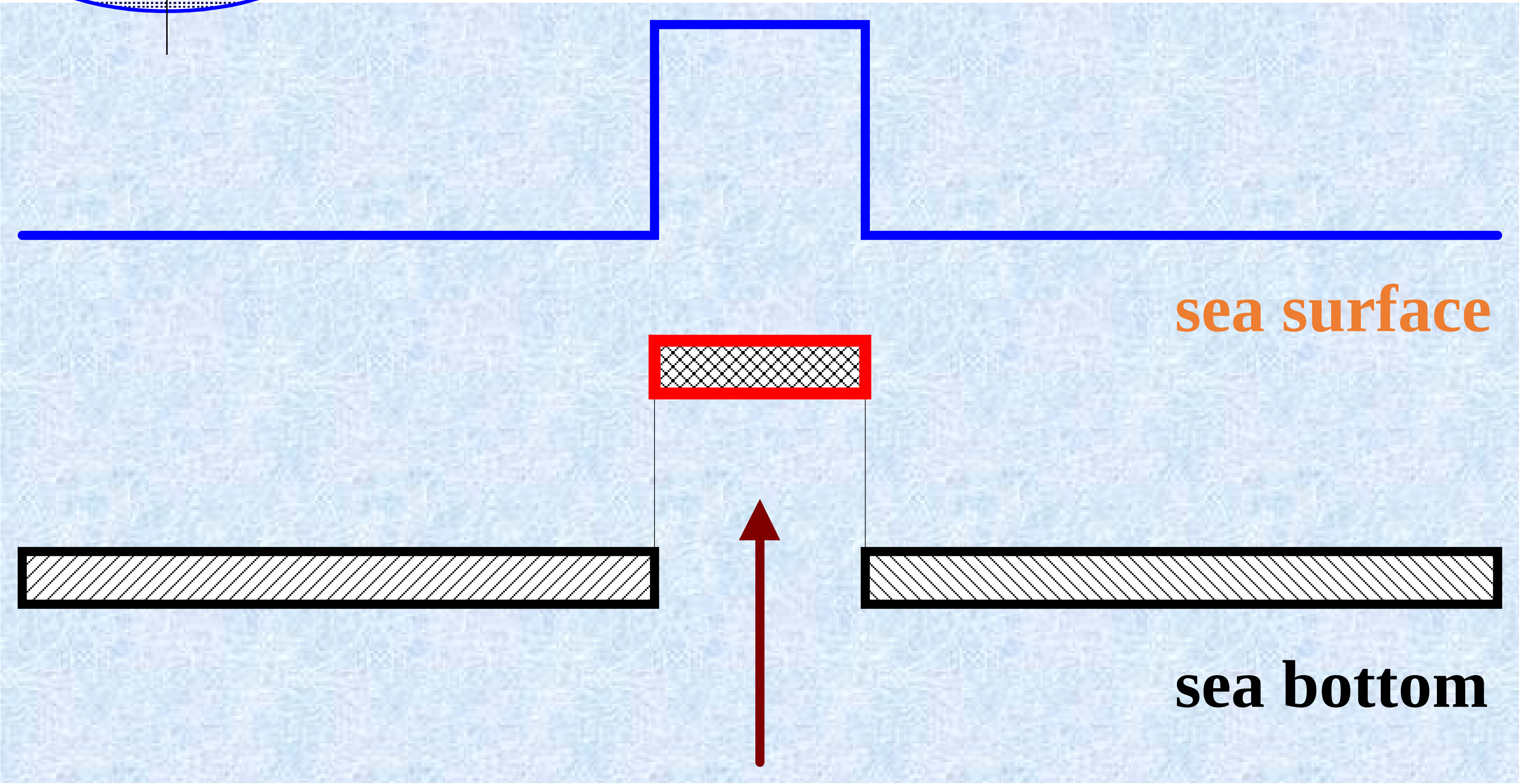

Dimensions – function of earthquake parameters

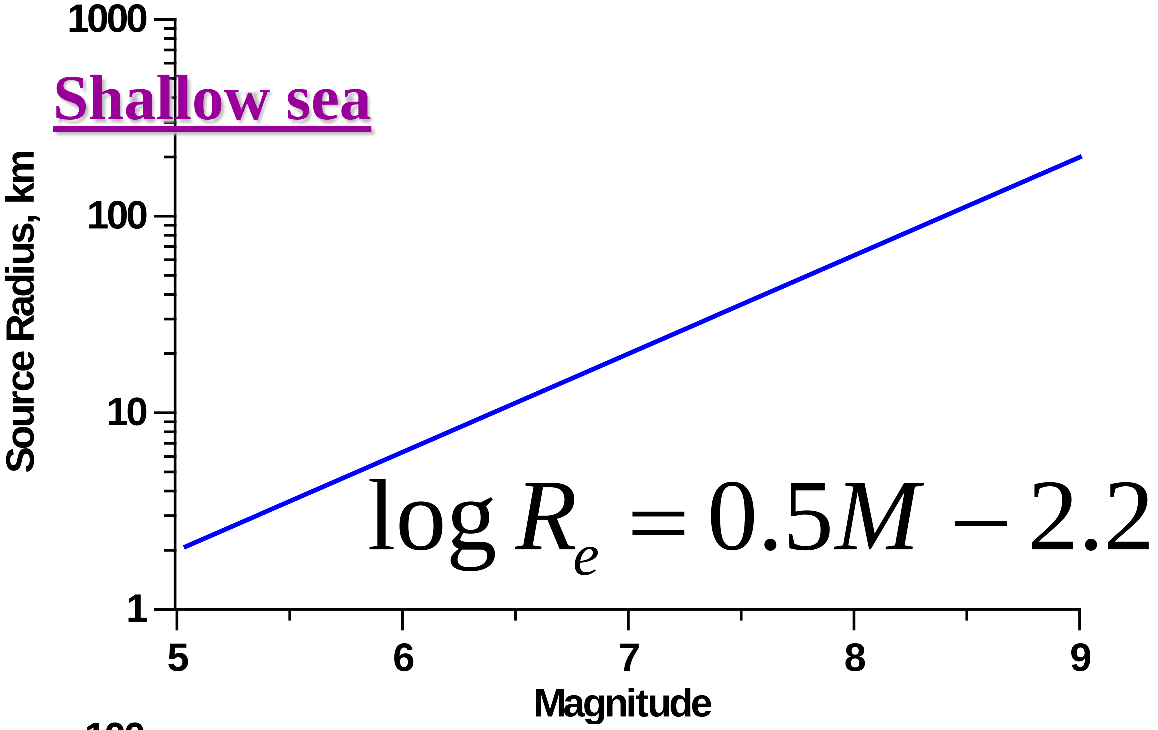

“Seismic” tsunami source

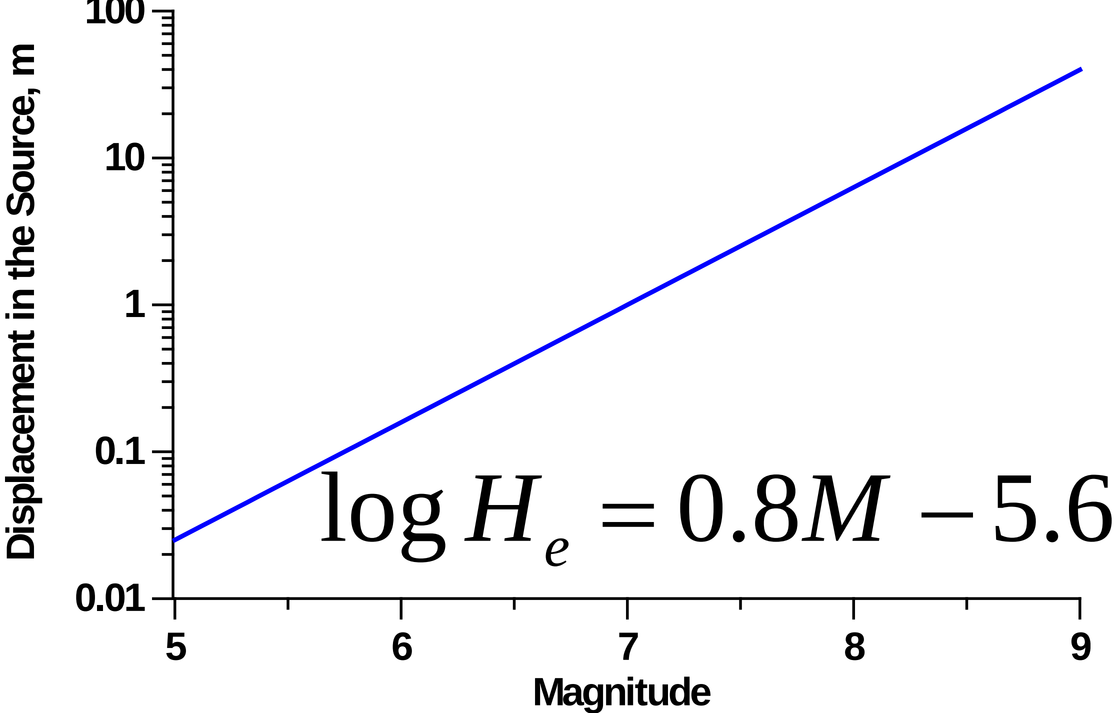

M is the earthquake magnitude

M = 6 is equiv. of 1 atomic bomb

Bulletin of the Seismological Society of America, Vol. 75, No. 4, pp. 1135–1154, August 1985

SURFACE DEFORMATION DUE TO SHEAR AND TENSILE FAULTS IN A HALF-SPACE

BY YOSHIMITSU OKADA*

ABSTRACT

A complete suite of closed analytical expressions is presented for the surface displacements, strains, and tilts due to inclined shear and tensile faults in a half-space for both point and finite rectangular sources. These expressions are particularly compact and free from field singular points which are inherent in the previously stated expressions of certain cases. The expressions derived here represent powerful tools not only for the analysis of static field changes associated with earthquake occurrence but also for the modeling of deformation fields arising from fluid-driven crack sources.

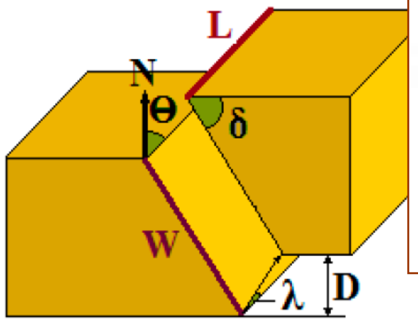

Steketee (1958) showed that the displacement field $u_i(x_1, x_2, x_3)$ due to a dislocation $\Delta u_j(\xi_1, \xi_2, \xi_3)$ across a surface Σ in an isotropic medium is given by

$$u_i = \frac{1}{F} \int \int_{\Sigma} \Delta u_j \left[\lambda \delta_{jk} \frac{\partial u_i^n}{\partial \xi_n} + \mu \left(\frac{\partial u_i^j}{\partial \xi_k} + \frac{\partial u_i^k}{\partial \xi_j} \right) \right] \nu_k \, d\Sigma \qquad (1)$$

ДОКЛАДЫ АКАДЕМИИ НАУК, 2019, том 487, № 4, с. 370–375

МЕХАНИКА

УДК 532

ПРОСТЫЕ РЕШЕНИЯ ЗАДАЧИ О ВОЛНАХ НА ПОВЕРХНОСТИ ЖИДКОСТИ В РАМКАХ ЛИНЕЙНОЙ ГИДРОУПРУГОЙ МОДЕЛИ

С. Ю. Доброхотов[1,2], Х. Х. Ильясов[1,*], С. Я. Секерж-Зенькович[1], О. Л. Толстова[2,3,]**

Представлено академиком РАН Д.М. Климовым 13.02.2019 г.

Поступило 20.02.2019 г.

Рассмотрена задача о возбуждении волн на поверхности слоя воды, расположенного на упругом основании. Предполагается, что источник возбуждения располагается внутри упругого полупространства. Используется подход Г.С. Подъяпольского, основанный на изучении решений совместной линейной системы уравнений теории упругости в полупространстве и теории волн в жидкости, связанных на границе раздела соответствующими граничными условиями. На основе полученного ранее упрощённого дисперсионного соотношения для водяной моды, учитывающего влияние упругого основания, выведена простая интегральная формула, связывающая начальное возмущение специального вида в упругом полупространстве и амплитуду волны на поверхности воды, порождённой этим источником. Проведено сравнение получаемых решений с решениями, основанными на известной поршневой модели возбуждения длинных волн.

26 December 2004 Earthquake

Vertical Seafloor Displacement

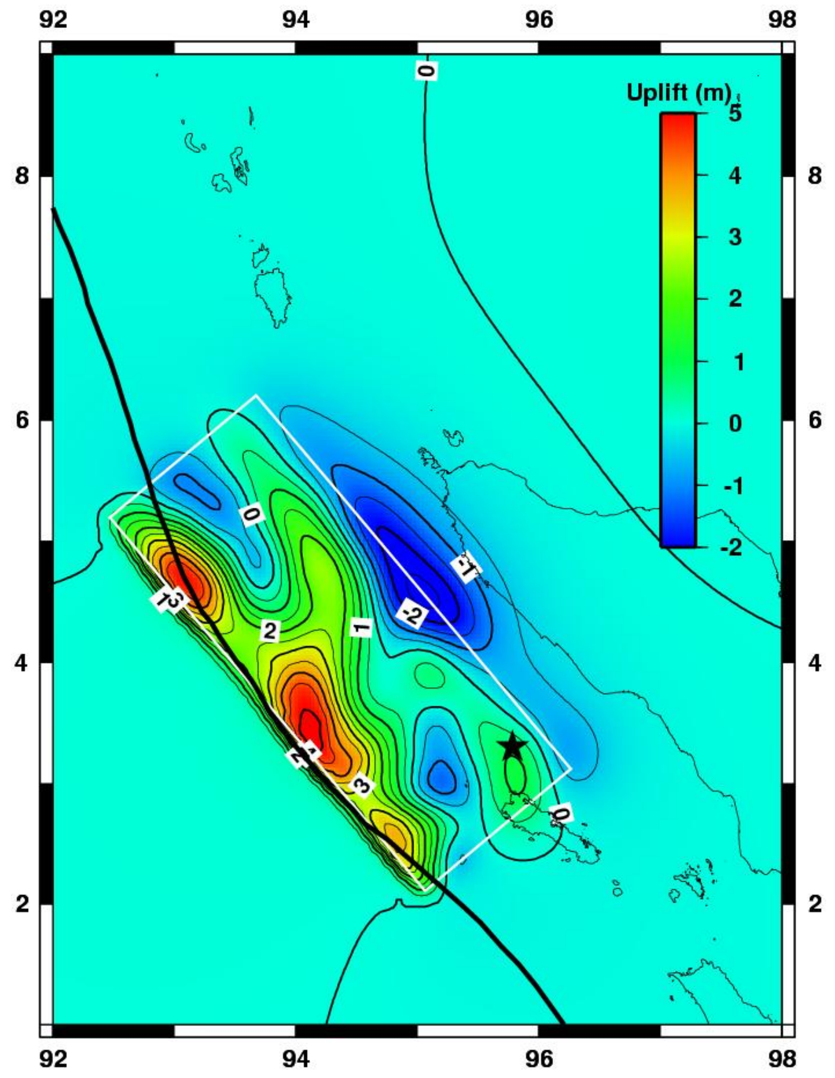

Horizontal Seafloor Displacement

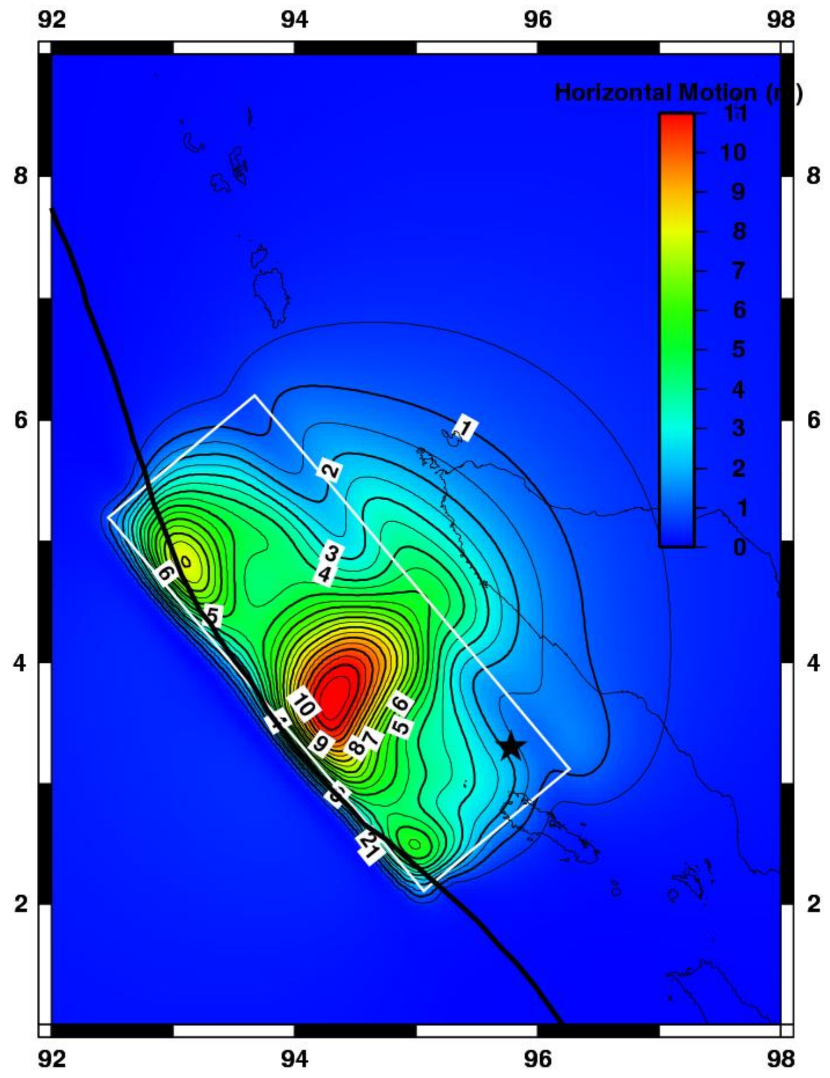

Practice of Tsunami Computing

$$\frac{\partial M}{\partial t} + \frac{gD}{R\cos\theta}\frac{\partial \eta}{\partial \varphi} = fN$$

$$\frac{\partial N}{\partial t} + \frac{gD}{R}\frac{\partial \eta}{\partial \theta} = -fM$$

$$\frac{\partial \eta}{\partial t} + \frac{1}{R\cos\theta}\left[\frac{\partial M}{\partial \varphi} + \frac{\partial}{\partial \theta}\left(N\cos\theta\right)\right] = 0$$

Open Sea

$$\frac{\partial M}{\partial t} + \frac{\partial}{\partial x}\left(\frac{M^2}{D}\right) + \frac{\partial}{\partial y}\left(\frac{MN}{D}\right) + gD\frac{\partial \eta}{\partial x} + \frac{k}{2D^2}M\sqrt{M^2+N^2} = 0$$

$$\frac{\partial N}{\partial t} + \frac{\partial}{\partial x}\left(\frac{MN}{D}\right) + \frac{\partial}{\partial y}\left(\frac{N^2}{D}\right) + gD\frac{\partial \eta}{\partial y} + \frac{k}{2D^2}N\sqrt{M^2+N^2} = 0$$

$$\frac{\partial \eta}{\partial t} + \frac{\partial M}{\partial x} + \frac{\partial N}{\partial y} = 0$$

Coastal Zone

Shallow Water Models

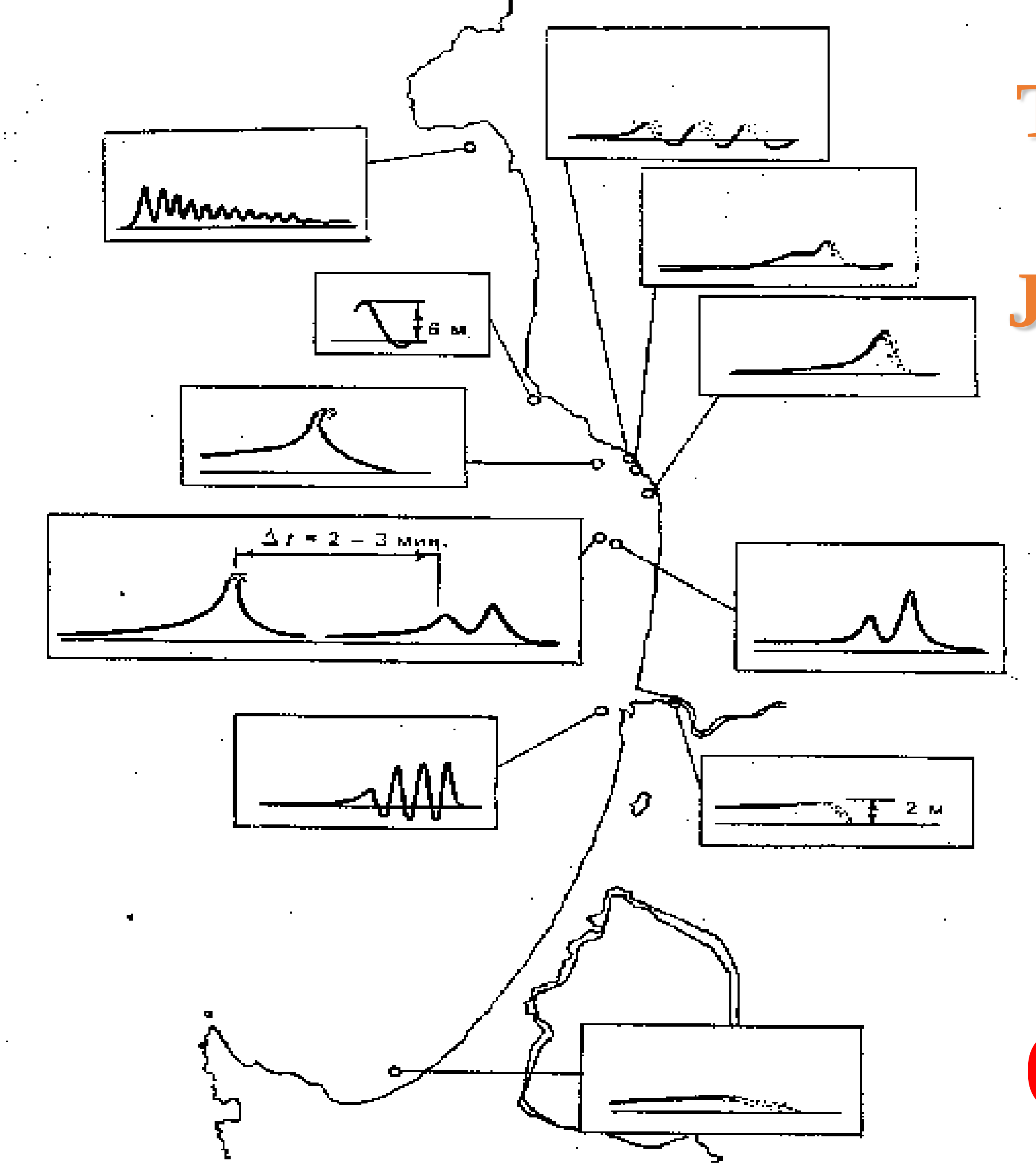

Tsunami wave Shapes at Japanese Coast

26 May 1983 Japan Sea (Shuto, 1983)

Thailand, 26/12/2004

Accuracy Comparison

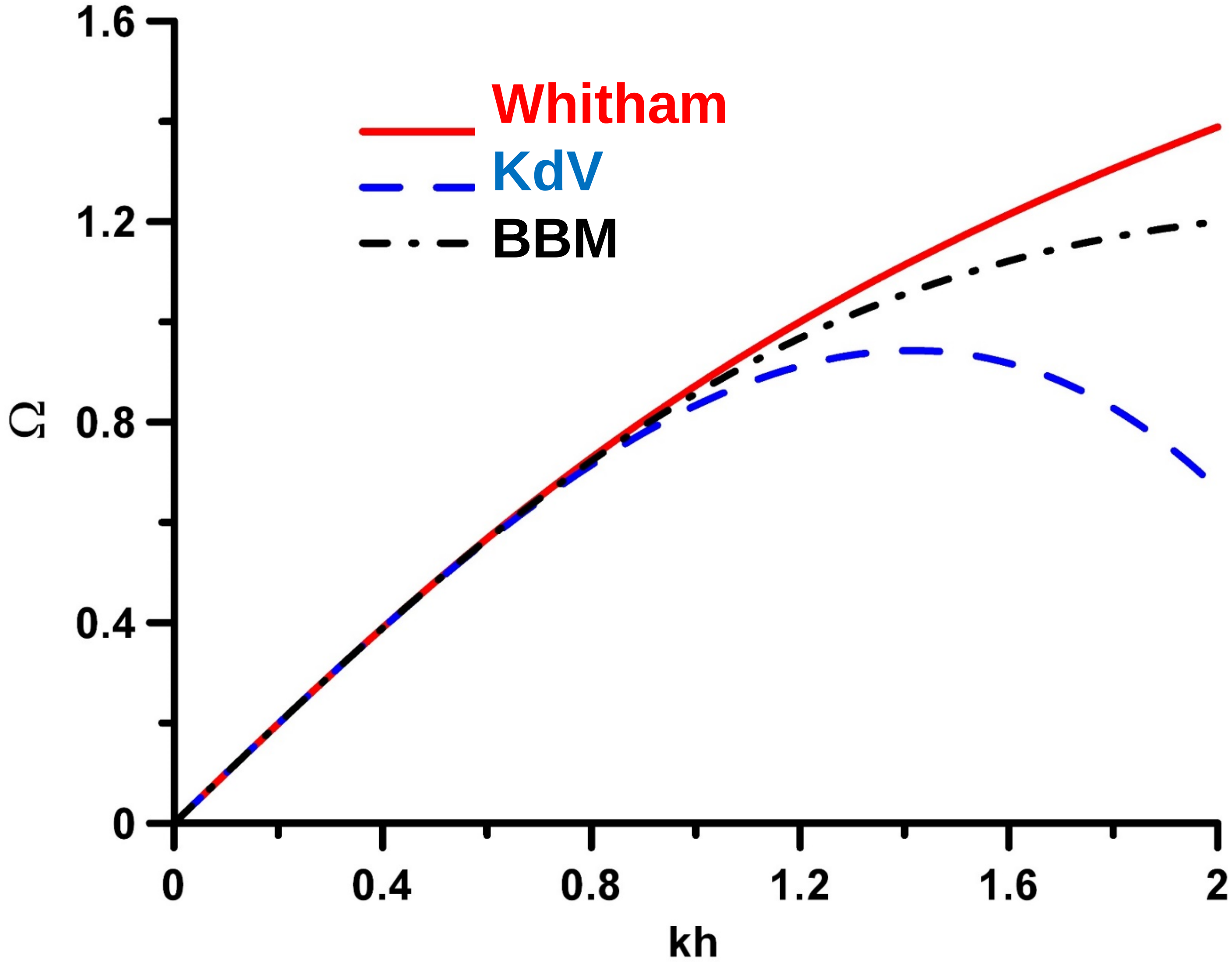

Exact - Whitham

$$\omega(k) = \sqrt{gk\tanh(kh)}$$

Korteweg-de Vries

$$\omega = c_0 k\left(1 - \frac{k^2h^2}{6}\right)$$

Benjamin-Bona-Maxoni

$$\omega = \frac{c_0 k}{1 + \frac{k^2h^2}{6}}$$

Proc. R. Soc. Lond. A (2003) **459**, 1075–1104
10.1098/rspa.2002.1067

THE ROYAL SOCIETY

Boussinesq-type formulations for fully nonlinear and extremely dispersive water waves: derivation and analysis

By P. A. Madsen[1], H. B. Bingham[1] and H. A. Schäffer[2]

$$\frac{\omega^2}{ghk^2} = \frac{1 + \frac{1}{6}k^2h^2 + \frac{1}{120}k^4h^4}{1 + \frac{1}{2}k^2h^2 + \frac{1}{24}k^4h^4},$$

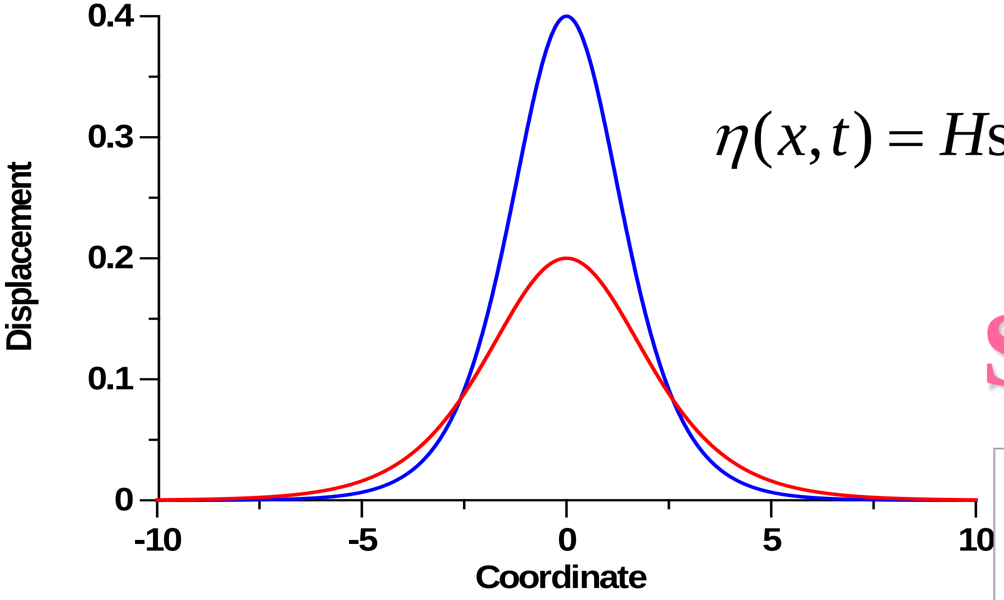

$$\eta(x,t) = H\mathrm{sech}^2\left[\sqrt{\frac{3H}{4h}}\frac{x-\sqrt{gh}(1+H/2h)t}{h}\right]$$

Soliton Length, km

H (m) height / h (m) depth	1	5	10	20
50	0.72	0.32	0.23	0.16
100	2	0.91	0.64	0.46
500	22.8	10.2	7.2	5.1
1000	64.4	28.8	20.4	14.4
5000	720	322	227	161

Coastal Zone, Many solitons, Ur >>1, but coast is not too far

$$\frac{\partial\eta}{\partial t} + \sqrt{gh}\left(1+\frac{3\eta}{2h}\right)\frac{\partial\eta}{\partial x} + \frac{\sqrt{gh}h^2}{6}\frac{\partial^3\eta}{\partial x^3} = 0$$

Open Sea, Big Scales of Nonlinearity and Dispersion

Journal of Dynamics and Differential Equations, Vol. 18, No. 3, July 2006 (© 2006)
DOI: 10.1007/s10884-006-9031-4

Surface Water Waves and Tsunamis

Walter Craig

JOURNAL OF GEOPHYSICAL RESEARCH, VOL. 113, C12012, doi:10.1029/2008JC004932, 2008

Click Here for Full Article

On the solitary wave paradigm for tsunamis

Per A. Madsen,[1] David R. Fuhrman,[1] and Hemming A. Schäffer[1]

Available online at www.sciencedirect.com
ScienceDirect
ELSEVIER
Fluid Dynamics Research 40 (2008) 175–211
FLUID DYNAMICS RESEARCH

Propagation of very long water waves, with vorticity, over variable depth, with applications to tsunamis

A. Constantin[a,b], R.S. Johnson[c,*]

J. Ocean Eng. Mar. Energy (2015) 1:145–156
DOI 10.1007/s40722-014-0011-1

RESEARCH ARTICLE

Changing forms and sudden smooth transitions of tsunami waves

R. H. J. Grimshaw · J. C. R. Hunt · K. W. Chow

PHILOSOPHICAL TRANSACTIONS OF THE ROYAL SOCIETY A
MATHEMATICAL, PHYSICAL & ENGINEERING SCIENCES

Seismically generated tsunamis

Diego Arcas and Harvey Segur

Phil. Trans. R. Soc. A 2012 **370**, 1505-1542
doi: 10.1098/rsta.2011.0457

JOURNAL OF GEOPHYSICAL RESEARCH, VOL. 113, C05008, doi:10.1029/2007JC004343, 2008

Formation of undular bores and solitary waves in the Strait of Malacca caused by the 26 December 2004 Indian Ocean tsunami

J. Grue,[1] E. N. Pelinovsky,[2] D. Fructus,[1] T. Talipova,[2] and C. Kharif[3]

Received 16 May 2007; revised 17 October 2007; accepted 28 December 2007; published 7 May 2008.

[1] Deformation of the Indian Ocean tsunami moving into the shallow Strait of Malacca and formation of undular bores and solitary waves in the strait are simulated in a model study using the fully nonlinear dispersive method (FNDM) and the Korteweg-deVries (KdV) equation. Two different versions of the incoming wave are studied where the waveshape is the same but the amplitude is varied: full amplitude and half amplitude. While moving across three shallow bottom ridges, the back face of the leading depression wave steepens until the wave slope reaches a level of 0.0036–0.0038, when short waves form, resembling an undular bore for both full and half amplitude. The group of short waves has very small amplitude in the beginning, behaving like a linear dispersive wave train, the front moving with the shallow water speed and the tail moving with the linear group velocity. Energy transfer from long to short modes is similar for the two input waves, indicating the fundamental role of the bottom topography to the formation of short waves. The dominant period becomes about 20 s in both cases. The train of short waves, emerging earlier for the larger input wave than for the smaller one, eventually develops into a sequence of rank-ordered solitary waves moving faster than the leading depression wave and resembles a fission of the mother wave. The KdV equation has limited capacity in resolving dispersion compared to FNDM.

KdV and FNDM Models

[12] Fully nonlinear dispersive methods (FNDM) for rapid computations of nonlinear wave motion in three dimensions have been developed in recent years by means of pseudospectral methods [e.g., *Bateman et al.*, 2001; *Clamond and Grue*, 2001; *Grue*, 2002; *Fructus et al.*, 2005] and highly nonlinear Boussinesq equations [e.g., *Madsen et al.*, 2002]. The highly nonlinear Boussinesq

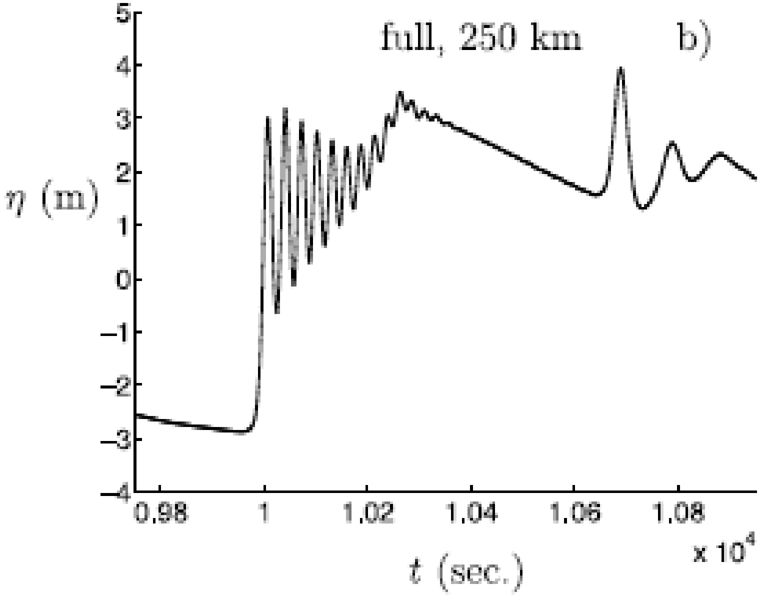
full, 250 km
b)
η (m)
t (sec.)
x 10^4

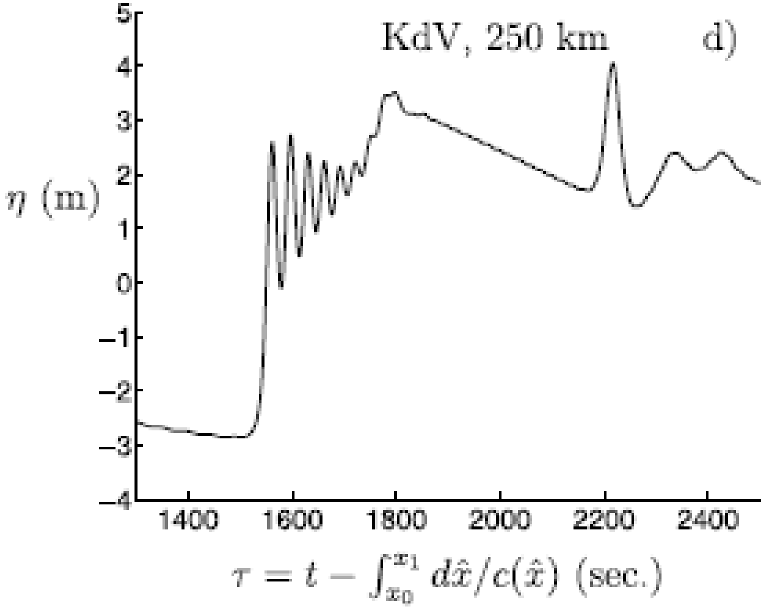
KdV, 250 km
d)
η (m)
τ = t − ∫_{x0}^{x1} dx̂/c(x̂) (sec.)

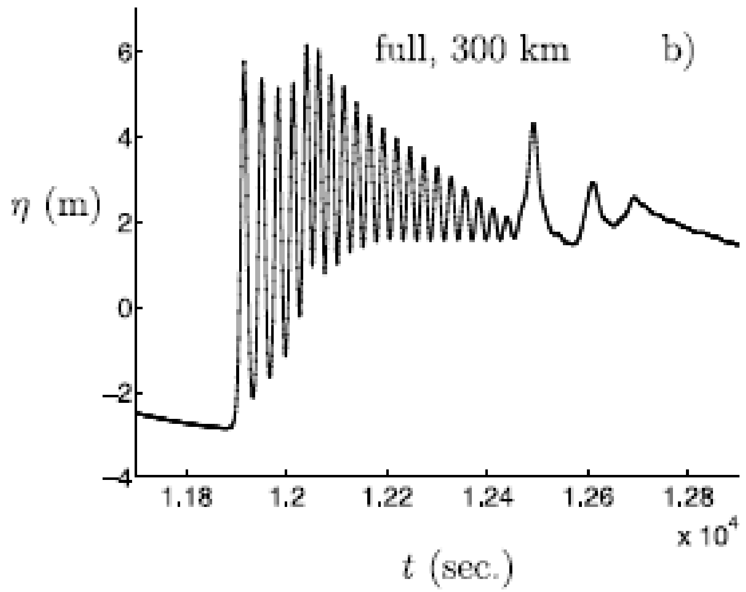
full, 300 km
b)
η (m)
t (sec.)
x 10^4

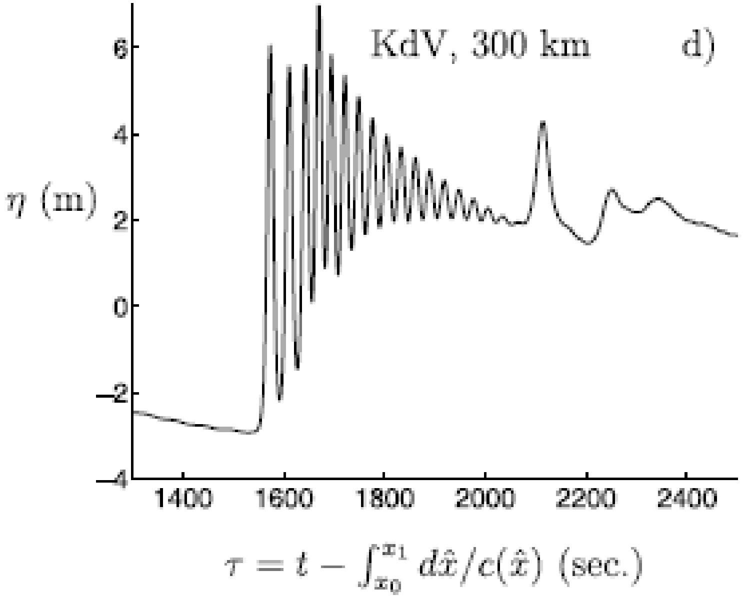
KdV, 300 km
d)
η (m)
τ = t − ∫_{x0}^{x1} dx̂/c(x̂) (sec.)

Explosive volcano eruption

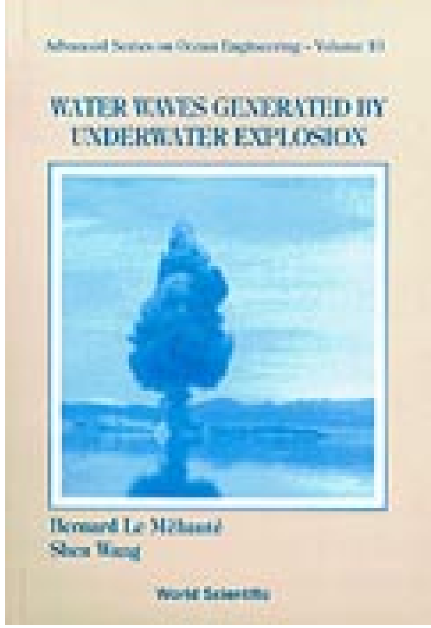

Equivalent source (*Le Mehaute*)

$$\eta_e(r) = H_e[2(r/R)^2 - 1]$$

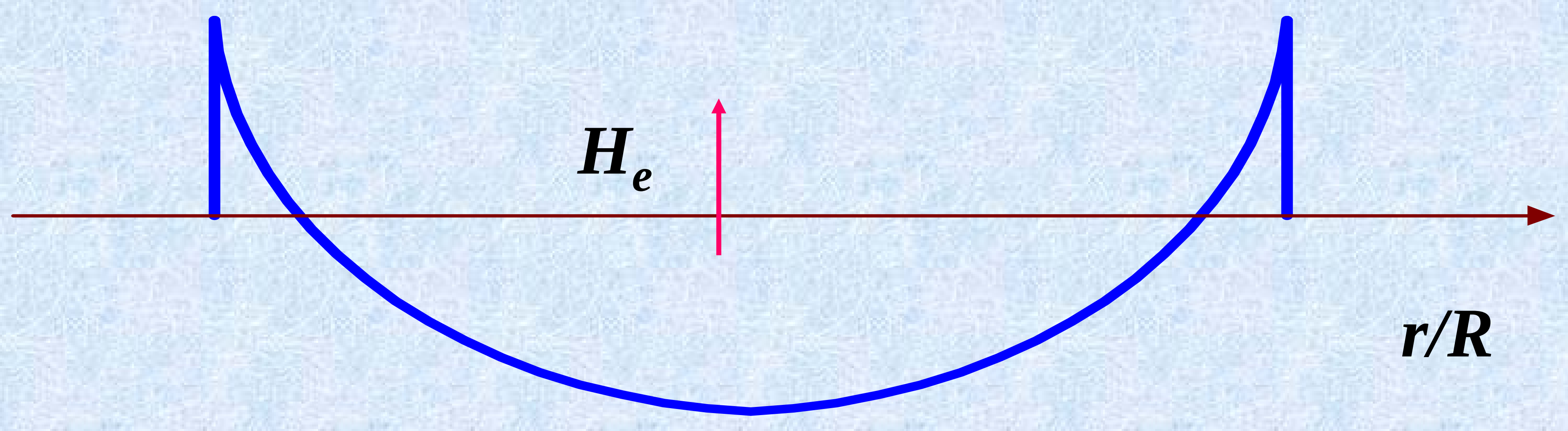

Explosive tsunamis

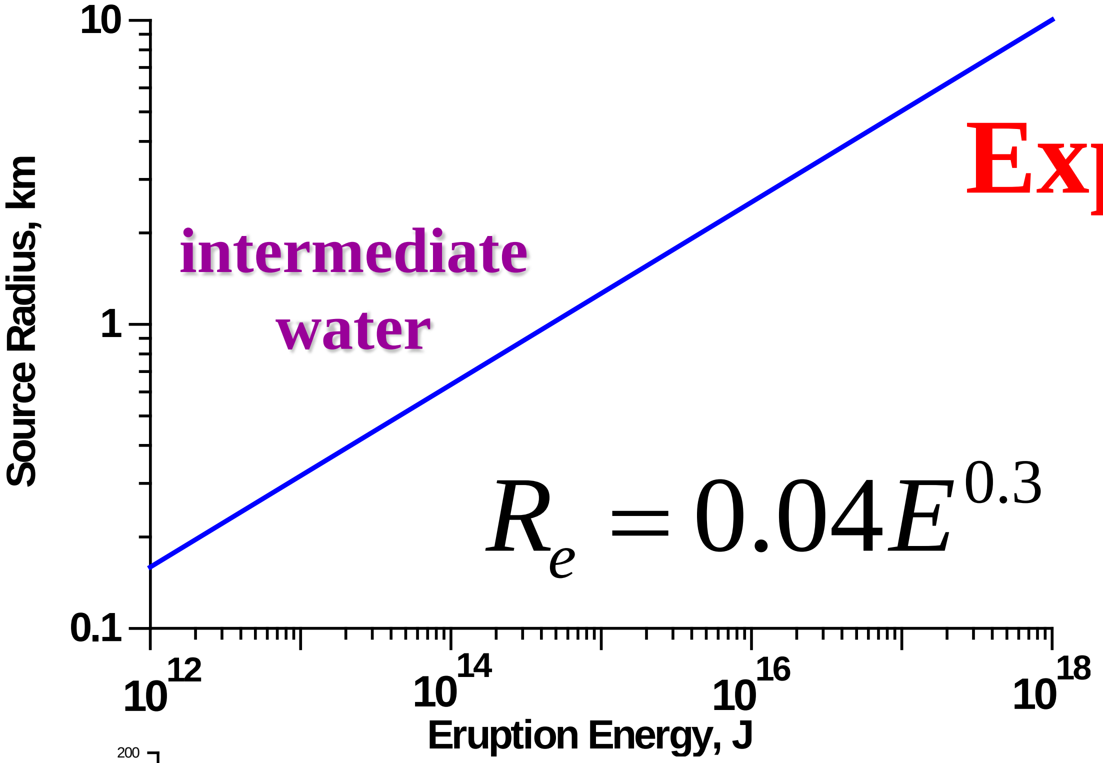

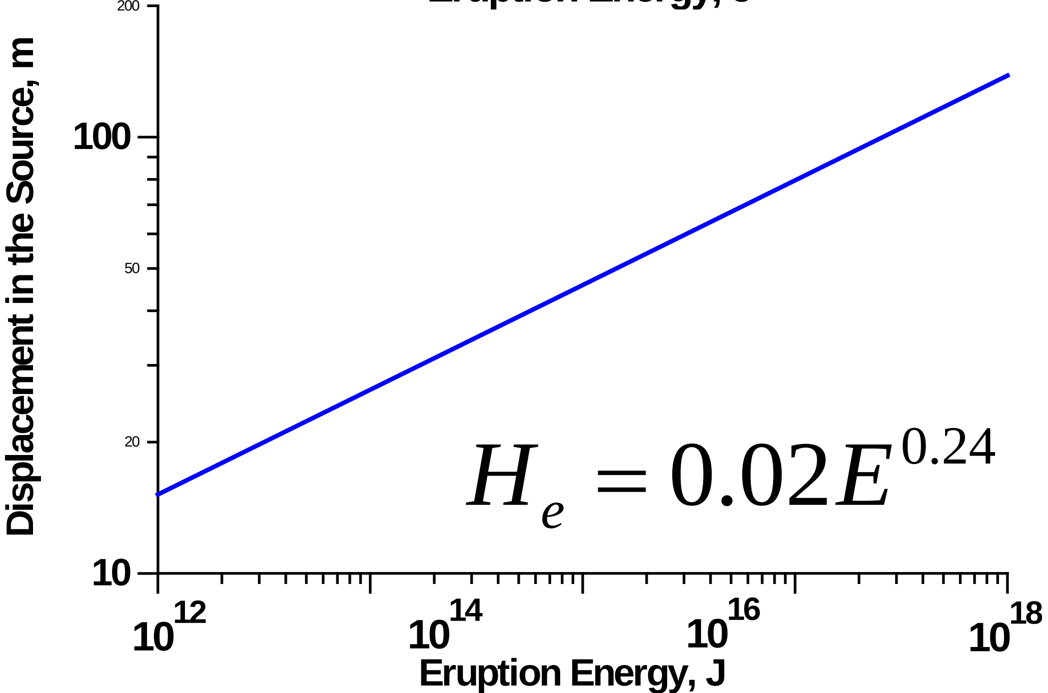

1883
Krakatau eruption
8.4×10^{17} Joules
$R_e \sim 3.5$ km
$H_e \sim 220$ m

Tsunami generated by subaquatic volcanic eruptions

PAGEOPH, 2000, v. 157, 1135-1143

January 2, 1996, Karymskoye Lake, Kamchatka, Russia

"Explosions occurred every 4 to 12 min. Six explosions were observed with an average interval of 6 min"

Nat. Hazards Earth Syst. Sci., 10, 2359–2369, 2010
www.nat-hazards-earth-syst-sci.net/10/2359/2010/
doi:10.5194/nhess-10-2359-2010

Natural Hazards and Earth System Sciences

Numerical simulation of a tsunami event during the 1996 volcanic eruption in Karymskoye lake, Kamchatka, Russia

T. Torsvik[1], R. Paris[2], I. Didenkulova[3,4], E. Pelinovsky[4], A. Belousov[5], and M. Belousova[5,6]

[1]Bergen Center for Computational Science, Uni Research, Bergen, Norway
[2]CNRS-GEOLAB, Clermont-Université, 4 rue Ledru, 63057 Clermont-Ferrand, France
[3]Laboratory of Wave Engineering, Institute of Cybernetics, Tallinn, Estonia
[4]Department of Nonlinear Geophysical Processes, Institute of Applied Physics, Nizhny Novgorod, Russia
[5]Earth Observatory of Singapore, Nanyang Technological University, Singapore
[6]Institute of Volcanology & Seismology, Petropavlovsk-Kamchatsky, Russia

Numerical code of nonlinear –dispersive shallow-water theory

COULWAVE

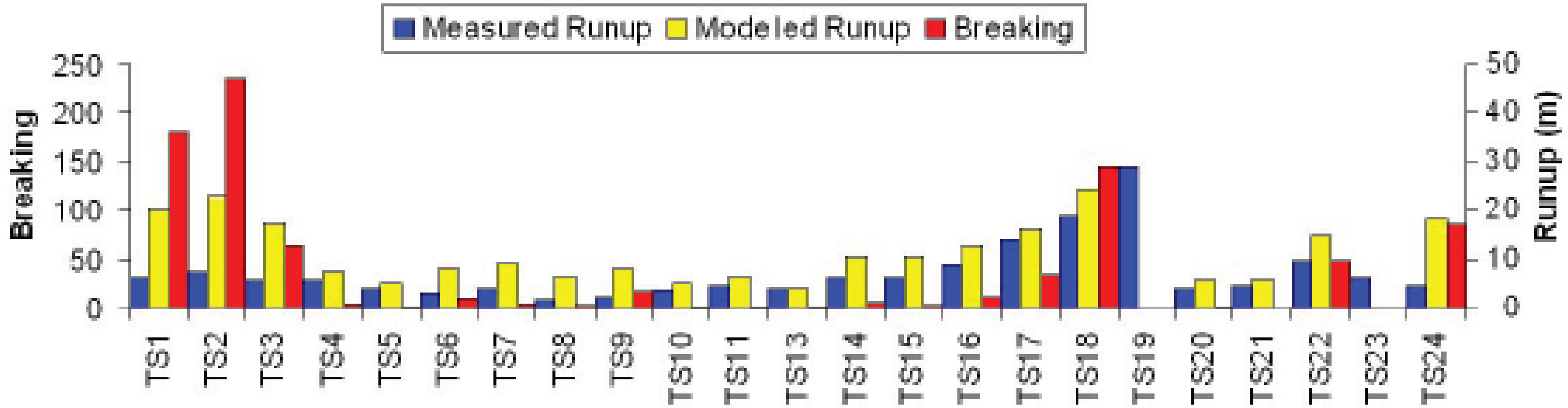

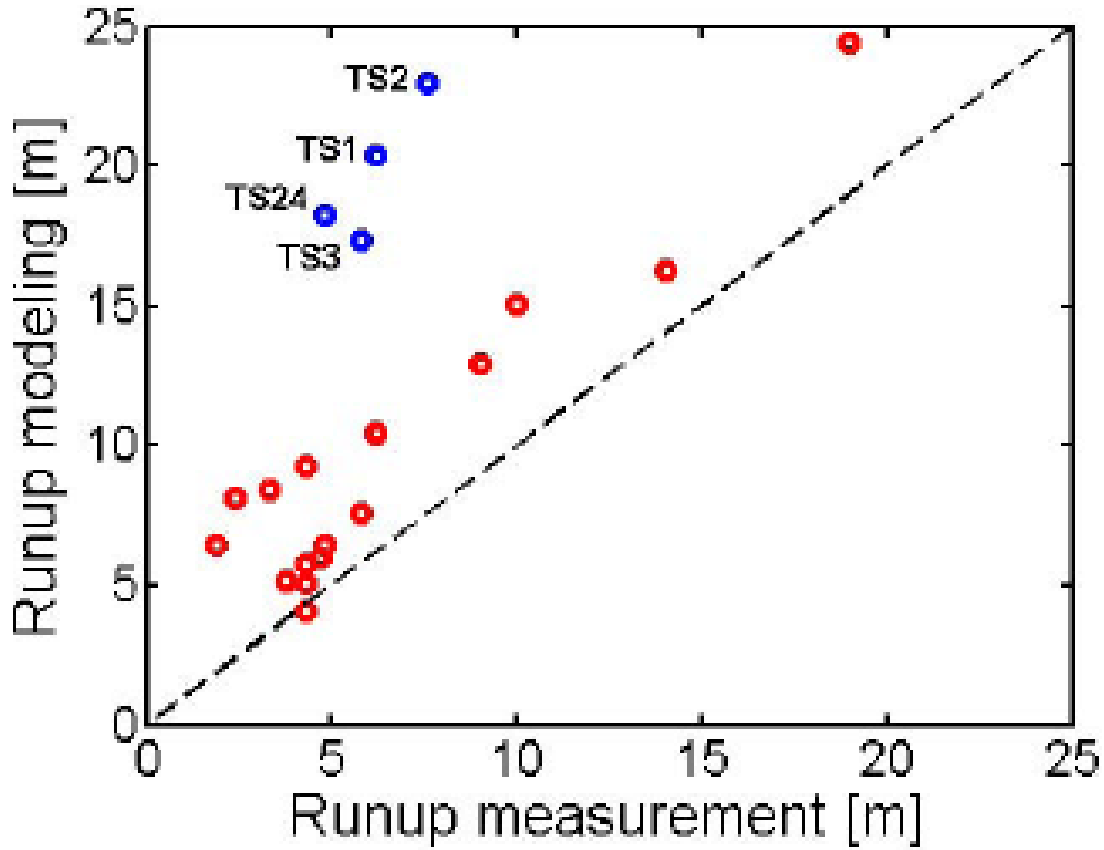

Very Good Comparison!

Navier-Stokes Equations (RANS and others)

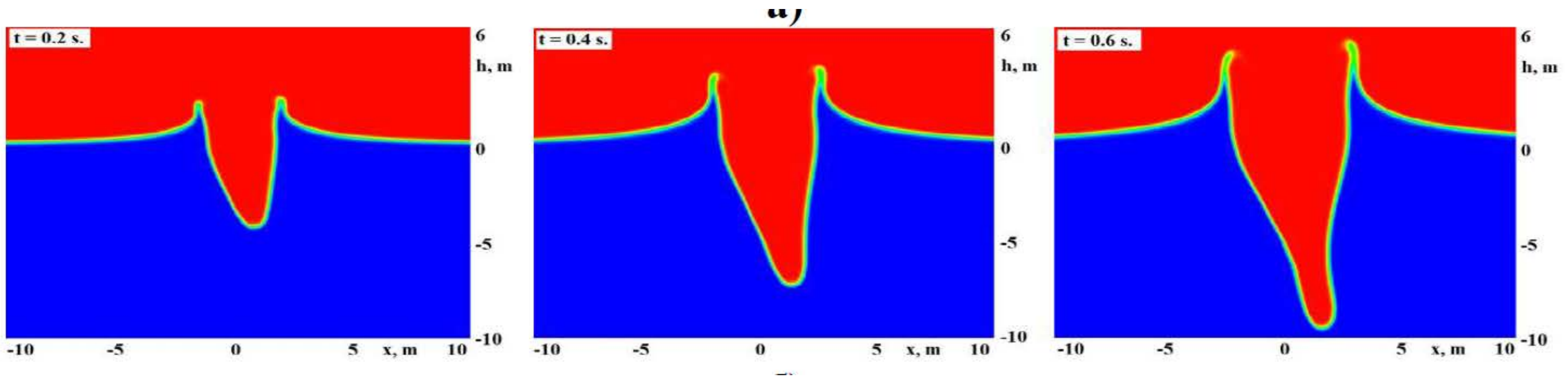

Body: diameter 1 m, angle 80 degree, velocity 30 m/s

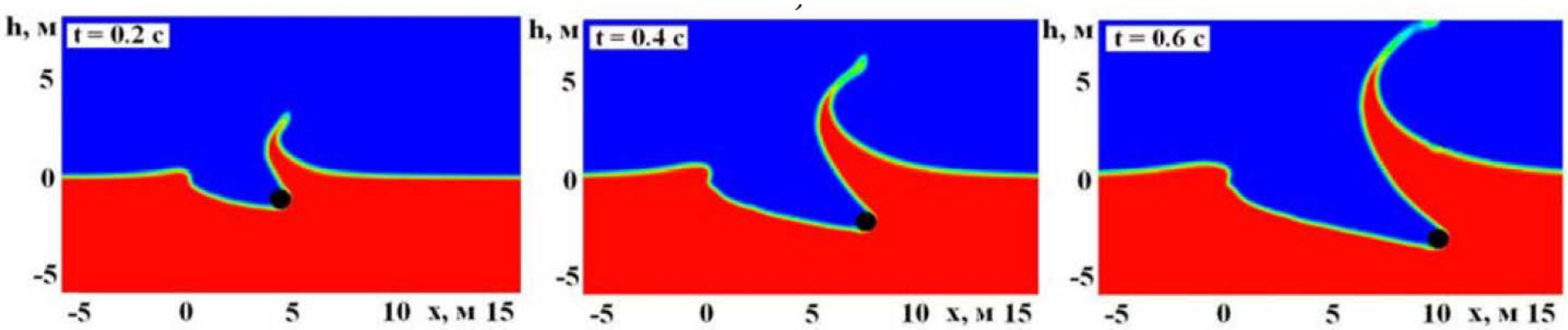

Body: diameter 1 m, angle 20 degree, velocity 30 m/s

Angle 5 degree

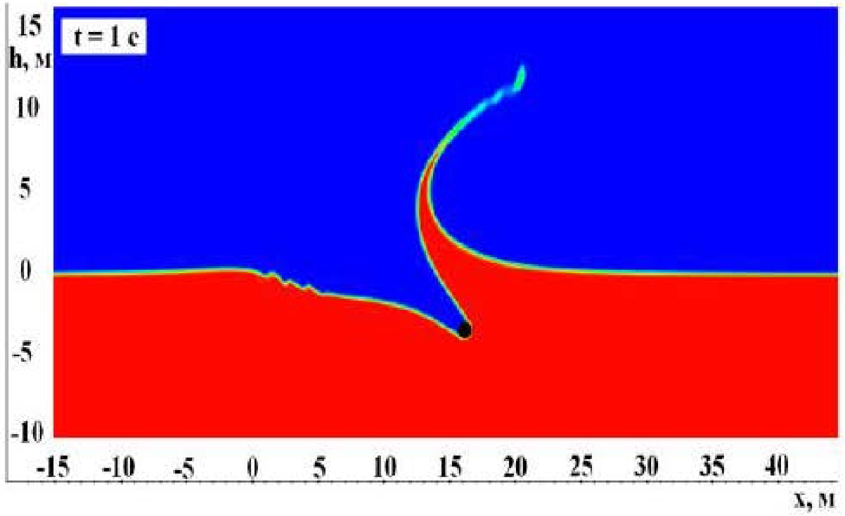

30 m/s

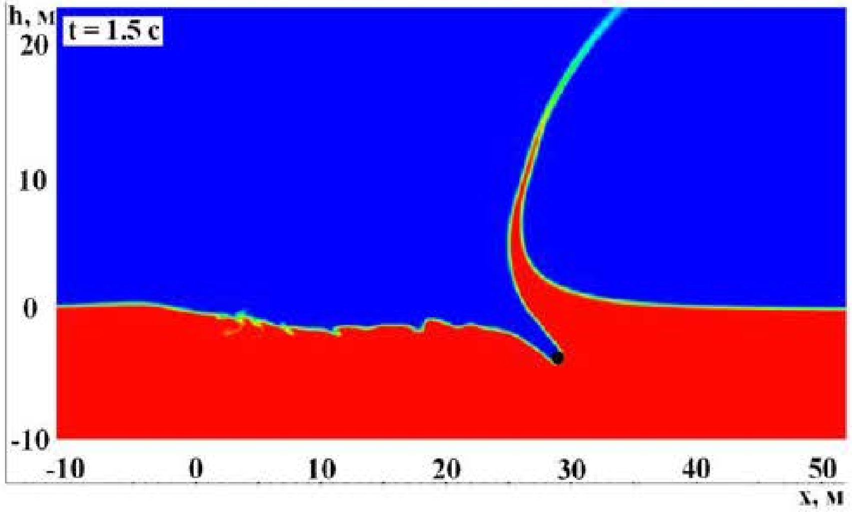

60 m/s

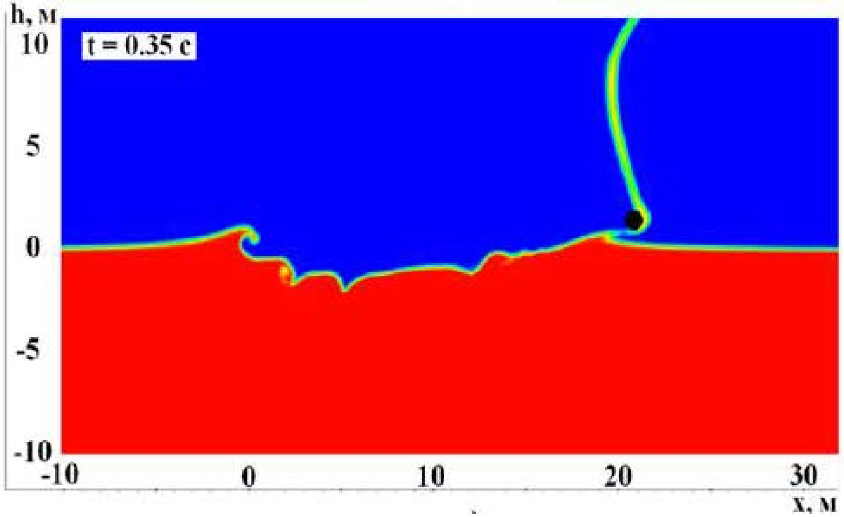

100 m/s

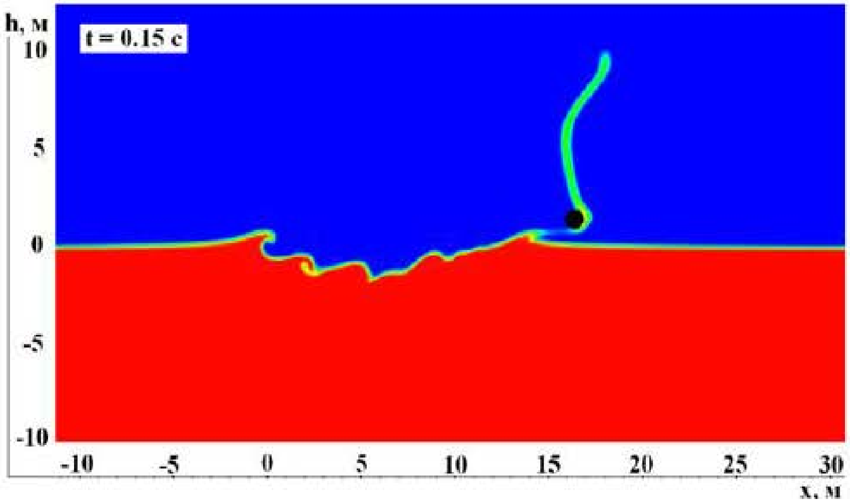

150 m/s

Jumping Frog Effect

Kozelkov A.S., Kurkin A.A., Pelinovskii E.N. Effect of the angle of water entry of a body on the generated wave heights. *Fluid Dynamics*, 2016, vol. 51, 288-298.

Landslide Solid Block Model

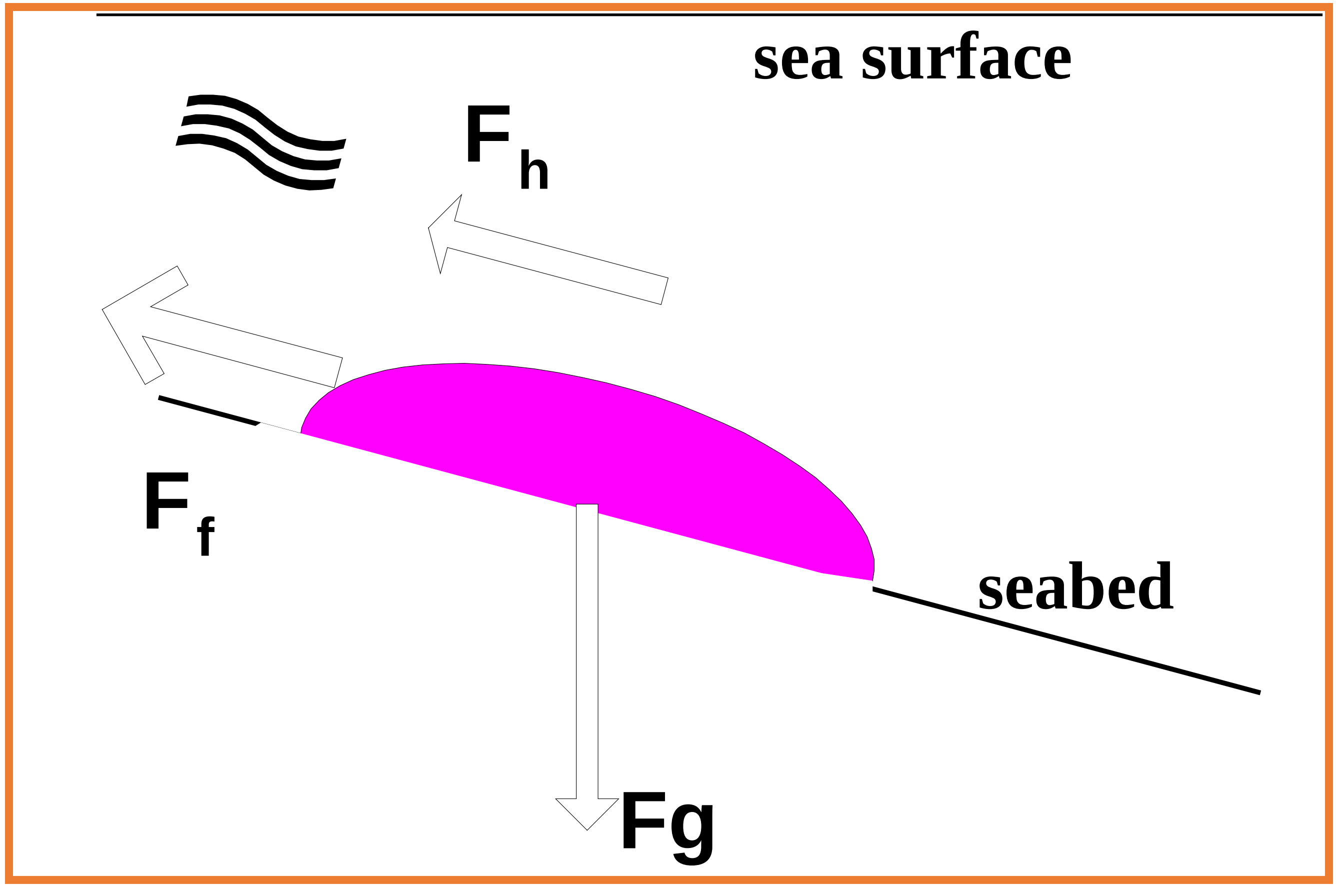

$$\rho V \frac{dU}{dt} = (\rho - \rho_0) g V (\sin\alpha - \mu \cos\alpha) - \frac{\rho_0}{2} C_D S U^2$$

Pergamon

Phys. Chem. Earth, Vol. 21, No. 12, pp. 13–17, 1996.

0079-1946/96 $15.00 + 0.00

PII: S0079-1946(97)00003-7

Simplified Model of Tsunami Generation by Submarine Landslides

E. Pelinovsky[1] and A. Poplavsky[2]

Solution

$$U(\tau) = U_\infty \tanh \tau$$

$$x(\tau) = x_0 + \frac{2\rho L}{\rho_0 C_D} \ln \cosh \tau$$

where

$$U_\infty = \sqrt{\frac{\rho - \rho_0}{\rho_0} \frac{2gL}{C_D} |\sin\alpha - \mu \cdot \cos\alpha|}$$

$$\tau = \frac{\rho_0 C_D U_\infty t}{2\rho L}$$

Pure appl. geophys. 158 (2001) 759–797
0033 – 4553/01/040759 – 39 $ 1.50 + 0.20/0

Pure and Applied Geophysics

Tsunami Excitation by Submarine Slides in Shallow-water Approximation

STEFANO TINTI,[1] ELISABETTA BORTOLUCCI[1] and CINZIA CHIAVETTIERI[1]

J. Fluid Mech. (2003), *vol.* 478, *pp.* 101–109.
DOI: 10.1017/S0022112002003385 Printed in the United Kingdom

Analytical solutions for forced long waves on a sloping beach

By PHILIP L.-F. LIU[1], PATRICK LYNETT[1]† AND COSTAS E. SYNOLAKIS[2]

Savage-Hutter model of granular flow (uniform on depth)

$$\frac{\partial h}{\partial t}+\frac{\partial}{\partial x}(hu)+\frac{\partial}{\partial y}(hv)=0 \qquad (1)$$

$$\frac{\partial}{\partial t}(hu)+\frac{\partial}{\partial x}(hu.u)+\frac{\partial}{\partial y}(hu.v)=$$

$$-\frac{1}{2}\frac{\partial}{\partial x}(gh^2\cos\theta)+gh\sin\theta_x+F_x \qquad (2)$$

$$\frac{\partial}{\partial t}(hv)+\frac{\partial}{\partial x}(hv.u)+\frac{\partial}{\partial y}(hv.v)=$$

$$-\frac{1}{2}\frac{\partial}{\partial y}(gh^2\cos\theta)+gh\sin\theta_y+F_y \qquad (3)$$

JOURNAL OF GEOPHYSICAL RESEARCH, VOL. 115, B03402, doi:10.1029/2009JB006515, 2010

Savage-Hutter model for avalanche dynamics in inclined channels: Analytical solutions

Narcisse Zahibo,[1] Efim Pelinovsky,[1,2] Tatiana Talipova,[1,2] and Irina Nikolkina[1,3]

Received 3 April 2009; revised 17 November 2009; accepted 10 December 2009; published 2 March 2010.

[1] The Savage-Hutter model is applied to describe gravity driven shallow water flows in inclined channels of parabolic-like shapes modeling avalanches moving in mountain valleys or landslide motions in underwater canyons. The Coulomb (sliding) friction term is included in the model. Several analytical solutions describing the nonlinear dynamics of avalanches are obtained: the nonlinear deformed (Riemann) wave, the dam break problem, self-similar solutions and others. Some of them extend the known solution for an inclined plate (one-dimensional geometry). The cross-section shape of the inclined channels significantly influences the speed of avalanche propagation and characteristic time of dynamical processes. Obtained analytical solutions can be used to test numerical models and to give insights into the structure of avalanche flow and to highlight basic mechanisms of avalanche dynamics.

Riemann invariants

$$I_{\pm} = u \pm 2\sqrt{\frac{m+1}{m} gh\cos\theta - g\alpha t}$$

$$\alpha = \sin\theta - \mu\cos\theta > 0$$

$$\frac{\partial I_{\pm}}{\partial t} + c_{\pm}\frac{\partial I_{\pm}}{\partial x} = 0$$

$$c_{\pm} = \frac{3m+2}{4(m+1)} I_{\pm} + \frac{m+2}{4(m+1)} I_{\mp} + g\alpha t$$

$$u(x,t) = g\alpha t + v(x,t)$$

$$v(x,t) = \frac{I_{+} + I_{-}}{2}$$

$$h = \frac{m}{16g\cos\theta(m+1)}\left(I_{+} - I_{-}\right)^{2}$$

Dam Break Problem

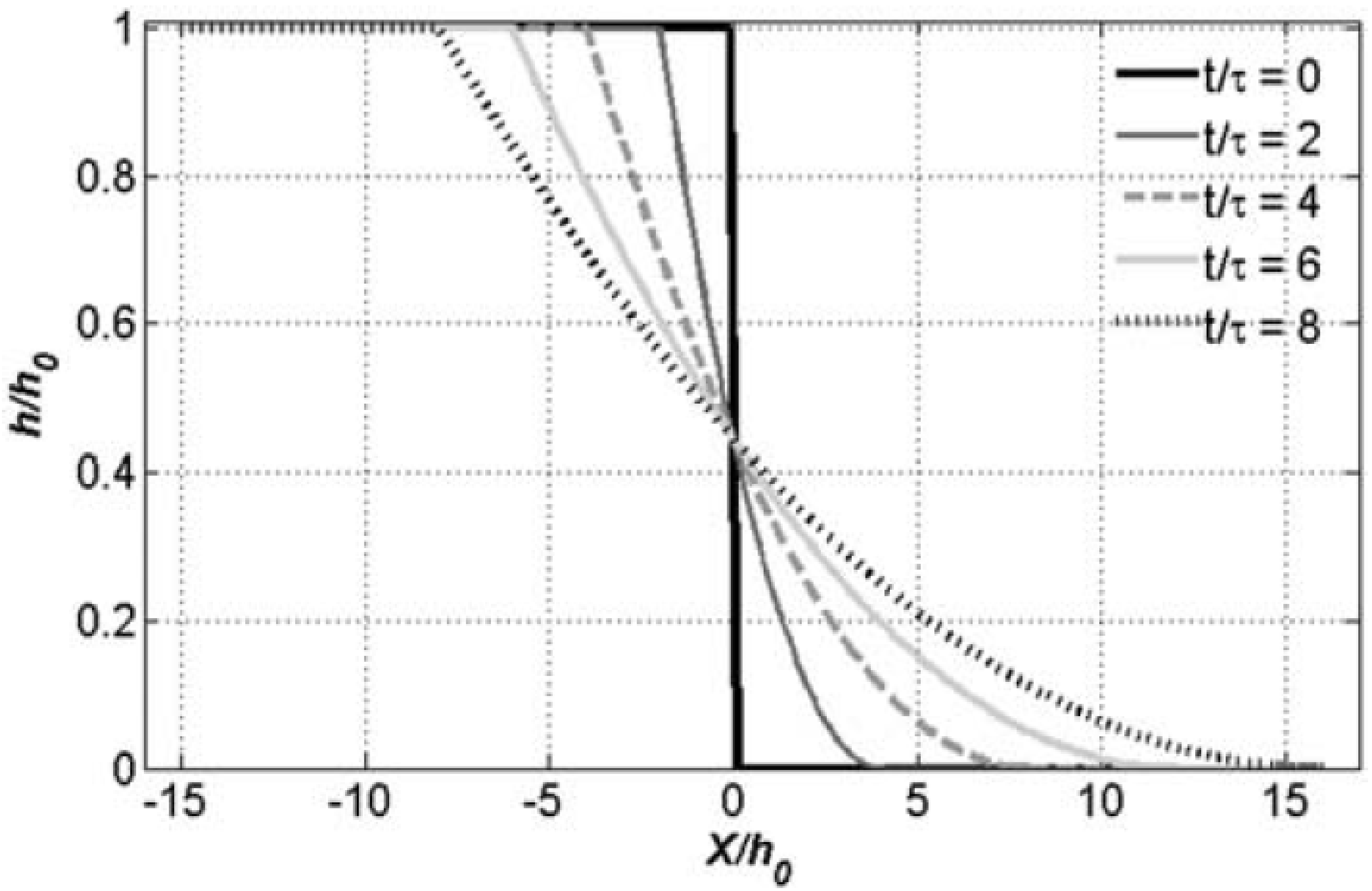

$$h(X,t) = \begin{cases} h_0 & X < -c_0 t \\ \dfrac{h_0}{9}\left(2 - \dfrac{X}{c_0 t}\right)^2 & -c_0 t < X < 2c_0 t \\ 0 & 2c_0 t < X, \end{cases}$$

2D Self-similar solutions (parabolic cap)

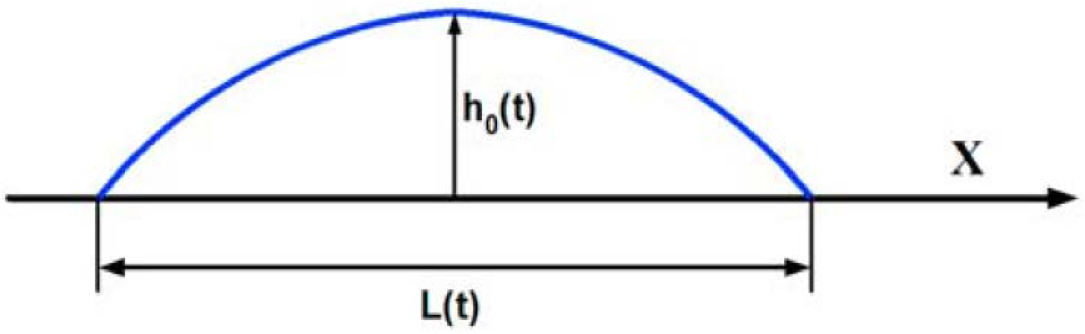

$$h(t) \sim L^{-\frac{m}{m+1}} \sim t^{-\frac{m}{m+1}}.$$

m – shape coefficient in cross-section

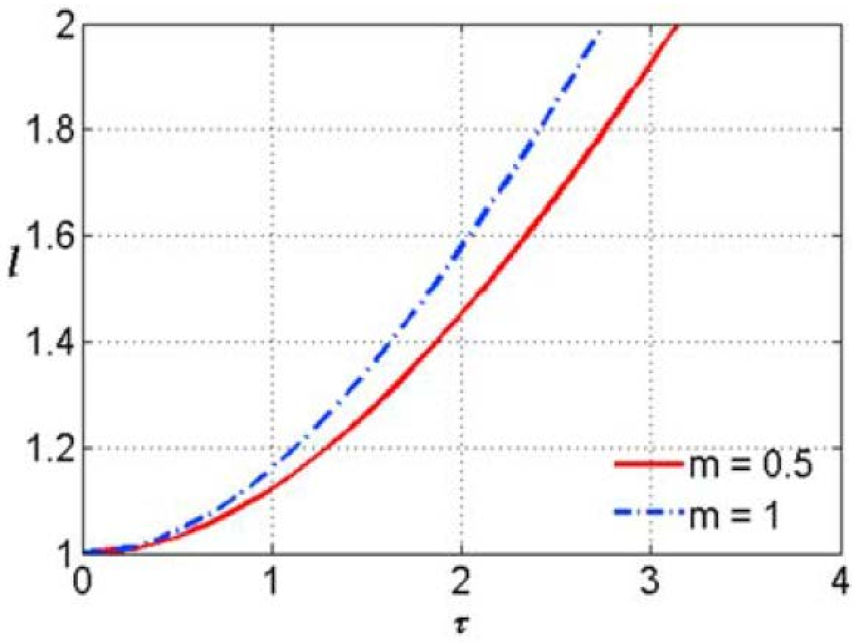

Landslide with parabolic profile of flow

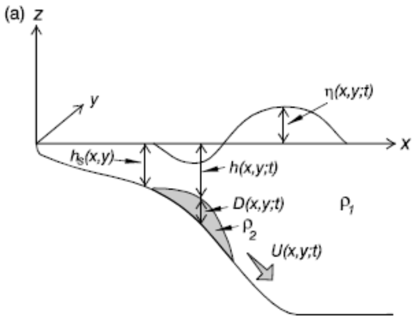

$$\frac{\partial D}{\partial t}+\frac{2}{3}\left[\frac{\partial (DU)}{\partial x}+\frac{\partial (DV)}{\partial y}\right]=0\;; \qquad (2)$$

$$\rho_2\frac{2}{3}\left[\frac{\partial U}{\partial t}-\frac{1}{5}\frac{U}{D}\frac{\partial D}{\partial t}+\frac{4}{5}\left(U\frac{\partial U}{\partial x}+V\frac{\partial U}{\partial y}\right)\right]=-g\left[(\rho_2-\rho_1)\left(\frac{\partial D}{\partial x}-\frac{\partial h_s}{\partial x}\right)+\rho_1\frac{\partial \eta}{\partial x}\right]-\frac{2\mu U}{D^2}\;; \qquad (3a)$$

$$\rho_2\frac{2}{3}\left[\frac{\partial V}{\partial t}-\frac{1}{5}\frac{V}{D}\frac{\partial D}{\partial t}+\frac{4}{5}\left(U\frac{\partial V}{\partial x}+V\frac{\partial V}{\partial y}\right)\right]=-g\left[(\rho_2-\rho_1)\left(\frac{\partial D}{\partial y}-\frac{\partial h_s}{\partial y}\right)+\rho_1\frac{\partial \eta}{\partial y}\right]-\frac{2\mu V}{D^2}. \qquad (3b)$$

Simplified 1D case

$$\frac{\partial D}{\partial t}+\frac{\partial M}{\partial x}=0 \qquad \frac{\partial M}{\partial t}+\frac{6}{5}\frac{\partial}{\partial x}\left(\frac{M^2}{D}\right)+gD\frac{\partial D}{\partial x}=g\theta D$$

where discharge $$M=\frac{2}{3}DU$$

JOURNAL OF GEOPHYSICAL RESEARCH, VOL. 97, NO. C8, PAGES 12,731–12,744, AUGUST 15, 1992

The Coupling of A Submarine Slide and The Surface Waves Which It Generates

L. JIANG AND P.H. LEBLOND

Forced Wave Equation

$$c = \sqrt{gh(x)}$$

$$\frac{\partial^2 \eta}{\partial t^2} - \frac{\partial}{\partial x}\left[c^2(x)\frac{\partial \eta}{\partial x}\right] = \frac{\partial^2 z_b}{\partial t^2}$$

$$\eta(x,0) = z_b(x,0)$$

$$\frac{\partial \eta}{\partial t}(x,0) = \frac{\partial z_b}{\partial t}(x,0)$$

$$\frac{\partial^2 u}{\partial t^2} - \frac{\partial^2}{\partial x^2}\left[c^2(x)u\right] = -g\frac{\partial^2 z_b}{\partial t \partial x}$$

$$u(x,0) = 0$$

$$\frac{\partial u}{\partial t}(x,0) = -g\frac{\partial z_b}{\partial x}(x,0)$$

$$h(x) = px^{4/3}$$

“Non-Reflected” Beach

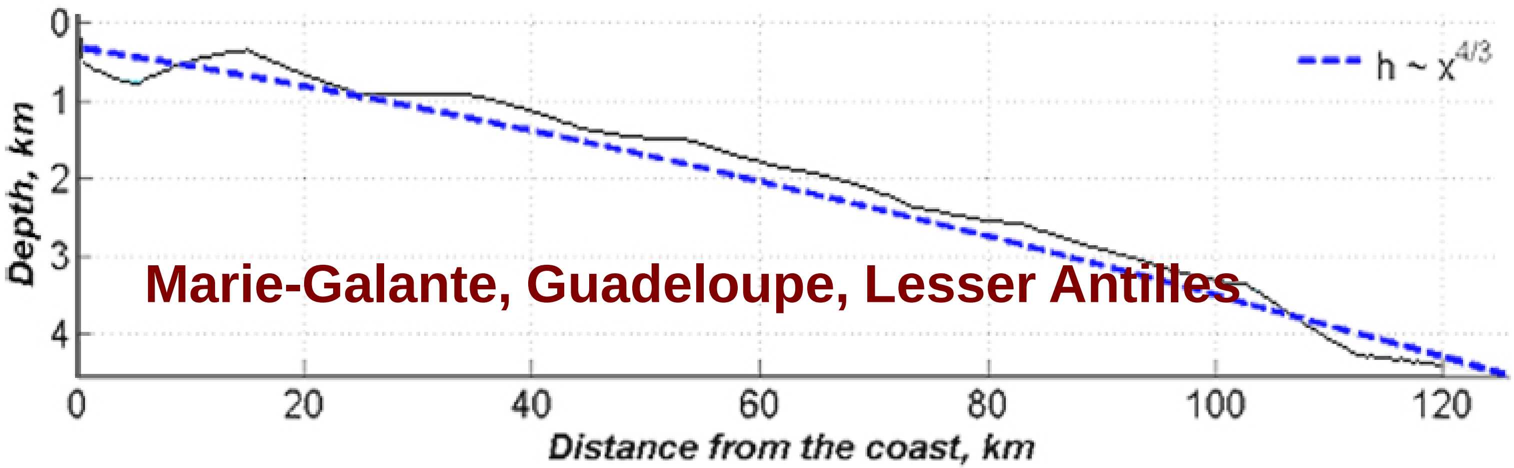

$$\eta(x,t) = A(x)H(\tau(x),t) \qquad \tau = \int_{x_0}^{x} \frac{dx'}{c(x')} \qquad A(x) = A_0\left[\frac{h_0}{h(x)}\right]^{1/4}$$

$$\frac{\partial^2 H}{\partial t^2} - \frac{\partial^2 H}{\partial \tau^2} = \frac{\partial^2}{\partial t^2}\left[\frac{z_b(\tau,t)}{A(\tau)}\right]$$

Duhamel Integral

$$H(\tau,t)=\frac{1}{2}\left[\frac{z_b(\tau-t)}{A(\tau-t)}+\frac{z_b(\tau+t)}{A(\tau+t)}\right]+\frac{1}{2}\int_{\tau-t}^{\tau+t}\frac{1}{A(\sigma)}\frac{\partial z_b}{\partial t}(\sigma,0)d\sigma+\frac{1}{2}\int_0^t d\rho\int_{\tau-(t-\rho)}^{\tau+(t-\rho)}\frac{1}{A(\varsigma)}\frac{\partial^2 z_b}{\partial\rho^2}(\varsigma,\rho)d\varsigma.$$

Landslide with variable volume and speed

$$z_b(\tau,t)=A(\tau)Z(\tau-Fr\cdot t)$$

$$V(x)=\frac{dx}{dt}=c(x)\cdot Fr$$

$$M(t)=\int z_b(x,t)dx\sim t$$

$$H(\tau,t)=\frac{Fr^2}{Fr^2-1}Z(\tau-Fr\cdot t)-\frac{1}{2(Fr-1)}Z(\tau-t)+\frac{1}{2(Fr+1)}Z(\tau+t)$$

Soliton interaction with external forcing within the Korteweg–de Vries equation

Andrei Ermakov[1] and Yury Stepanyants[1,2]

Chaos 29, 013117 (2019); doi: 10.1063/1.5063561

$$\frac{\partial u}{\partial t} + c\frac{\partial u}{\partial x} + \alpha u\frac{\partial u}{\partial x} + \beta\frac{\partial^3 u}{\partial x^3} = \varepsilon\frac{\partial f}{\partial x}$$

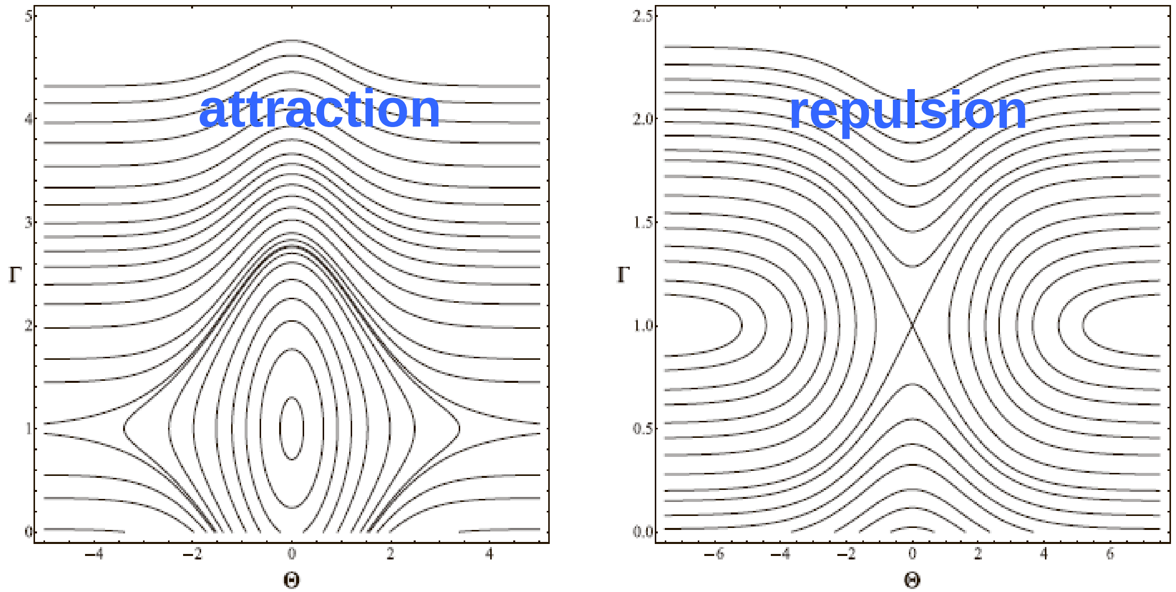

(a) (b)

Two –layer model of landslide tsunamis

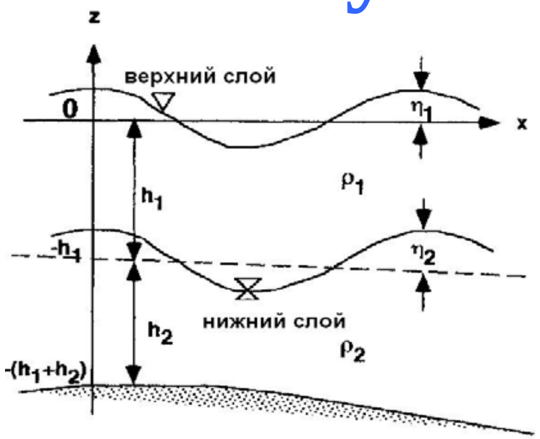

$$\frac{\partial M_1}{\partial t}+\frac{\partial}{\partial x}\left(\frac{M_1^2}{D_1}\right)+\frac{\partial}{\partial y}\left(\frac{M_1 N_1}{D_1}\right)+gD_1\frac{\partial \eta_1}{\partial x}+\frac{gm_1^2}{2D_1^{7/3}}M_1\sqrt{M_1^2+N_1^2}=0$$

$$\frac{\partial N_1}{\partial t}+\frac{\partial}{\partial y}\left(\frac{N_1^2}{D_1}\right)+\frac{\partial}{\partial x}\left(\frac{M_1 N_1}{D_1}\right)+gD_1\frac{\partial \eta_1}{\partial y}+\frac{gm_1^2}{2D_1^{7/3}}M_1\sqrt{M_1^2+N_1^2}=0$$

$$\frac{\partial(\eta_1-\eta_2)}{\partial t}+\frac{\partial M_1}{\partial x}+\frac{\partial N_1}{\partial y}=0$$

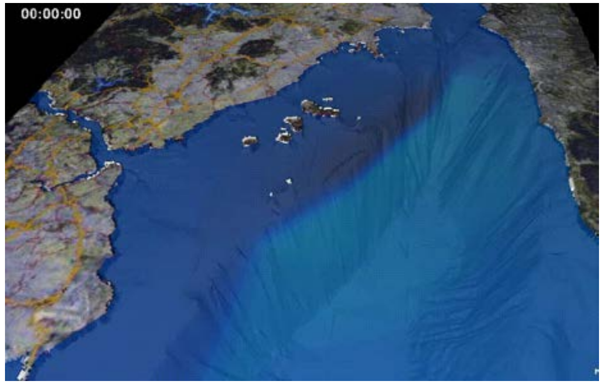

$$\frac{\partial \eta_2}{\partial t}+\frac{\partial M_2}{\partial x}+\frac{\partial N_2}{\partial y}-\beta\left(\frac{\partial^2\eta_2}{\partial x^2}+\frac{\partial^2\eta_2}{\partial y^2}\right)=0$$

$$\frac{\partial M_2}{\partial t}+\frac{\partial}{\partial x}\left(\frac{M_2^2}{D_2}\right)+\frac{\partial}{\partial y}\left(\frac{M_2 N_2}{D_2}\right)+gD_2\left[\frac{\rho_1}{\rho_2}\frac{\partial}{\partial x}(\eta_1+h_1-\eta_2)+\frac{\partial}{\partial x}(\eta_2-h_1)\right]+\frac{gm_2^2}{2D_2^{7/3}}M_2\sqrt{M_2^2+N_2^2}=0,$$

$$\frac{\partial N_2}{\partial t}+\frac{\partial}{\partial y}\left(\frac{N_2^2}{D_2}\right)+\frac{\partial}{\partial x}\left(\frac{M_2 N_2}{D_2}\right)+gD_2\left[\frac{\rho_1}{\rho_2}\frac{\partial}{\partial y}(\eta_1+h_1-\eta_2)+\frac{\partial}{\partial y}(\eta_2-h_1)\right]+\frac{gm_2^2}{2D_2^{7/3}}N_2\sqrt{M_2^2+N_2^2}=0,$$

Potential landslide tsunami in Nile Delta

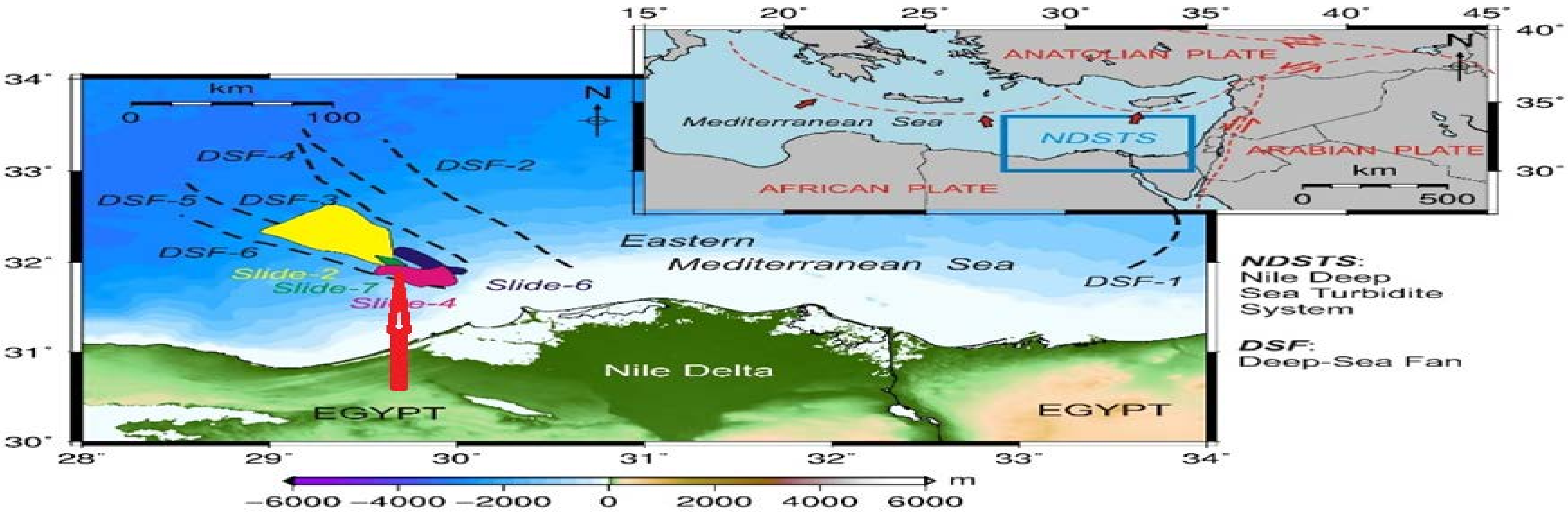

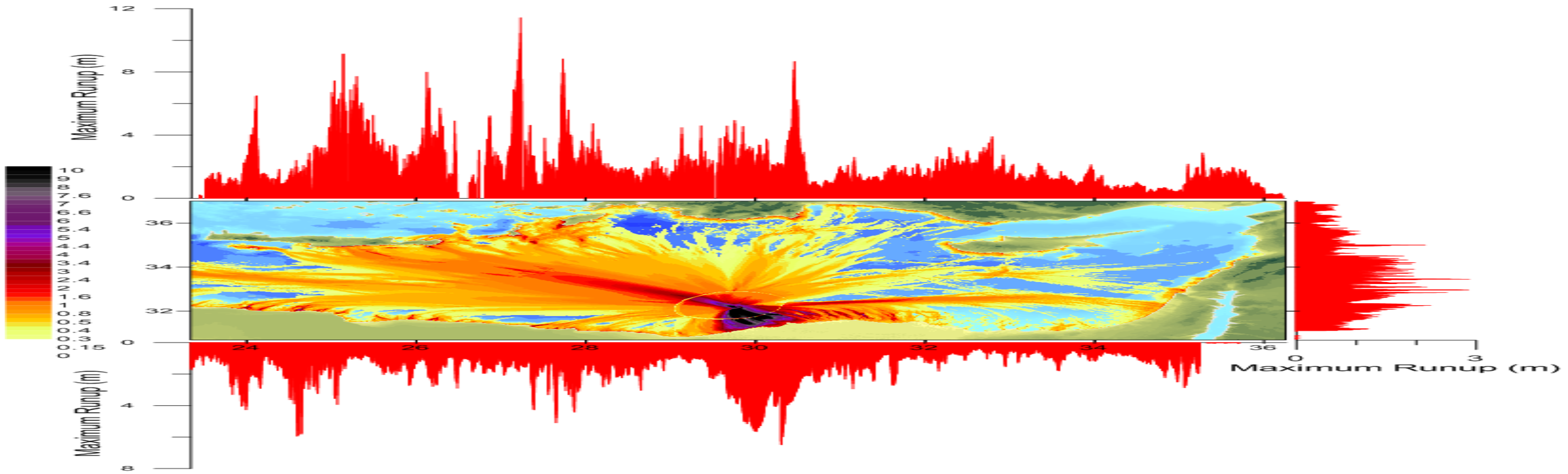

Maximum wave height distribution

Navier-Stokes Model

$$\begin{cases} \nabla \cdot \mathbf{u} = 0, \\ \frac{\partial}{\partial t} \sum_k \alpha^{(k)} \rho^{(k)} \mathbf{u} = -\nabla \cdot \sum_k \left(\alpha^{(k)} \rho^{(k)} \mathbf{u}\mathbf{u} \right) + \nabla \cdot \sum_k \left(\alpha^{(k)} \mu^{(k)} \nabla \mathbf{u} \right) - \nabla p + \sum_k \alpha^{(k)} \rho^{(k)} \mathbf{g}, \\ \frac{\partial}{\partial t} \alpha^{(k)} \rho^{(k)} + \nabla \cdot \left(\alpha^{(k)} \rho^{(k)} \mathbf{u} \right) = 0, \end{cases}$$

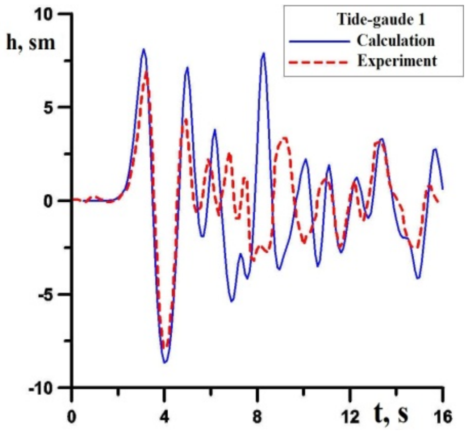

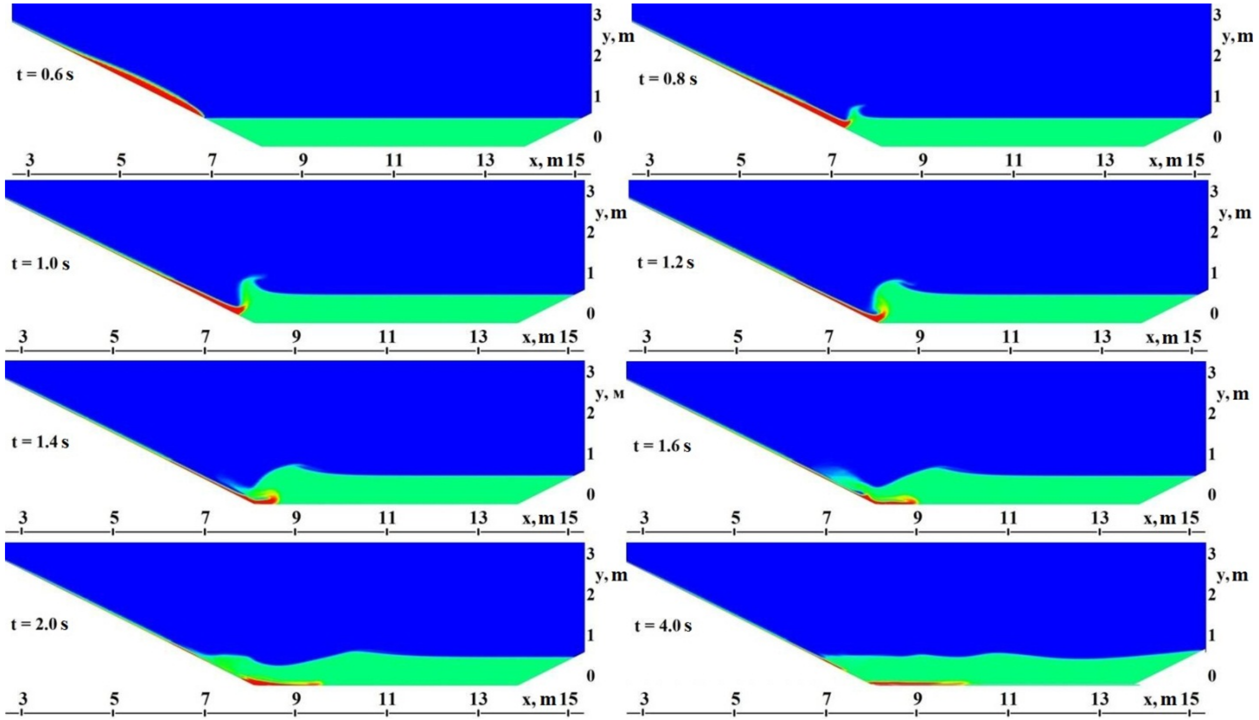

Verification on experimental data Fritz et al, 2009; Mohammed, 2010

Цунами в Волге

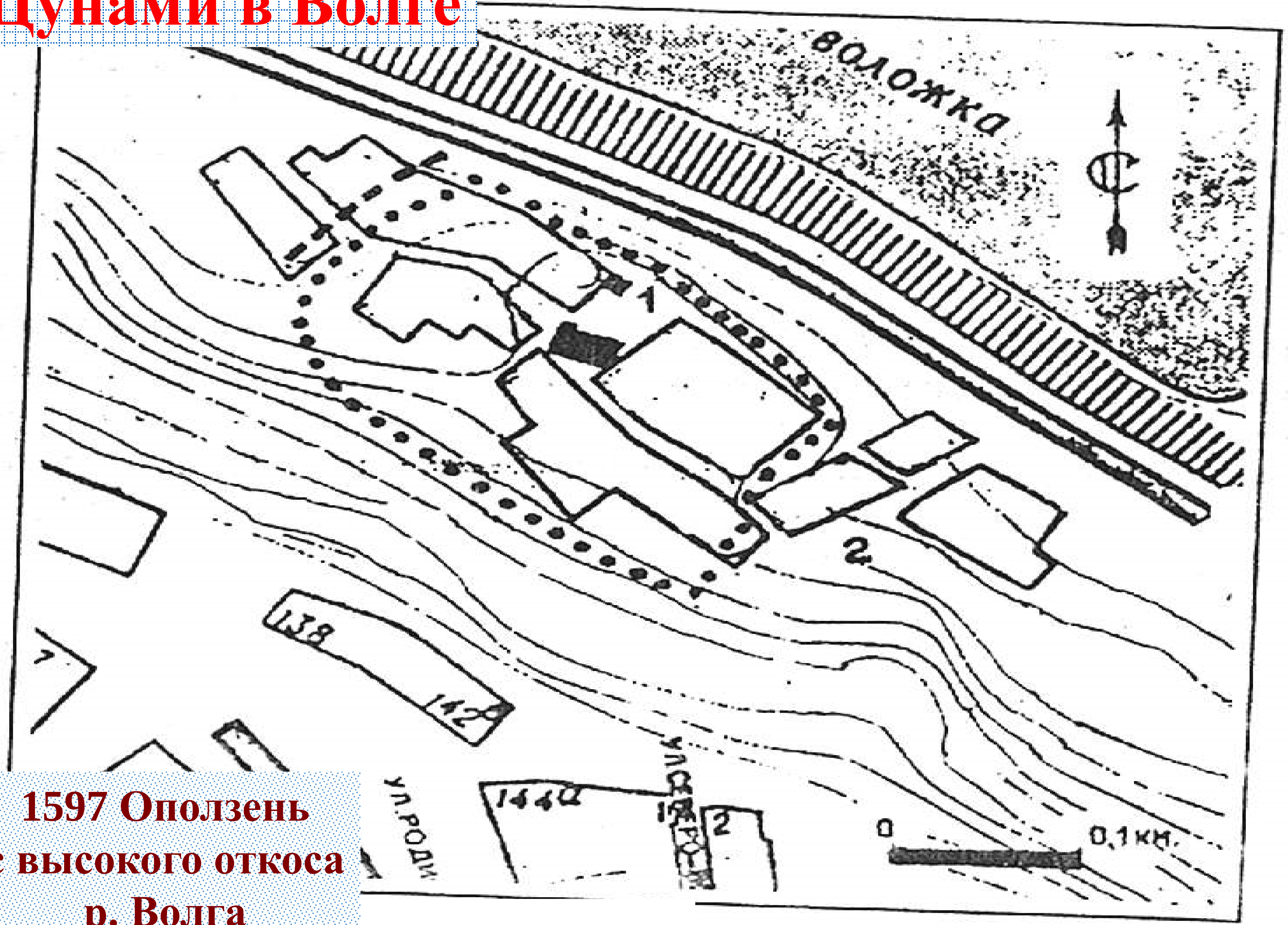

1597 Оползень с высокого откоса р. Волга

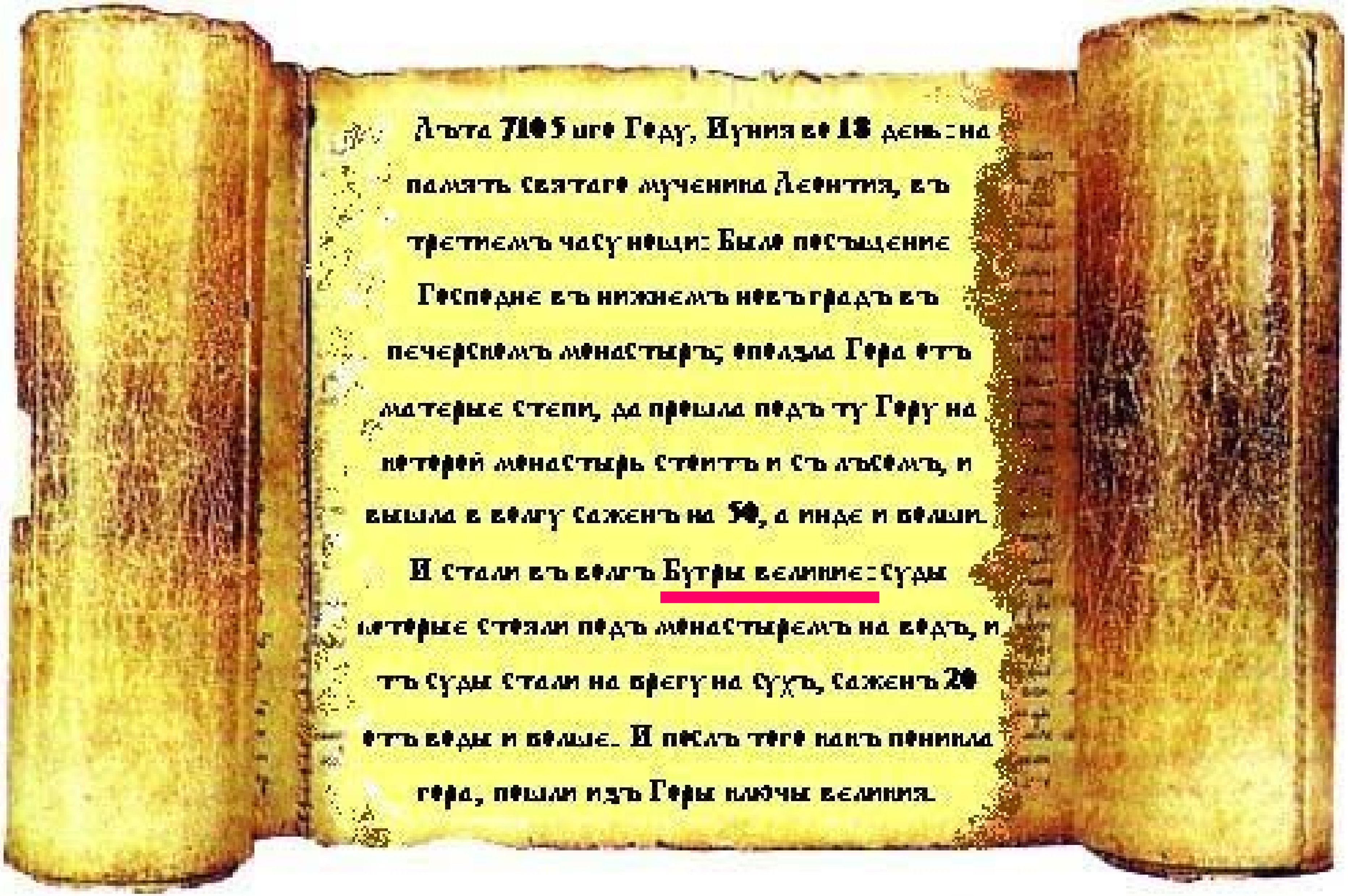

Лѣта 7105 иго Году, Иуния во 18 день: на
память святаго мученика Леонтия, въ
третиемъ часу нощи: Было посѣщение
Господне въ нижнемъ новѣградѣ въ
печерскомъ монастырѣ; оползла Гора отъ
матерые степи, да прошла подъ ту Гору на
которой монастырь стоитъ и съ лѣсомъ, и
вышла в волгу саженъ на 50, а инде и больши.
И стали въ волгѣ Бугры великие: суды
которые стояли подъ монастыремъ на водѣ, и
тѣ суды стали на брегу на сухѣ, саженъ 20
отъ воды и болше. И послѣ того какъ покинула
гора, пошли изъ Горы ключы великия.

Из летописи 1597 года

На месте разрушенного монастыря

Discovered in 1493 by Ch. Coulomb, first people from 1632

Population: before 1995 - 12,000, now – 4,400

Plymouth – former capital


MONTSERRAT


26.12. 2001


03.08.2003


03.08.2003


Pyroclastic Flow
12-13 July 2003
Tar River Valley
Tsunami
generation

Tsunami Traces

4 m high,
100-200 m inland

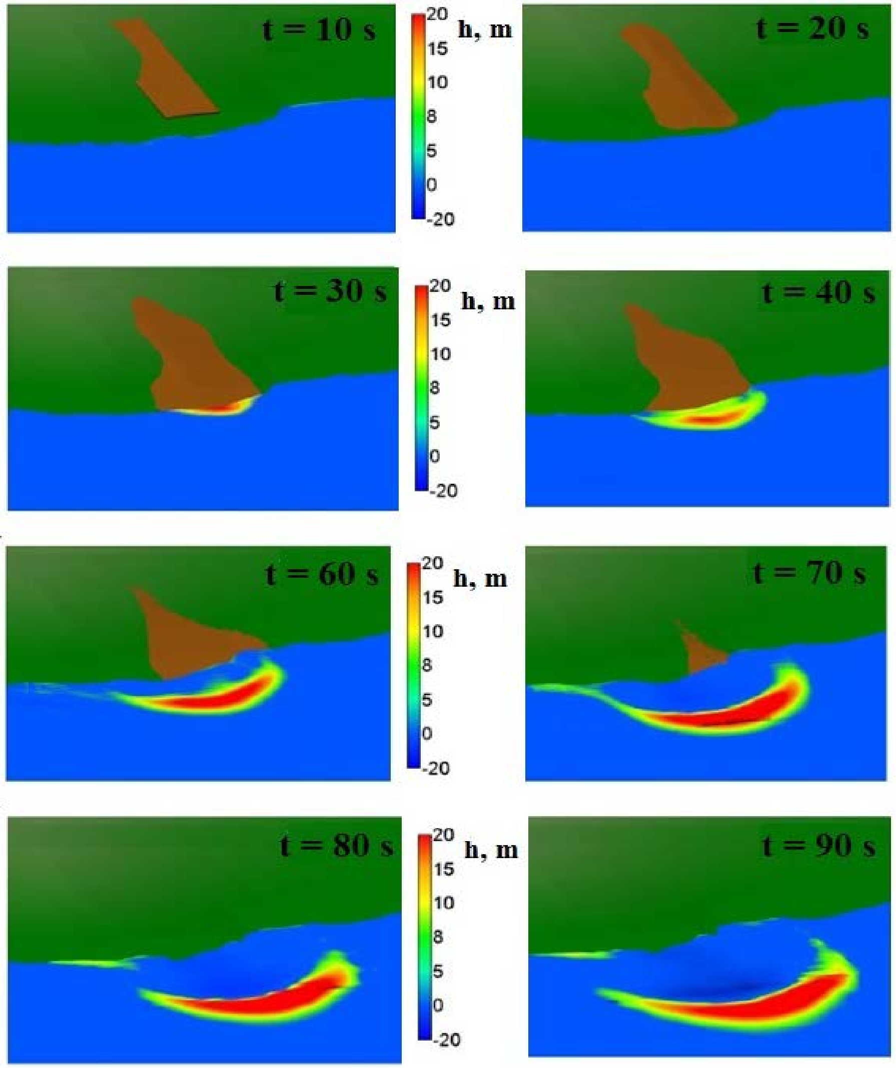

Computations and comparison with:

Tunami – shallow water
Geowave – Boussinesq
Logos – Navier Stokes

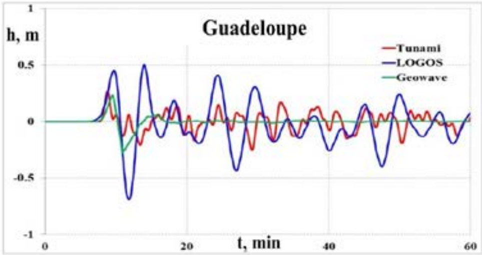

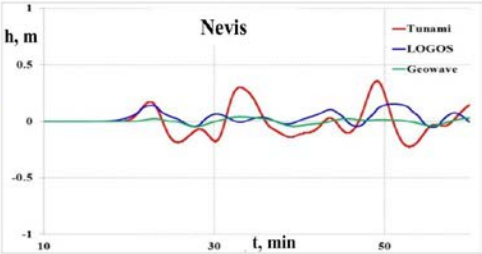

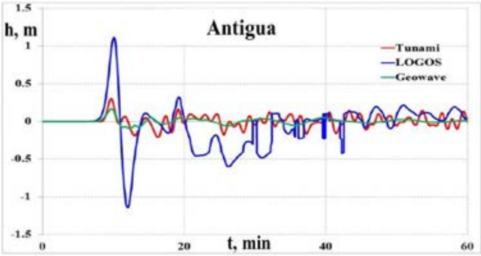

Distribution Functions of Tsunamis

(statistical reliability)

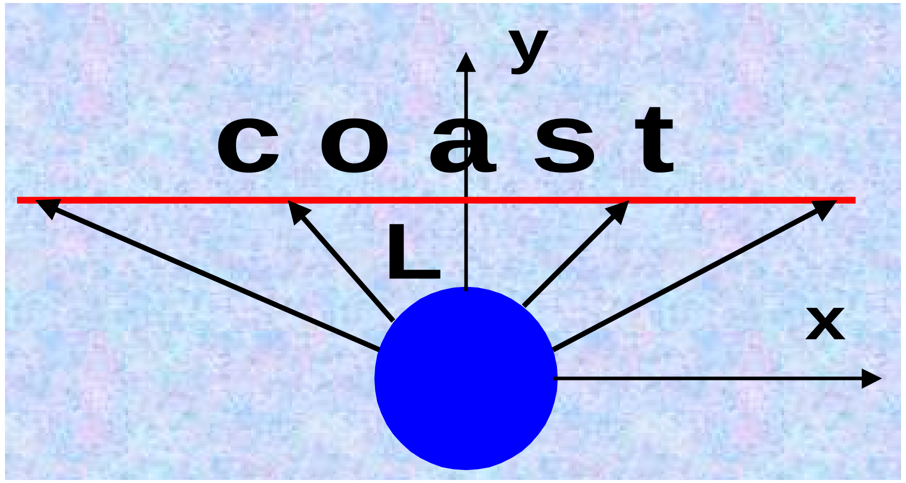

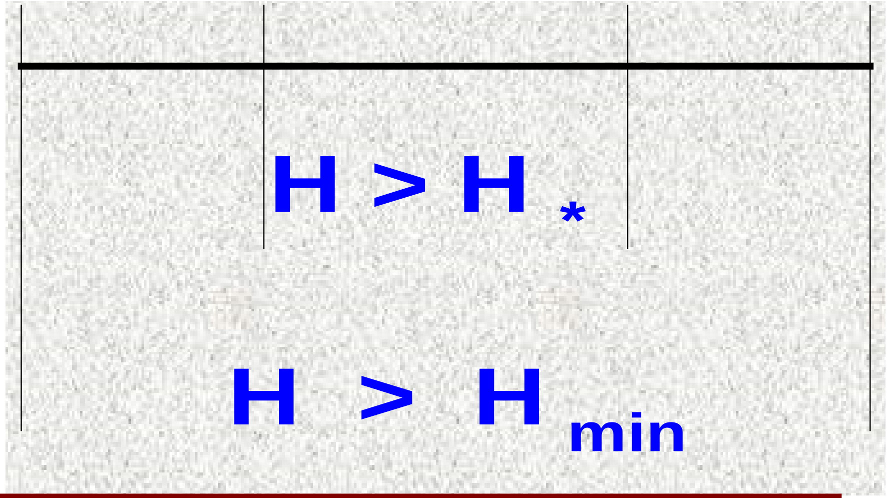

Constant Depth

$$H = H_e \left(\frac{R_e}{R} \right)^{\alpha}$$

$$R = \sqrt{x^2 + L^2}$$

Probability:

$P(H_*) = x(H>H_*)/x_{max}$

$$P(H) = \sqrt{\frac{\left(\frac{H_{max}}{H} \right)^{2/\alpha} - 1}{\left(\frac{H_{max}}{H_{min}} \right)^{2/\alpha} - 1}}$$

Random Wave Paths

$$H = K\,H_e$$

or

$$\log H = \log K + \log H_e$$

$$K = \prod_i K_i$$ – random amplification

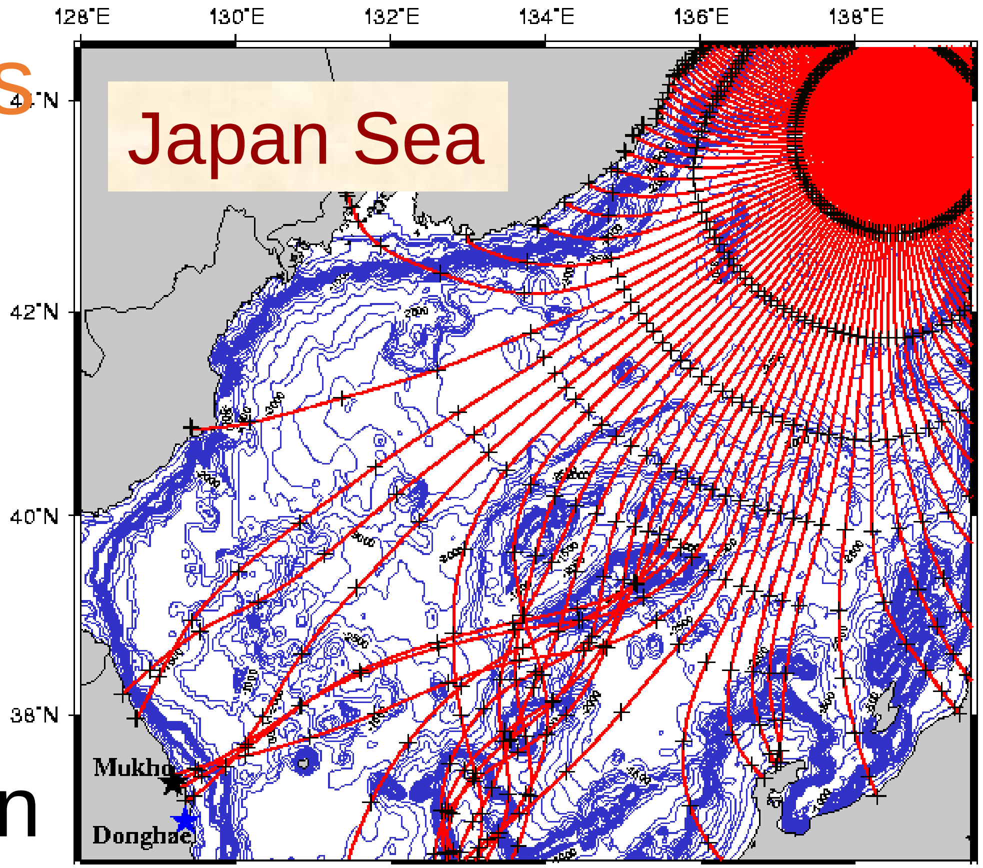

According to the central limit theorem logH is the gaussian process

$$f(H) = \frac{1}{H\sigma\sqrt{2\pi}\ln 10}\exp\left(-\frac{(\log H - <\log H>)^2}{2\sigma^2}\right)$$

Distribution functions of tsunamis 1992–2000

$$P(\varsigma) = \frac{1}{\sqrt{2\pi}\,\ln 10}\int_{\varsigma}^{\infty} \exp\left(-\frac{1}{2}(\log\theta)^2\right)\frac{d\theta}{\theta}$$

$$\zeta = \left(\frac{H}{\overline{H}}\right)^{1/\sigma}$$

$$\overline{H} = 10^{a}$$

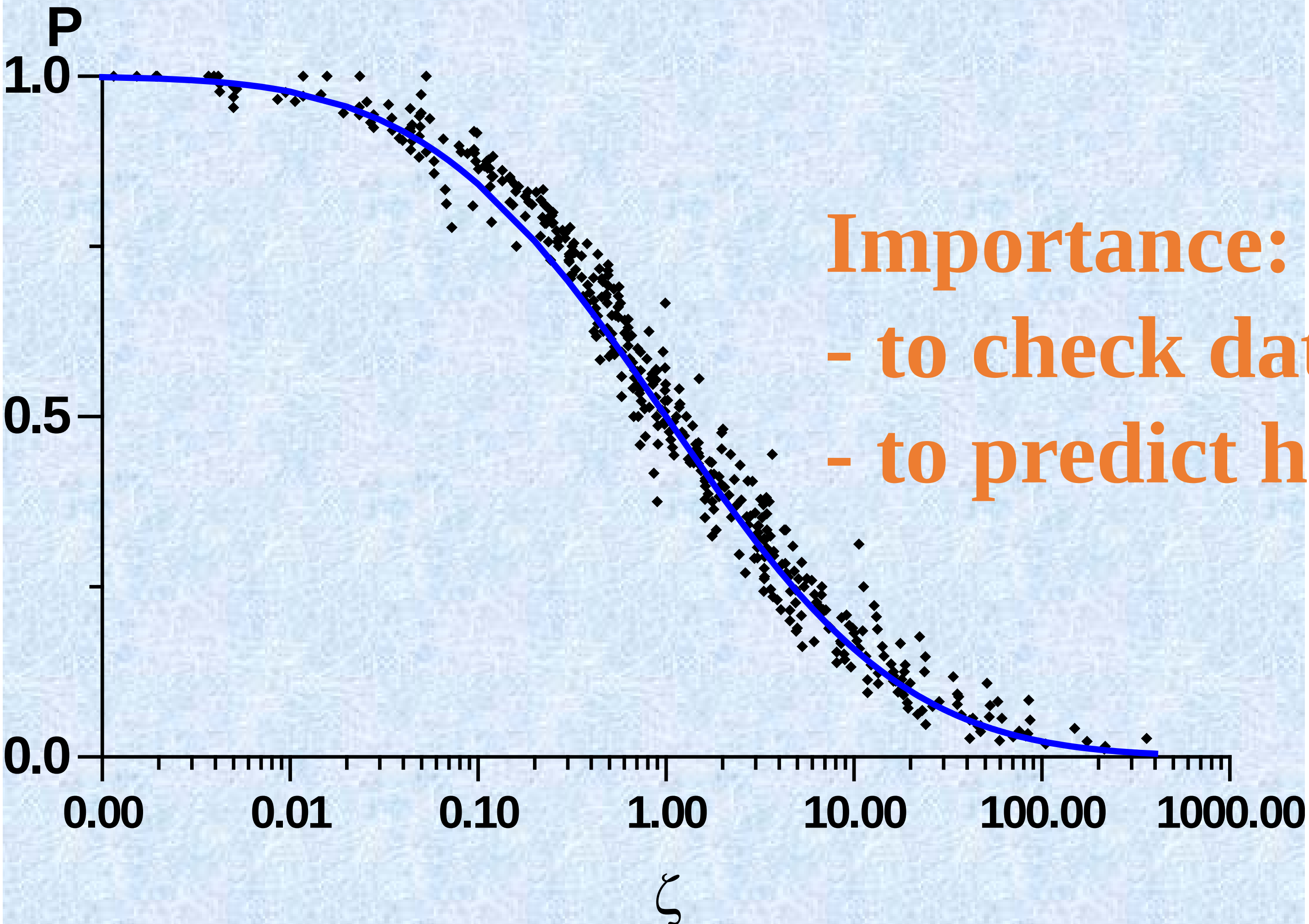

Importance:

- to check data and

- to predict huge heights

Choi, Pelinovsky, et al, 2002

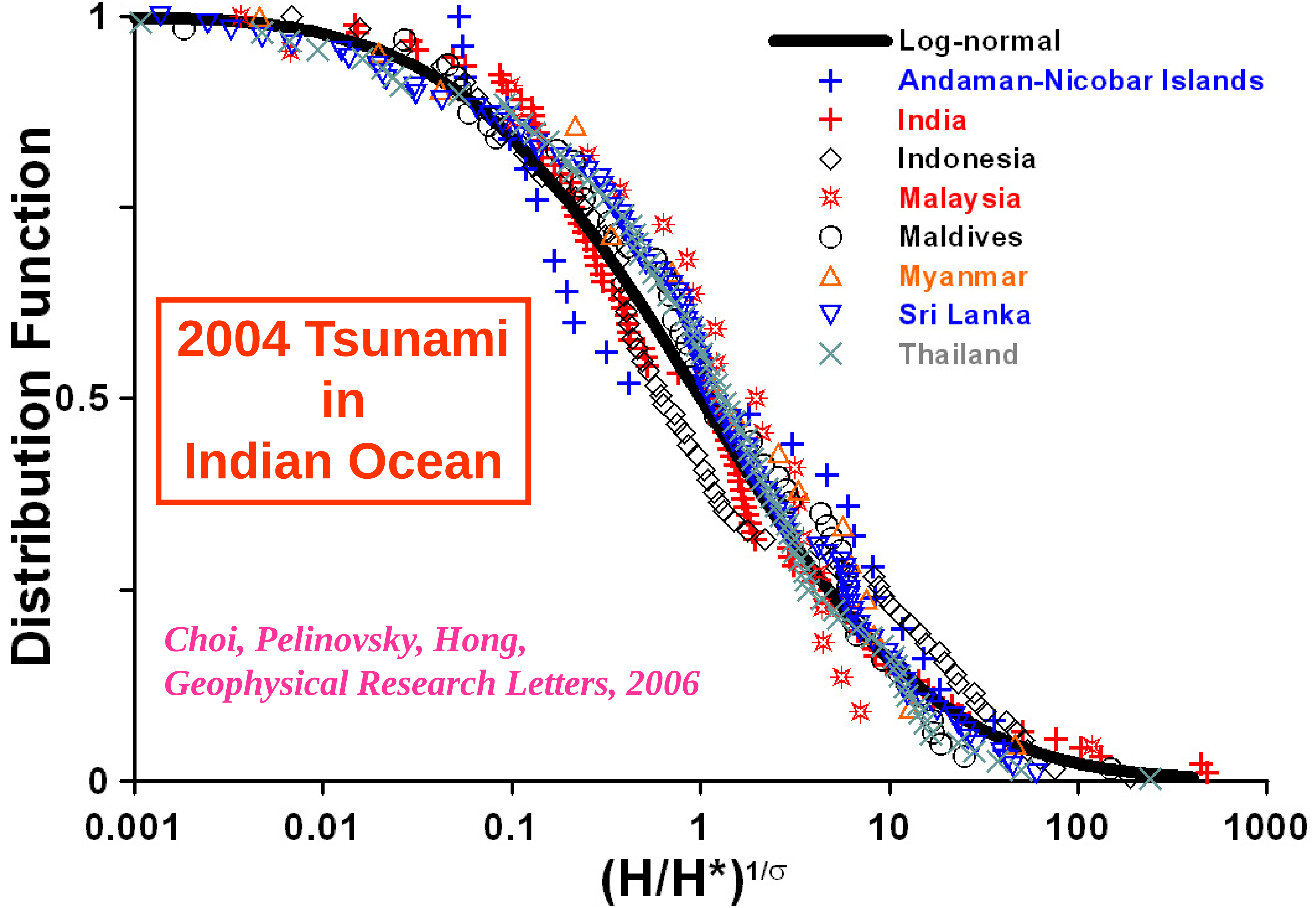
Distribution Function
1
0.5
0
0.001
0.01
0.1
1
10
100
1000
(H/H*)^1/σ
Log-normal
Andaman-Nicobar Islands
India
Indonesia
Malaysia
Maldives
Myanmar
Sri Lanka
Thailand
2004 Tsunami
in
Indian Ocean
Choi, Pelinovsky, Hong,
Geophysical Research Letters, 2006

Short-term prediction – the Operation Warning System

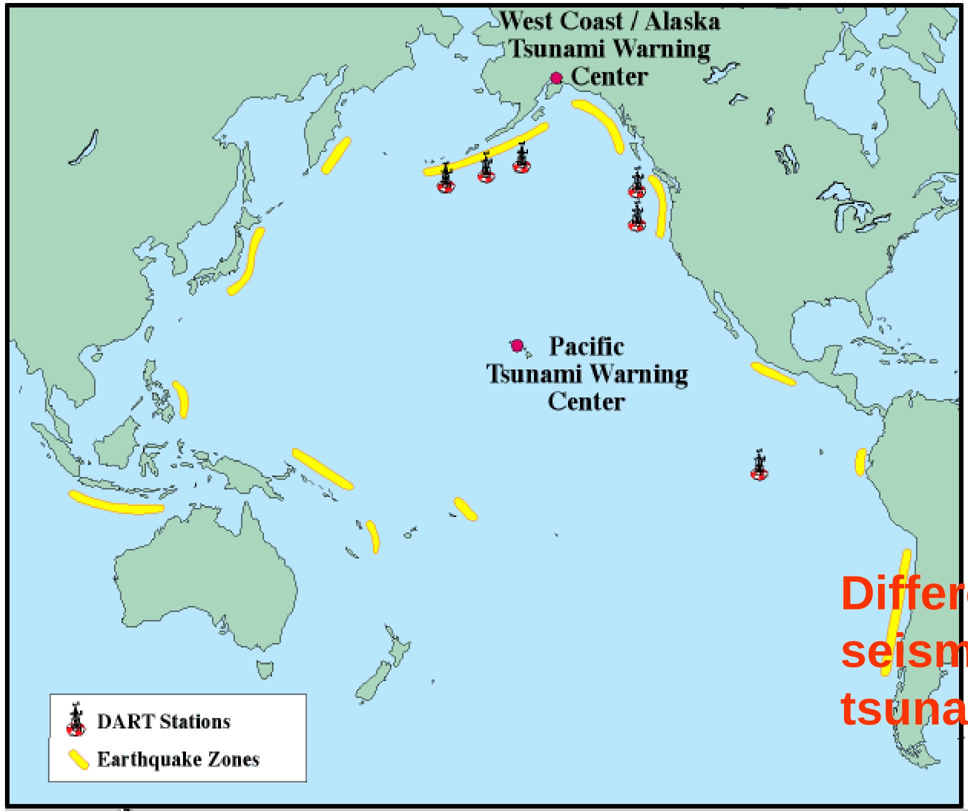

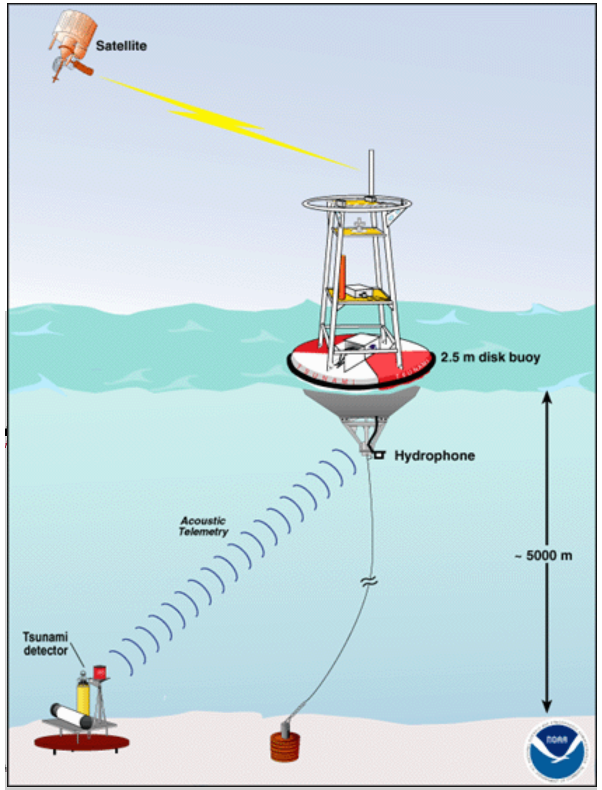

Different Speeds:
seismic -8 km/s,
tsunami – 200 m/s

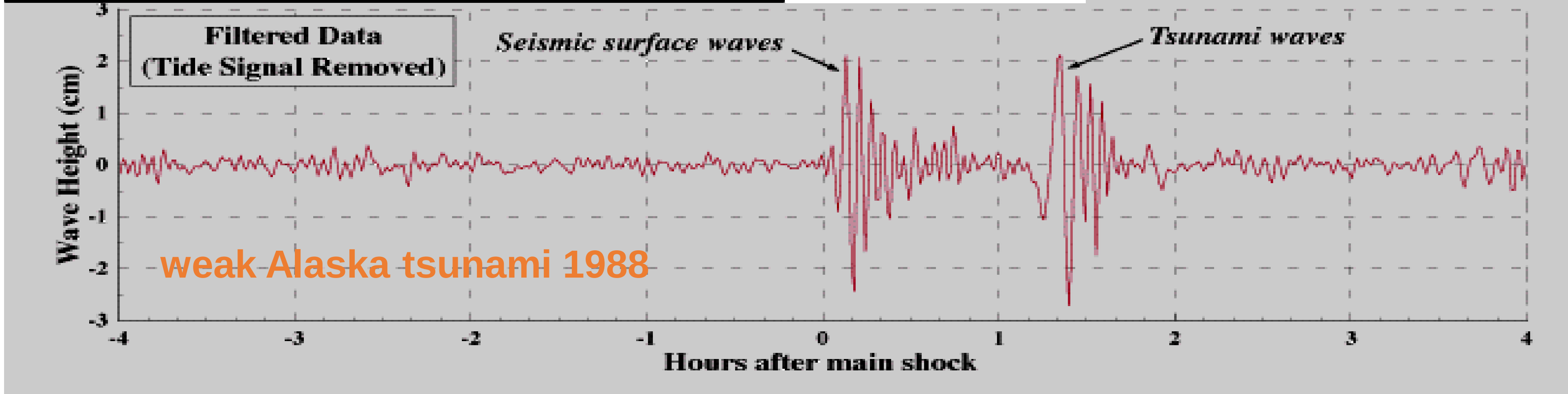

weak Alaska tsunami 1988

Tsunami was predicted by NOAA on-line within the framework of shallow water theory (MOST).

DART data is effective for the good prediction!

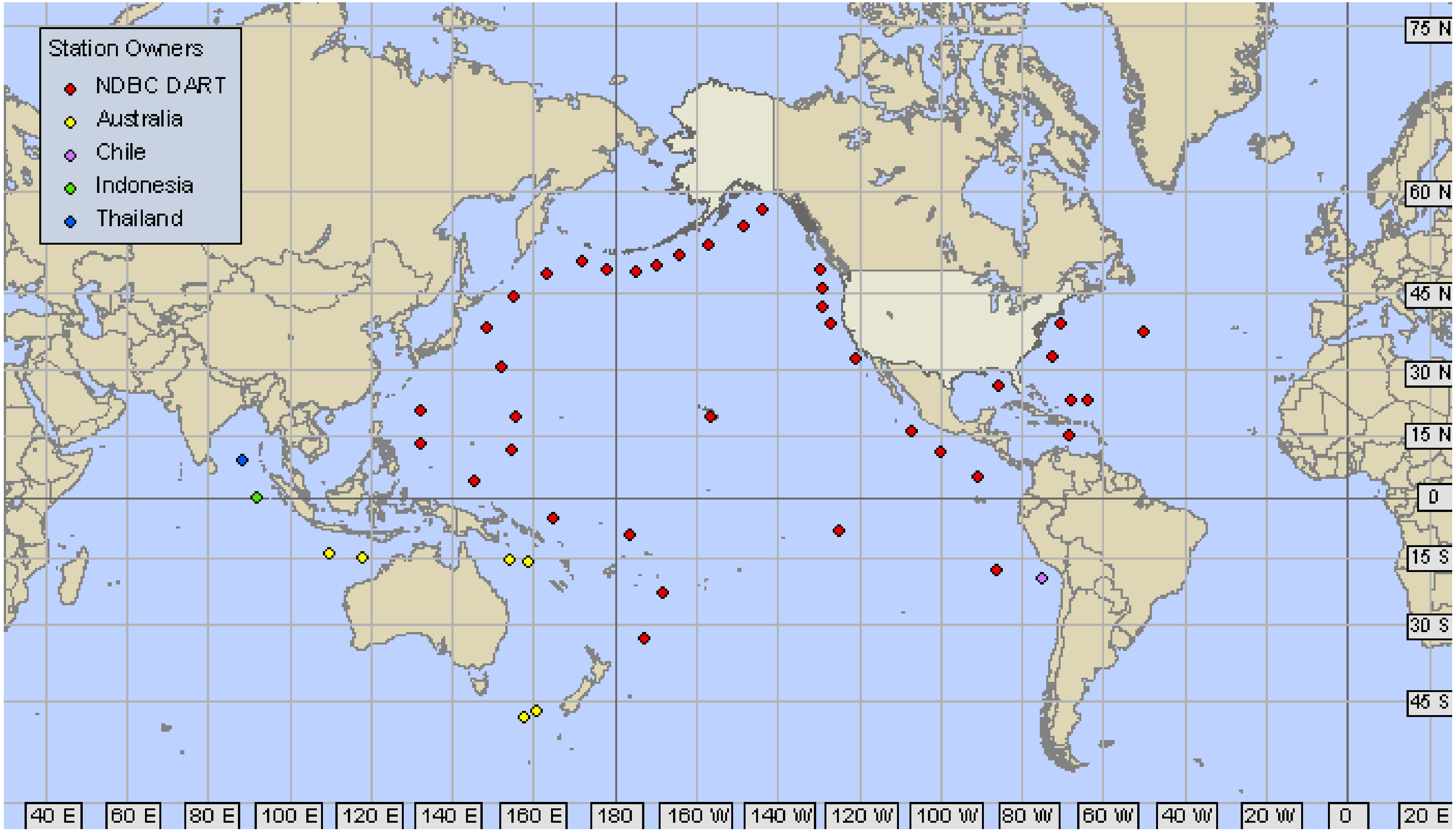

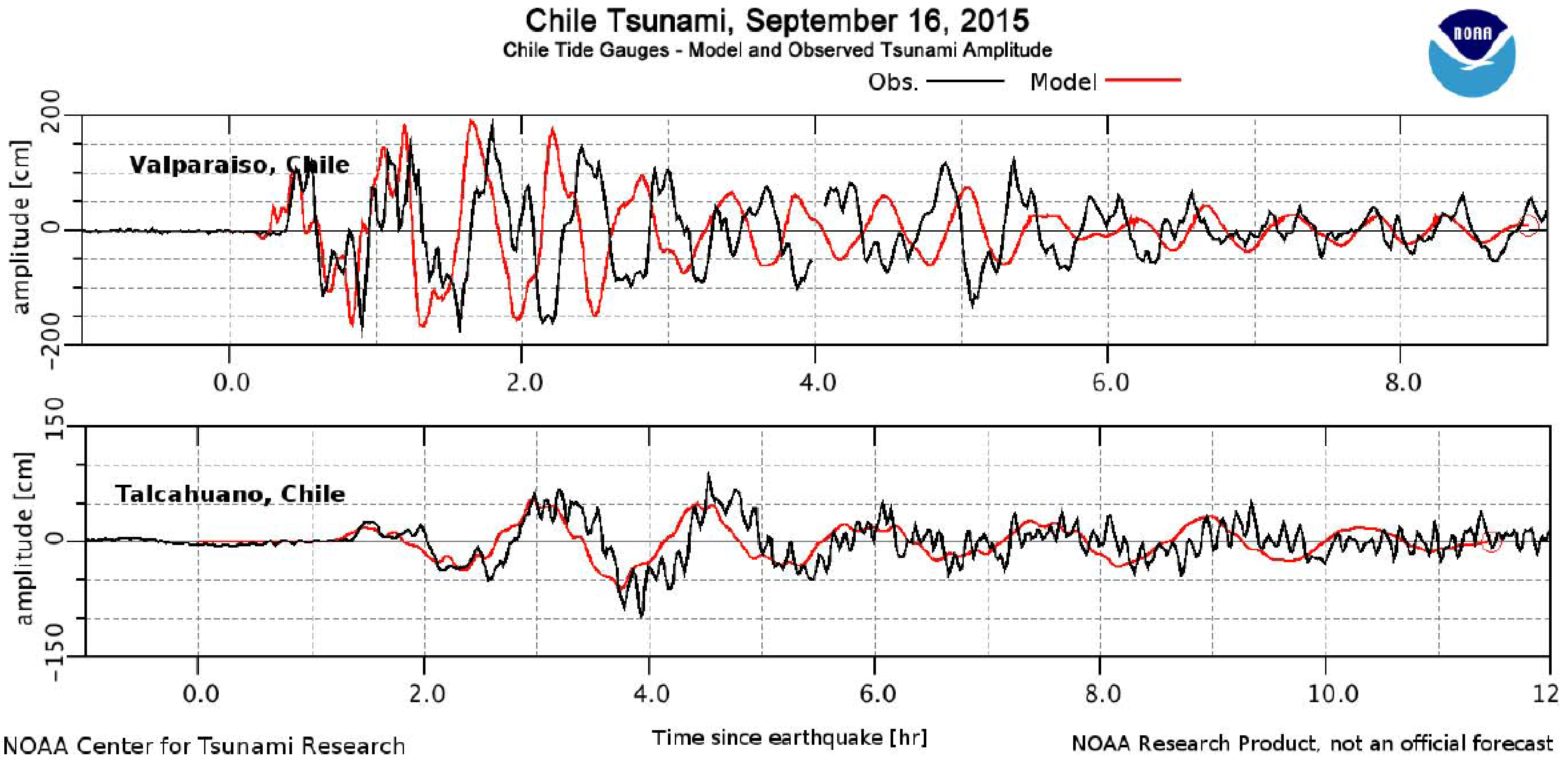

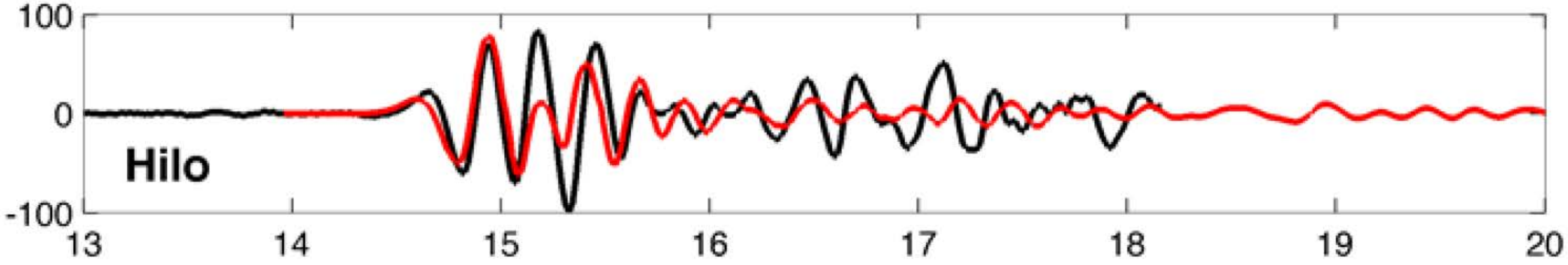

Black - observations, Red - simulations

Long-term tsunami forecasting

Probability (Poisson distribution)

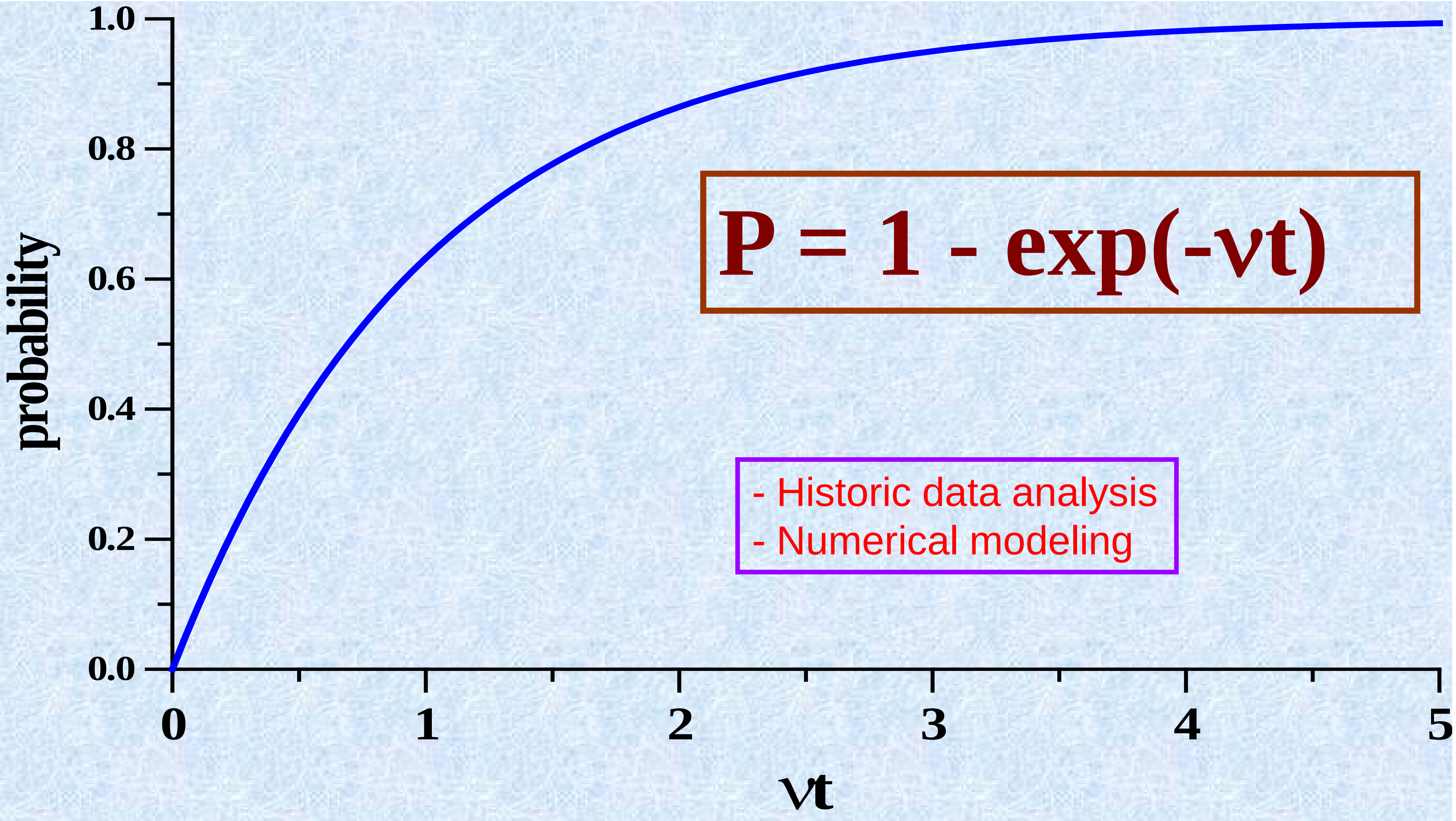

ISSN 0001-4338, Izvestiya, Atmospheric and Oceanic Physics, 2019, Vol. 55, No. 5, pp. 462–469. © Pleiades Publishing, Ltd., 2019.
Russian Text © The Author(s), 2019, published in Izvestiya Rossiiskoi Akademii Nauk, Fizika Atmosfery i Okeana, 2019, Vol. 55, No. 5.

Tsunami Hazard Assessment on the Egyptian Coast of the Mediterranean

A. I. Zaytsev[a, b], **, A. Yu. Babeyko[c], ***, A. A. Kurkin[a], *,
A. C. Yalciner[d], ****, and E. N. Pelinovsky[e, f, g], *****
[a]Nizhny Novgorod State Technical University n.a. R.E. Alekseev, Nizhny Novgorod, 603950 Russia
[b]Special Research Bureau for Automation of Marine Research, Russian Academy of Sciences, Far East Branch, Yuzhno-Sakhalinsk, 693023 Russia
[c]GFZ German Research Centre for Geosciences, Telegrafenberg, Potsdam, 14473 Germany
[d]Middle East Technical University, bldng K5-014, Ankara, 06800 Turkey
[e]Federal Research Center Institute of Applied Physics, Russian Academy of Sciences, Nizhny Novgorod, 603950 Russia
[f]National Research University-Higher School of Economics, Moscow, 101000 Russia
[g]University of Southern Queensland, West St., Darling Heights, Toowoomba, QLD 4350 Australia

Nuclear Plant in Egypt will be created by Russia

The probabilistic estimates obtained in [32] were based only on tsunamis of seismic origin, taking into account the large amount of data on possible earthquakes. The catalog of earthquakes over the past 1000 years for the Mediterranean Sea can be found in [33]. This catalog was used in [32] to create a synthetic catalog of potential tsunamigenic earthquakes for the next 100000 years. It retains the same distribution of magnitudes and focal mechanisms as in the catalogs of real events. The synthetic catalog contains almost 85000 earthquakes with a magnitude of $M > 6.5$ for 100000 years. The spatial distribution of earthquakes over 10000 years [32] demonstrates that the tsunami sources completely cover the Aegean Sea, and many of them are located close to Egypt.

Abstract—Tsunami forecast possibilities for areas with a small base of historical tsunamis have been discussed using the Probabilistic Tsunami Hazard Assessment (PTHA) method, which is based on a statistical analysis of a sufficiently large number of real and predictive earthquakes with a subsequent calculation of possible tsunami waves. This method has been used for a long-term tsunami hazard assessment on the Mediterranean coast of Egypt. The predicted wave heights have been shown to vary along the coastline due to the inhomogeneity of the coastal topography and specific features of the tsunami radiation pattern in the sea. The predicted wave heights for 1000 years vary in the range between 0.8 and 3.4 m.

The new directions in the numerical modeling

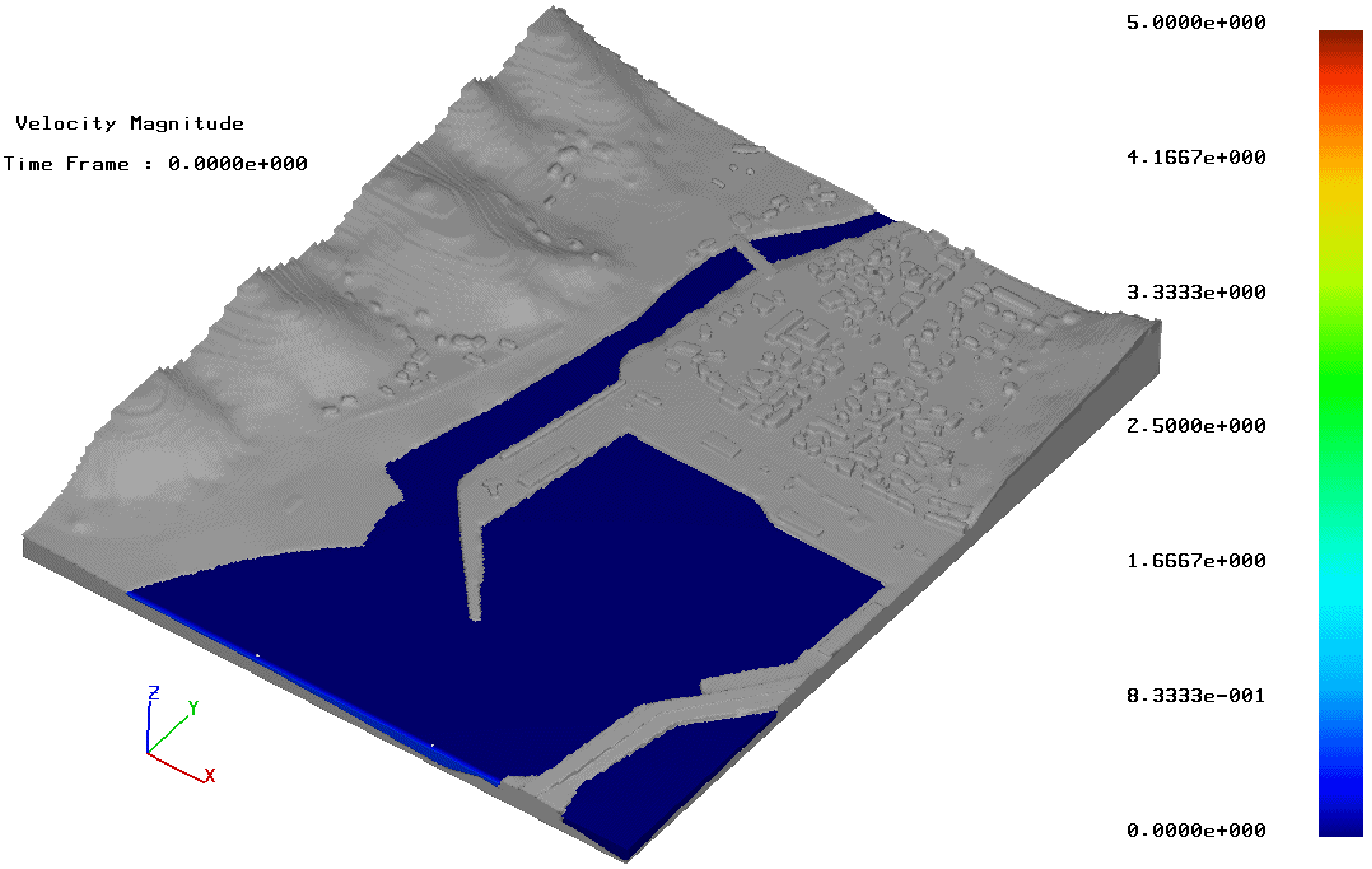

Dam in Kamaishi, Japan
Tsunami 2011

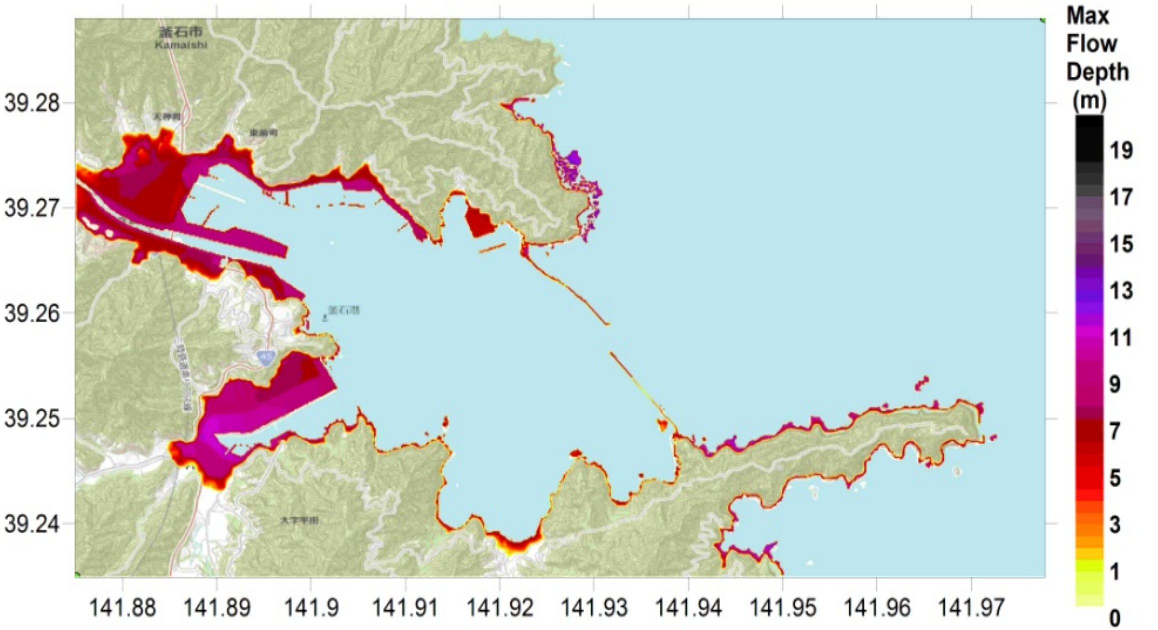

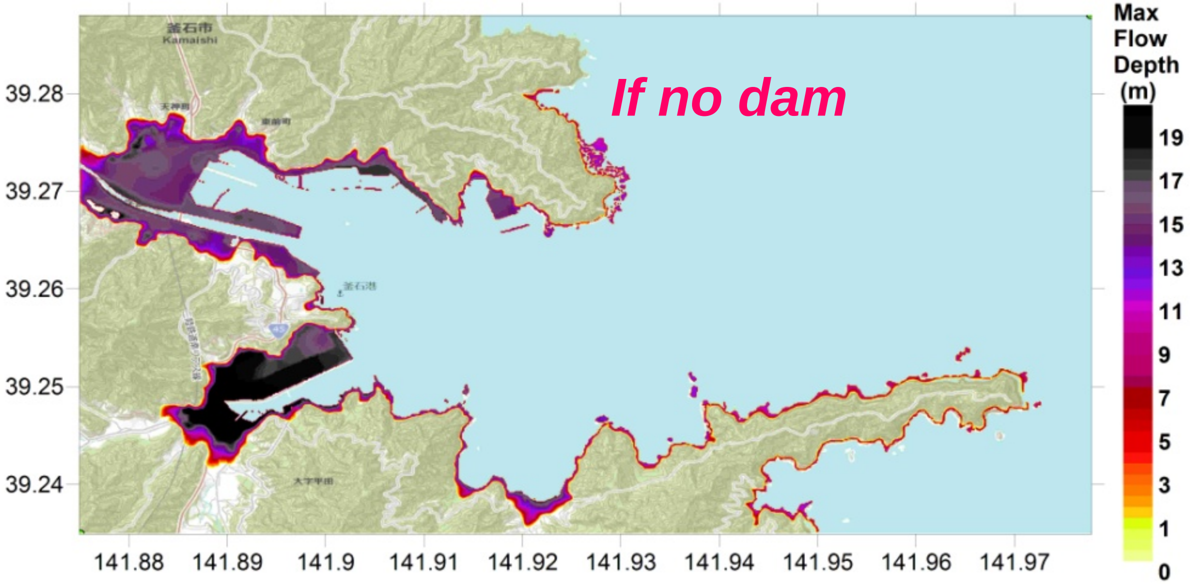

Difference in velocities

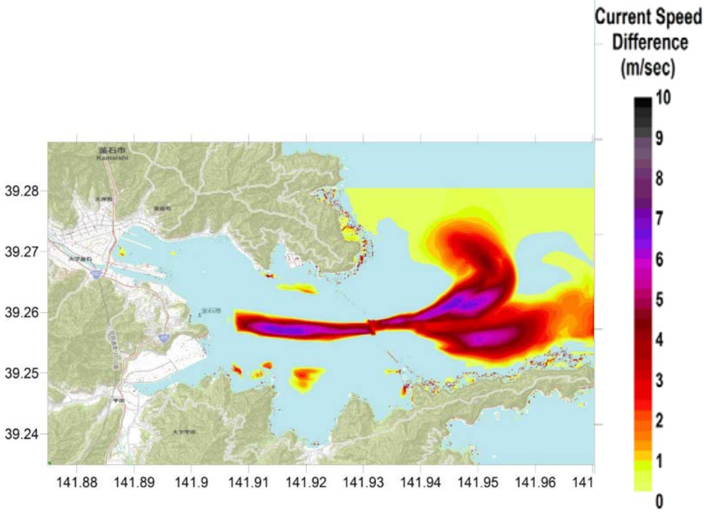

Порт Хайдарпаша, Турция (контейнерный порт)

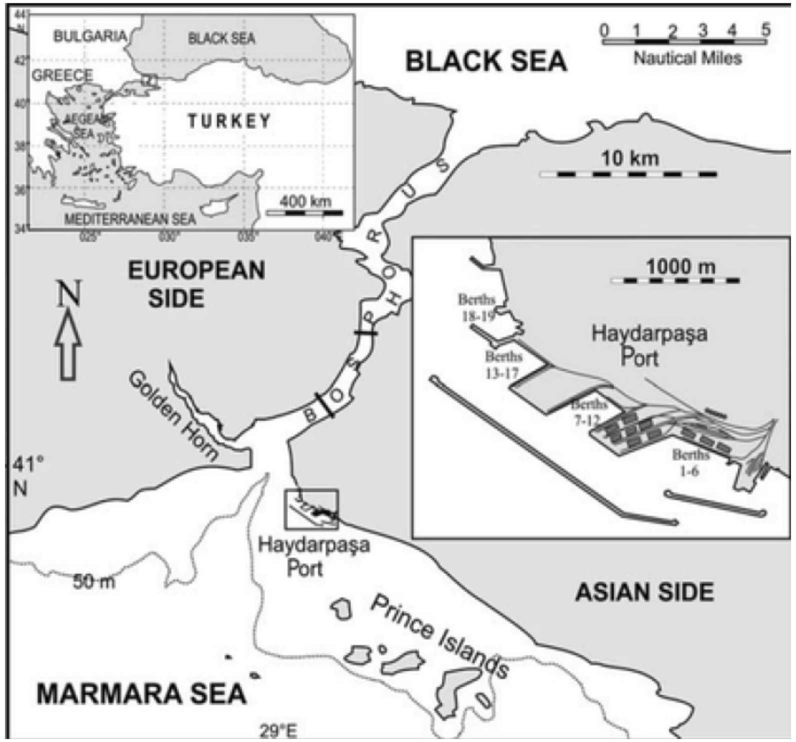

Расчеты вплоть до шага 1 м

Волна приходит через 5 мин и становится максимальной к 20 мин

Вода стоит в порту более часа

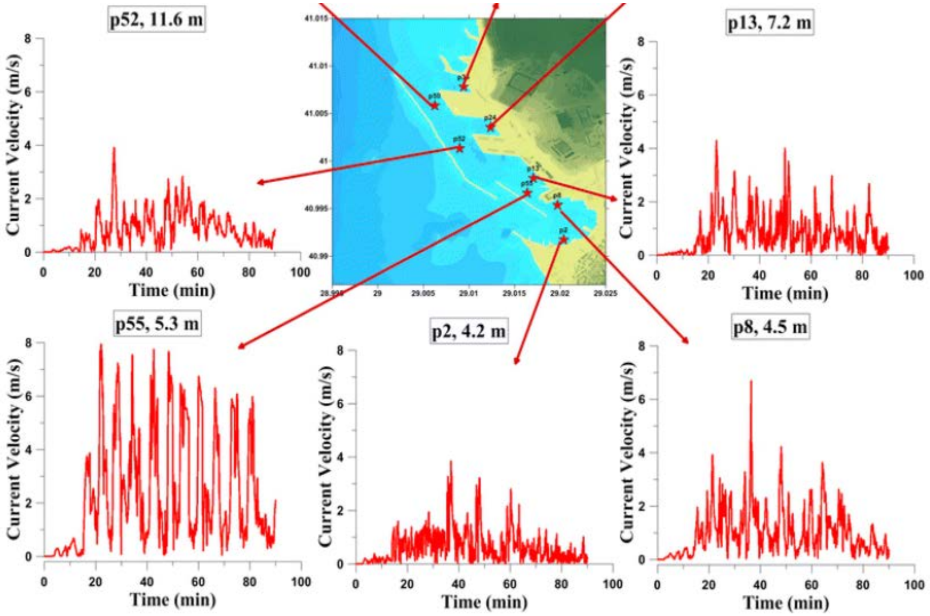

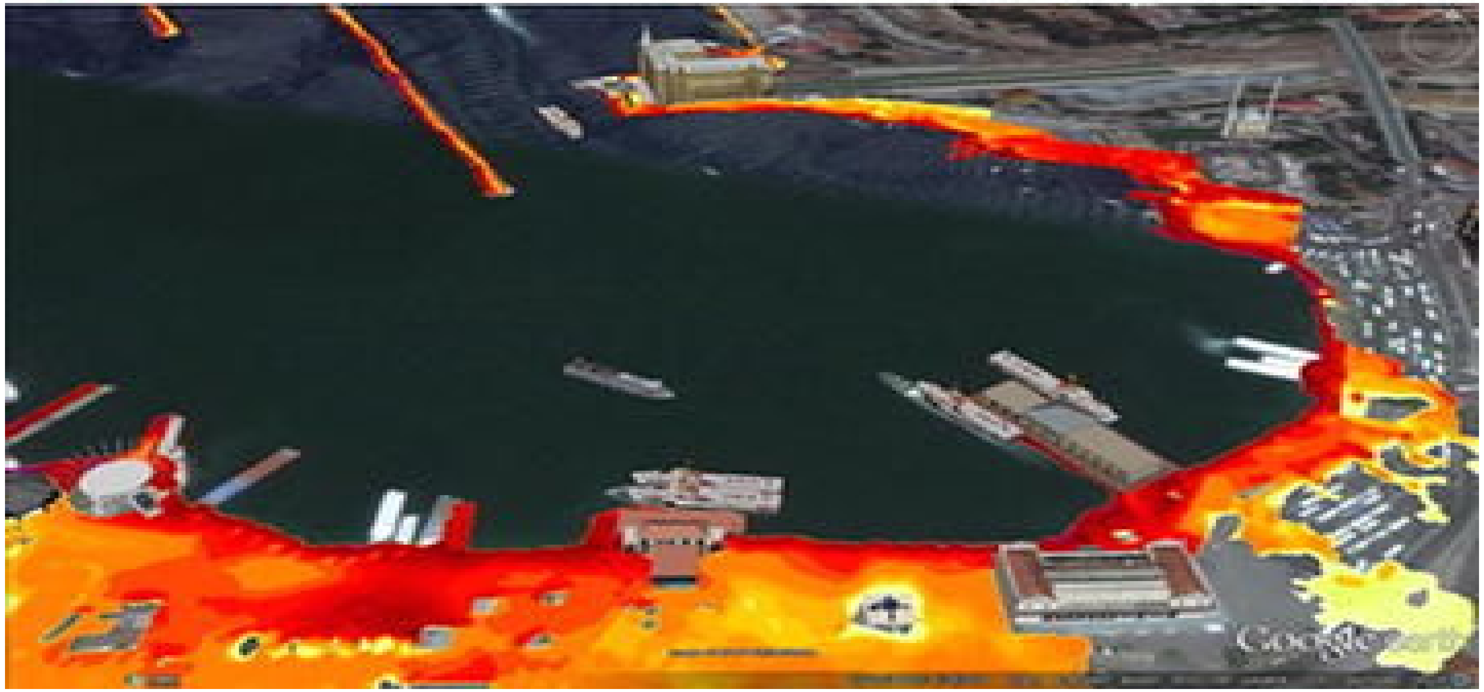

Высота 5 м,

Дистанция 340 м

Nat. Hazards Earth Syst. Sci., 11, 2835–2846, 2011
www.nat-hazards-earth-syst-sci.net/11/2835/2011/
doi:10.5194/nhess-11-2835-2011

Natural Hazards and Earth System Sciences

New tsunami damage functions developed in the framework of SCHEMA project: application to European-Mediterranean coasts

N. Valencia[1], A. Gardi[1,*], A. Gauraz[2], F. Leone[2], and R. Guillande[1]

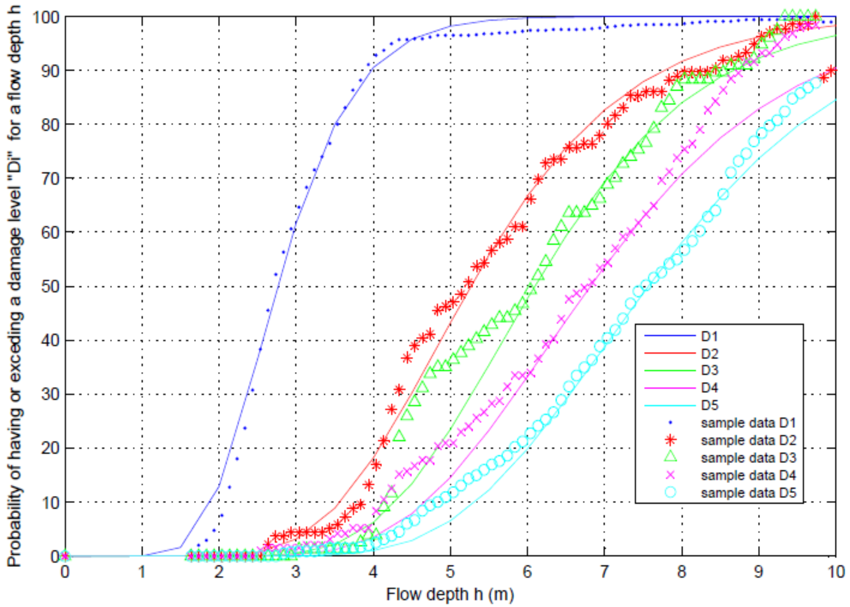

	Field recognition criteria	Field view	Aerial view	Recognition criteria by EO
A	Beach or sea front light constructions: Wooden, timber, clay materials, or zinc slabs.			Flat roof, steel sheets Small to very small surfaces. Extended surfaces in case of beach activities (restaurants, bars)
B	Brick not reinforced Cement mortar wall, Fieldstone, Masonry. One storey.			Simple geometry (square, rectangle). Flat or slope roofs, tile roofs. Little extension or surface. Located in the old town.
C	Individual buildings, villas: Brick with reinforced column & masonry filling. One or two storeys.			More complex geometry. Several levels of roof and several annex. Pitched roof. Medium to big dimensions.
D	Non-ingeneered reinforced concrete buildings. Collective use. Two to four floors			Tiles roofs. Located in old town. Elongated geometry.

Fragility Function

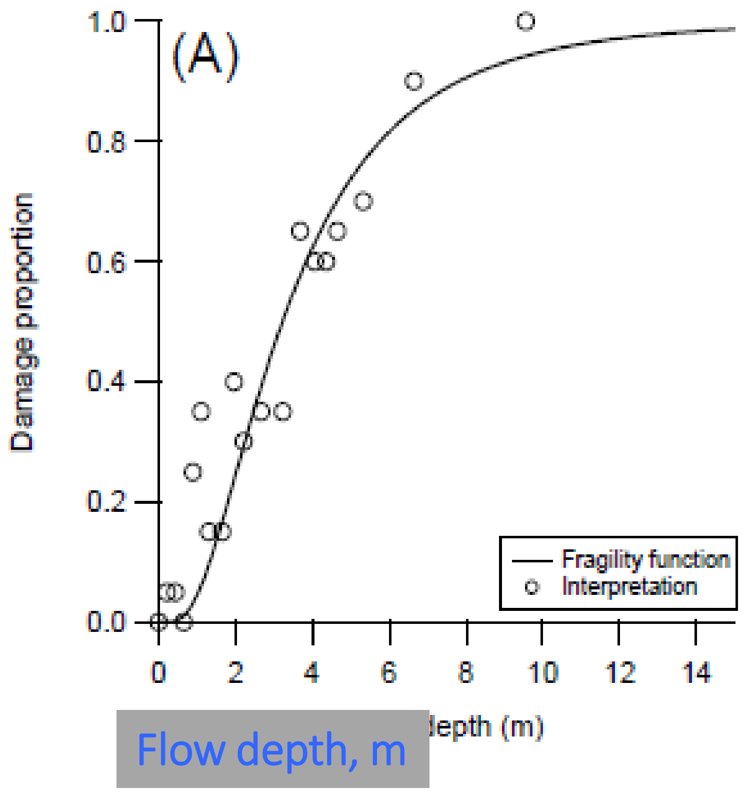

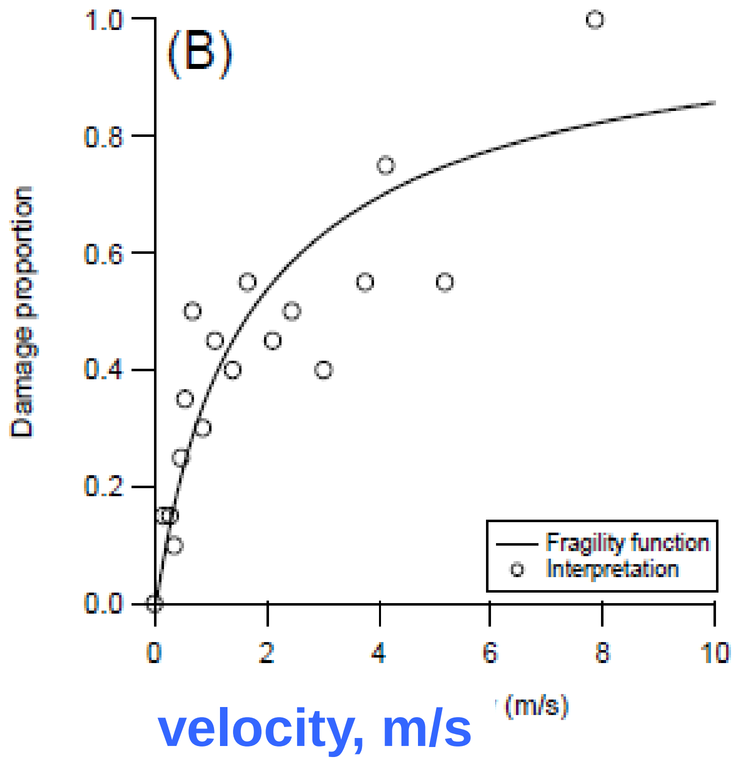

МИНИСТЕРСТВО СТРОИТЕЛЬСТВА
И ЖИЛИЩНО-КОММУНАЛЬНОГО ХОЗЯЙСТВА
РОССИЙСКОЙ ФЕДЕРАЦИИ

СВОД ПРАВИЛ СП 292.1325800.2017

ЗДАНИЯ И СООРУЖЕНИЯ В ЦУНАМИОПАСНЫХ РАЙОНАХ.
Правила проектирования

Издание официальное

Дата регистрации 07 августа 2017г.

Москва

2017

**Министерство строительства
и жилищно-коммунального хозяйства
Российской Федерации**

**Федеральное автономное учреждение
«Федеральный центр нормирования, стандартизации
и оценки соответствия в строительстве»**

Методическое пособие

ПРОЕКТИРОВАНИЕ ЗДАНИЙ И СООРУЖЕНИЙ В ЦУНАМИОПАСНЫХ РАЙОНАХ

Москва 2018

2011 Japan evacuation (Shuto)

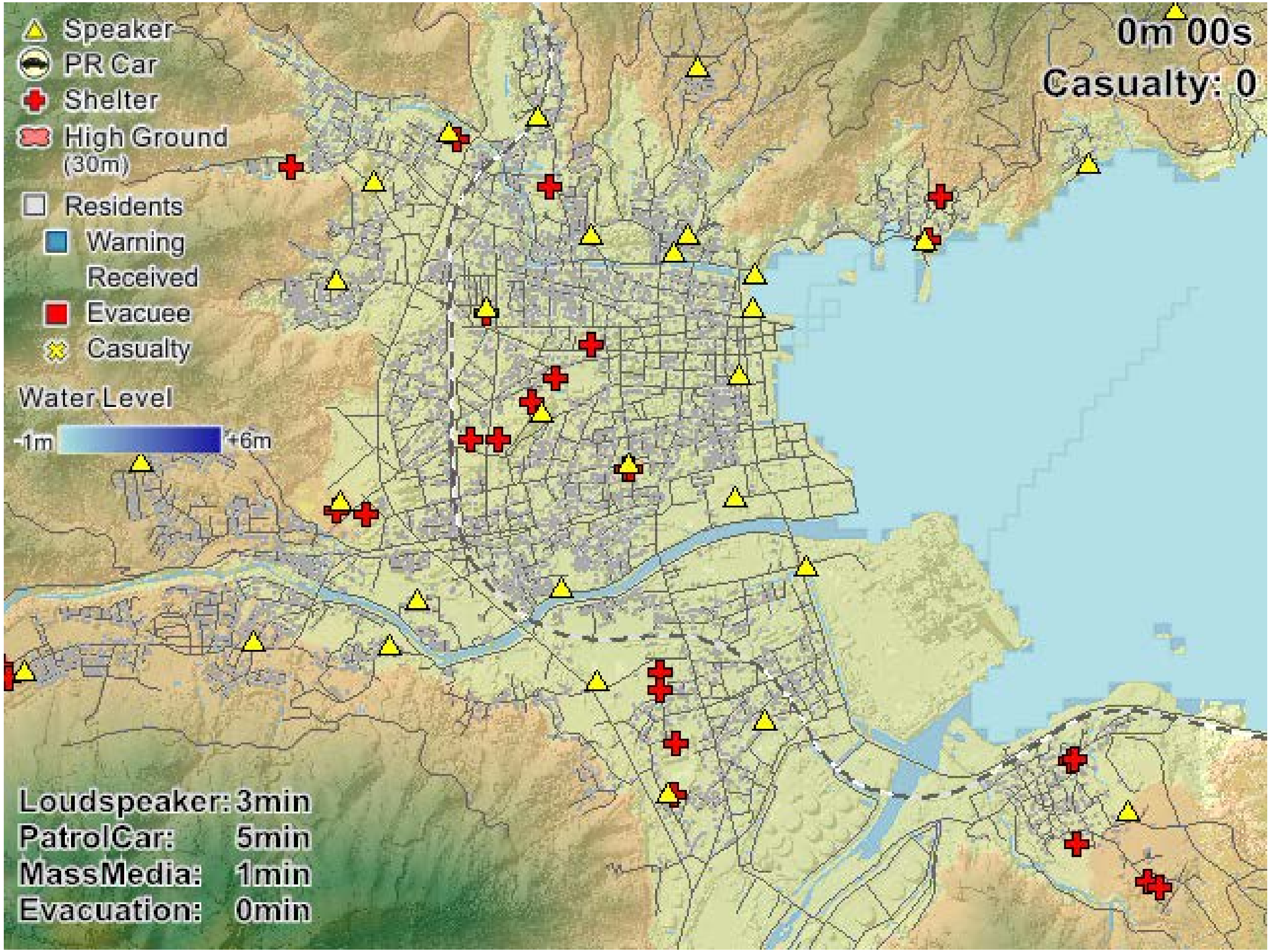

Risk mitigation:

1. Evacuation plan
(each house and telephone)
2. Education (books)
3. Training
4. Reserve (food)
5. Communications

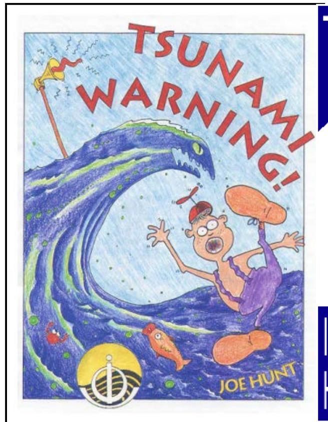

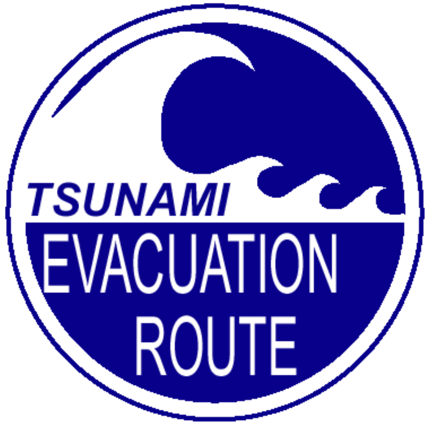

Главнейшие задачи:

1. Откуда взять расчетное землетрясение, оползень, вулкан, астероид?
2. Как оперативно предсказать источники ближних цунами?
3. Точные модели (физика, механика) или параметризация?
4. Обрушение – необрушение, многофазные потоки на берегу
5. Роль нейронных сетей – «убивцев» уравнений
6. Эффекты волн-убийц в цунами и предсказание особенностей дна
7. Социальное поведение в природных катастрофах
8. Воздействие на экологию и климат

Нелинейная физика - пункты 1, 3, 4, 6